Interactive Freeform Architectural Design with Nearly Developables and Cold Bent Glass

Doctoral Defense

Konstantinos Gavriil
TU Wien

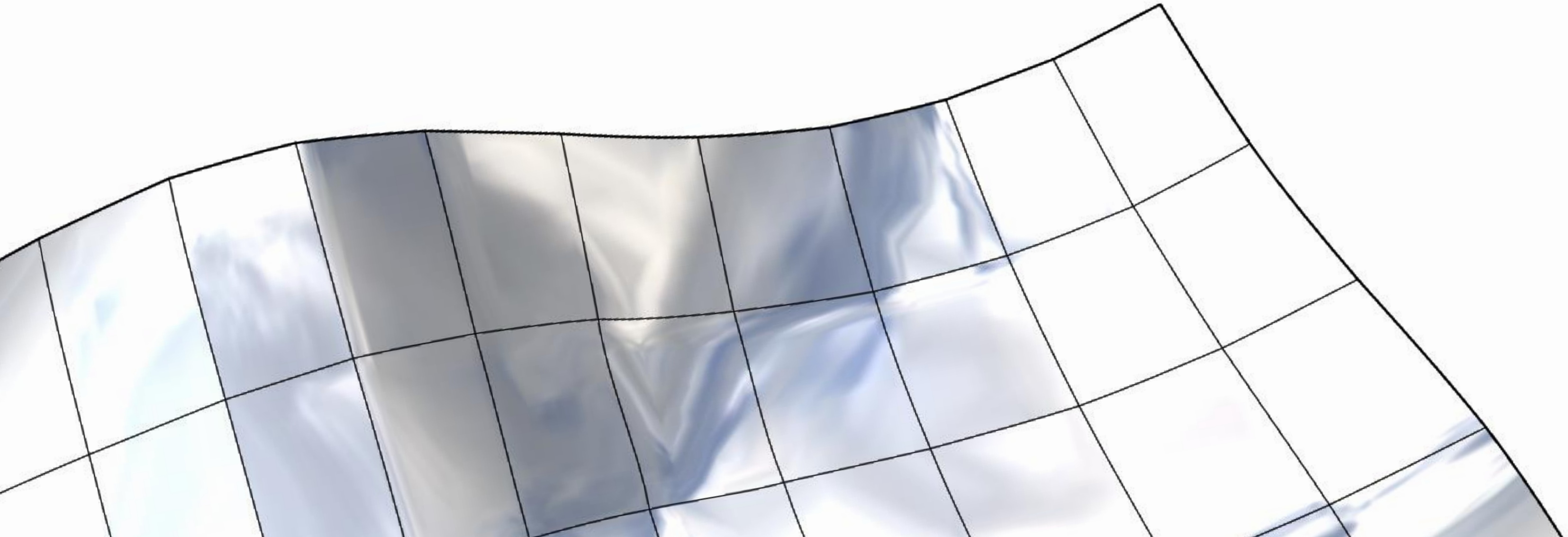


Vienna, Austria
Athens, Greece
Tashkent, Uzbekistan


Vienna, Austria
Athens, Greece
Tashkent, Uzbekistan


Vienna, Austria
Athens, Greece
Tashkent, Uzbekistan

Background

Past

- BSc in Mathematics & MSc in Computational Science — University of Athens

Recently

- Marie Skłodowska-Curie Fellow — Evolute GmbH
- PhD student — TU Wien

Secondments

- Invited PhD Student — Inria Sophia-Antipolis
- -------- ” -------- — SINTEF Digital

People


Helmut Pottmann


Alexander Schiftner


Ioannis Emiris

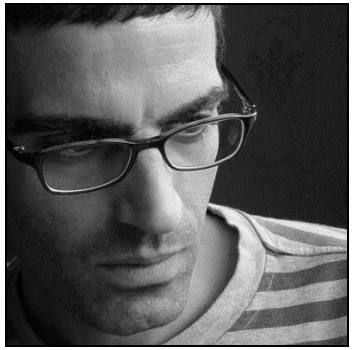
Christos Konaxis


Georg Muntingh


Oliver J.D. Barrowclough


Bernd Bickel


Ruslan Guseinov


Jesús Pérez


Davide Pellis


Paul Henderson


Florian Rist

Research output

- Optimizing B-spline surfaces for developability and paneling architectural freeform surfaces.
  K. Gavriil, A. Schiftner, H. Pottmann.
  Computer-Aided Design, 2019.

- Computational Design of Cold Bent Glass Façades.
  K. Gavriil, R. Guseinov, J. Pérez, D. Pellis, P. Henderson, F. Rist, H. Pottmann, B. Bickel.
  ACM Transactions on Graphics (Proceedings of ACM SIGGRAPH Asia), 2020.

- Void filling of digital elevation models with deep generative models.
  K. Gavriil, G. Muntingh, O. J.D. Barrowclough.
  IEEE Geoscience and Remote Sensing Letters, 2019.

- Interpolation of syzygies for implicit matrix representations.
  I. Emiris, K. Gavriil, and C. Konaxis.
  International Conference on Algebraic Informatics, 2017.

Research output

- Optimizing B-spline surfaces for developability and paneling architectural freeform surfaces.
  K. Gavriil, A. Schiftner, H. Pottmann.
  Computer-Aided Design, 2019.
  ✓

- Computational Design of Cold Bent Glass Façades.
  K. Gavriil, R. Guseinov, J. Pérez, D. Pellis, P. Henderson, F. Rist, H. Pottmann, B. Bickel.
  ACM Transactions on Graphics (Proceedings of ACM SIGGRAPH Asia), 2020.
  ✓

- Void filling of digital elevation models with deep generative models.
  K. Gavriil, G. Muntingh, O. J.D. Barrowclough.
  IEEE Geoscience and Remote Sensing Letters, 2019.

- Interpolation of syzygies for implicit matrix representations.
  I. Emiris, K. Gavriil, and C. Konaxis.
  International Conference on Algebraic Informatics, 2017.

Guggenheim Museum Bilbao by Frank Gehry.
Bilbao, Spain

Interactive Design with nearly developables & cold bent glass

Konstantinos Gavriil

Interactive Design with nearly developables & cold bent glass

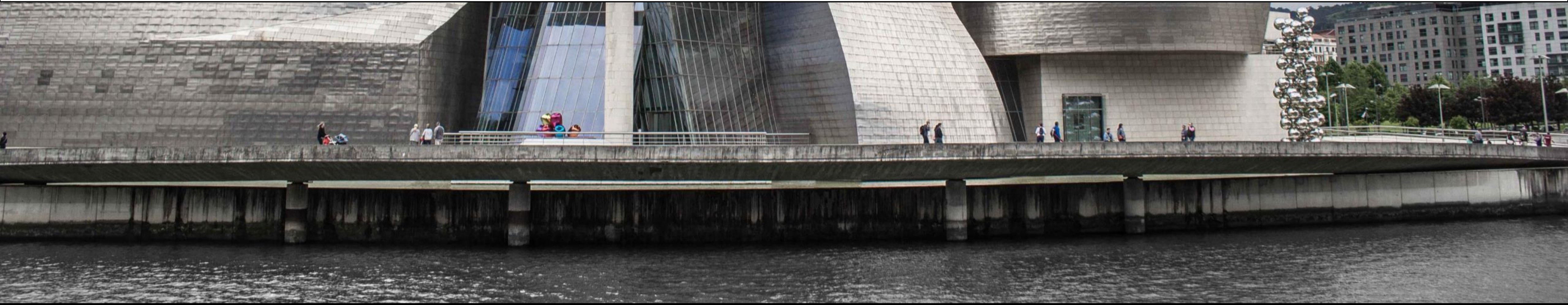

Konstantinos Gavriil

TU WIEN

Contributions

- Novel optimization method for increasing the developability of an arbitrary surface.

- Panelization of freeform architectural surfaces with panels that are
  - cylindrical (rotational),
  - conical (rotational),
  - planar.

- Computational framework for interactively designing panelizations with cold bent glass panels.

Contributions

- Novel optimization method for increasing the developability of an arbitrary surface.

- Panelization of freeform architectural surfaces with panels that are
  - cylindrical (rotational),
  - conical (rotational),
  - planar.

- Computational framework for interactively designing panelizations with cold bent glass panels.

Contributions

- Novel optimization method for increasing the developability of an arbitrary surface.

- Panelization of freeform architectural surfaces with panels that are
  - cylindrical (rotational),
  - conical (rotational),
  - planar.

- Computational framework for interactively designing panelizations with cold bent glass panels.

Contributions

- Novel optimization method for increasing the developability of an arbitrary surface.
- Panelization of freeform architectural surfaces with panels that are
  - cylindrical (rotational),
  - conical (rotational),
  - planar.
- Computational framework for interactively designing panelizations with cold bent glass panels.

Developability

A surface is **developable** when at every point it is locally isometric to the plane.

Properties.

- Locally isometric to the plane.
- The Gaussian curvature is zero at every point.
- A surface geodesic maps to a straight line in the developed plane.
- It is a ruled surface which has the same tangent plane across a ruling.
- The Gauss image is 1-dimensional.

Developability

A surface is **developable** when at every point it is locally isometric to the plane.

Properties.

- Locally isometric to the plane.
- The Gaussian curvature is zero at every point.
- A surface geodesic maps to a straight line in the developed plane.
- It is a ruled surface which has the same tangent plane across a ruling.
- The Gauss image is 1-dimensional.

Developability

A surface is **developable** when at every point it is locally isometric to the plane.

Properties.

- Locally isometric to the plane.
- The Gaussian curvature is zero at every point.
- A surface geodesic maps to a straight line in the developed plane.
- It is a ruled surface which has the same tangent plane across a ruling.
- The Gauss image is 1-dimensional.

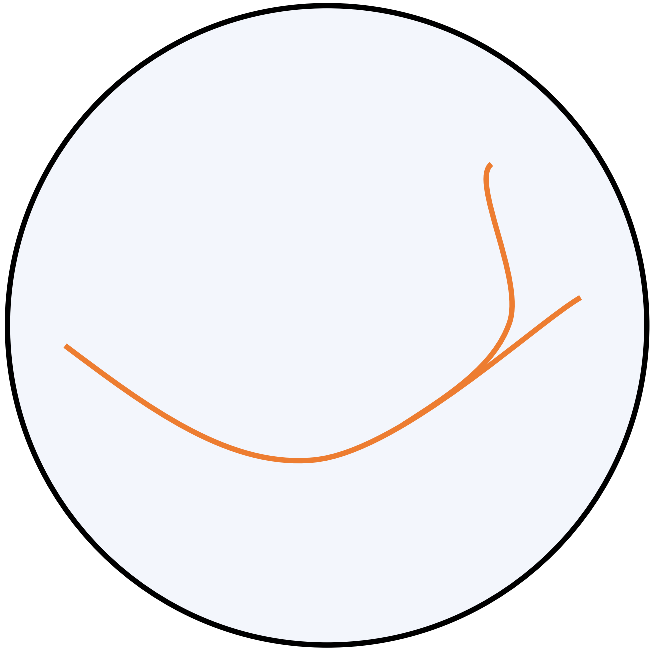

Local approximation of developable surfaces

Lemma. Along each ruling r, a non-planar developable ruled surface has second order contact with a rotational cone Γ (osculating cone). The vertex of this cone is the singular point of r (regression point). Γ degenerates to a rotational cylinder for a cylinder S and to a plane if r is an inflection ruling.

Theorem. At each regular point p of a developable ruled surface S, there is a developable surface with a planar Gauss image, which has second order contact with S along the entire ruling through p and interpolates a curve $a \in S$ through p.

Local approximation of developable surfaces

Lemma. Along each ruling r, a non-planar developable ruled surface has second order contact with a rotational cone Γ (osculating cone). The vertex of this cone is the singular point of r (regression point). Γ degenerates to a rotational cylinder for a cylinder S and to a plane if r is an inflection ruling.

Theorem. At each regular point p of a developable ruled surface S, there is a developable surface with a planar Gauss image, which has second order contact with S along the entire ruling through p and interpolates a curve $a \in S$ through p.

Local approximation of developable surfaces

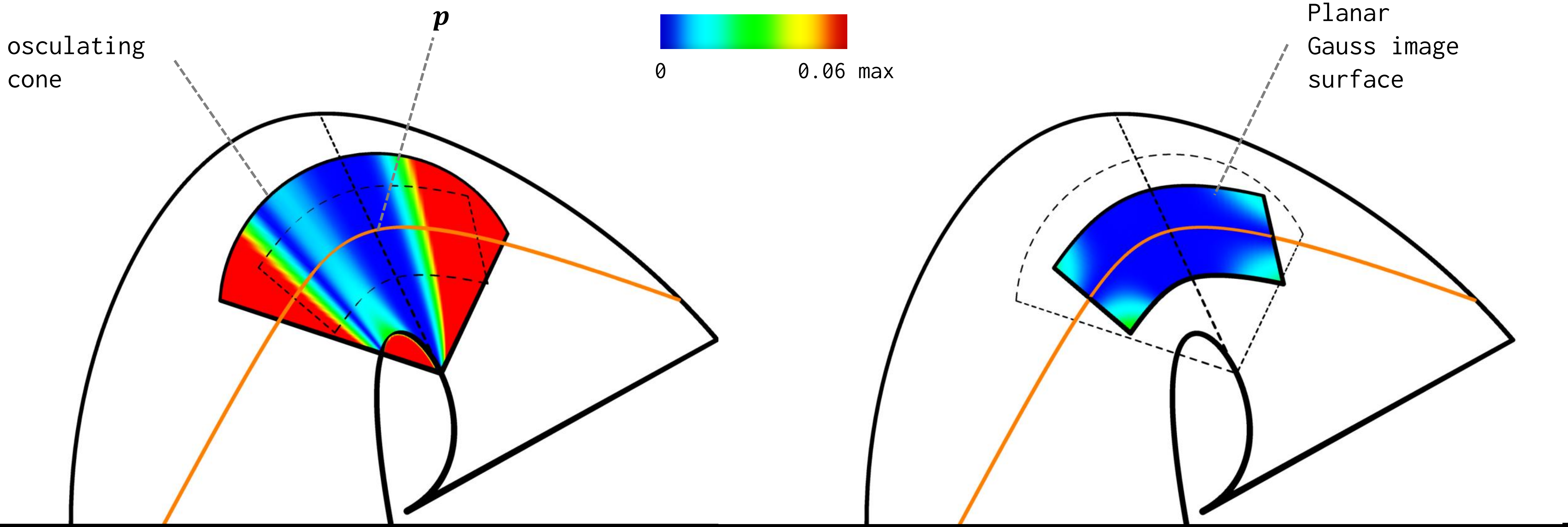

Methodology

sample points $\mathbf{p}_i$

group $\mathbf{p}_i$ to P_j

compute normals $\mathbf{n}_i$

optimize for planarity of $\mathbf{n}_i$ per P_j

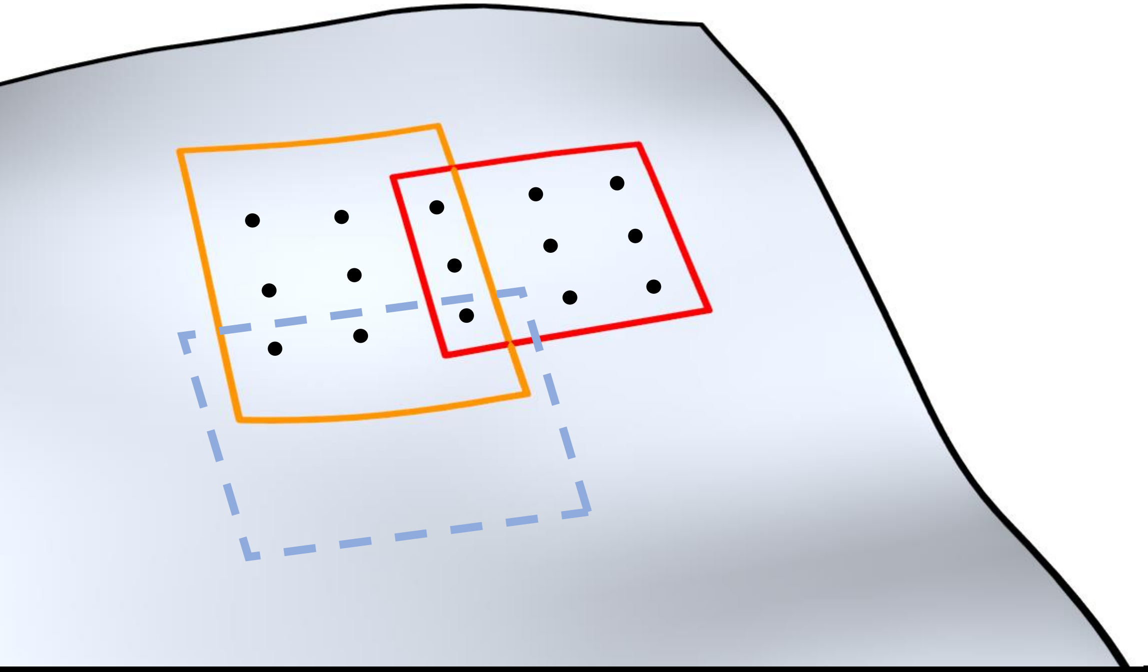

Methodology

sample points $\mathbf{p}_i$

group $\mathbf{p}_i$ to P_j

compute normals $\mathbf{n}_i$

optimize for planarity of $\mathbf{n}_i$ per P_j

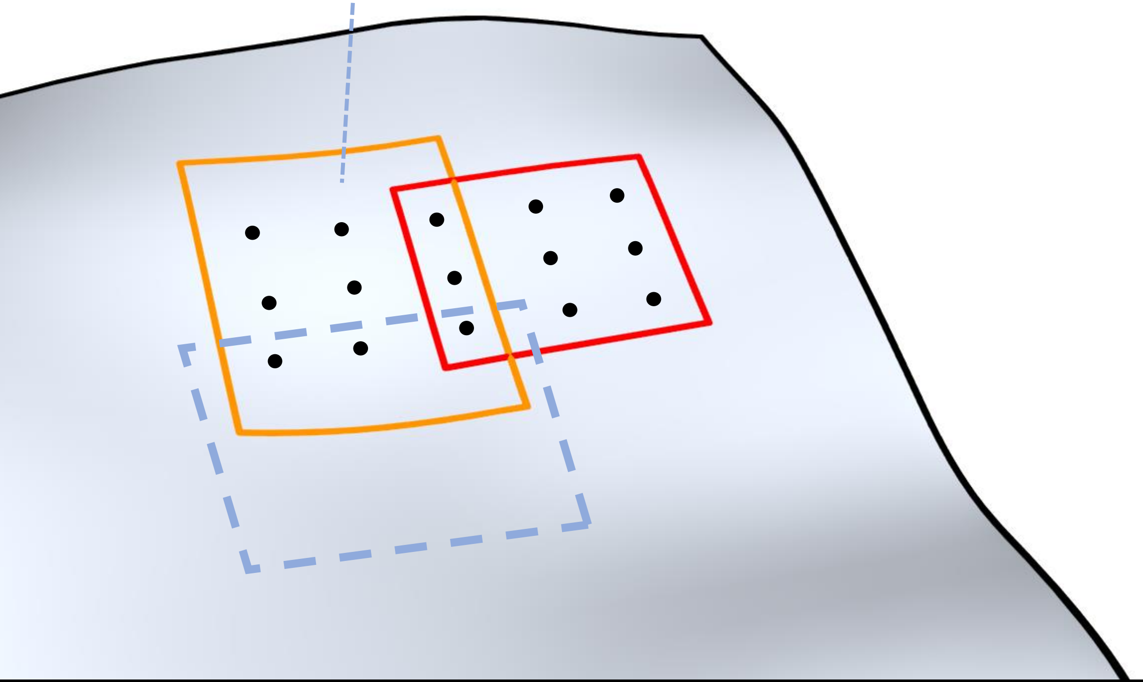

Methodology

sample points $\mathbf{p}_i$

group $\mathbf{p}_i$ to P_j

compute normals $\mathbf{n}_i$

optimize for planarity of $\mathbf{n}_i$ per P_j

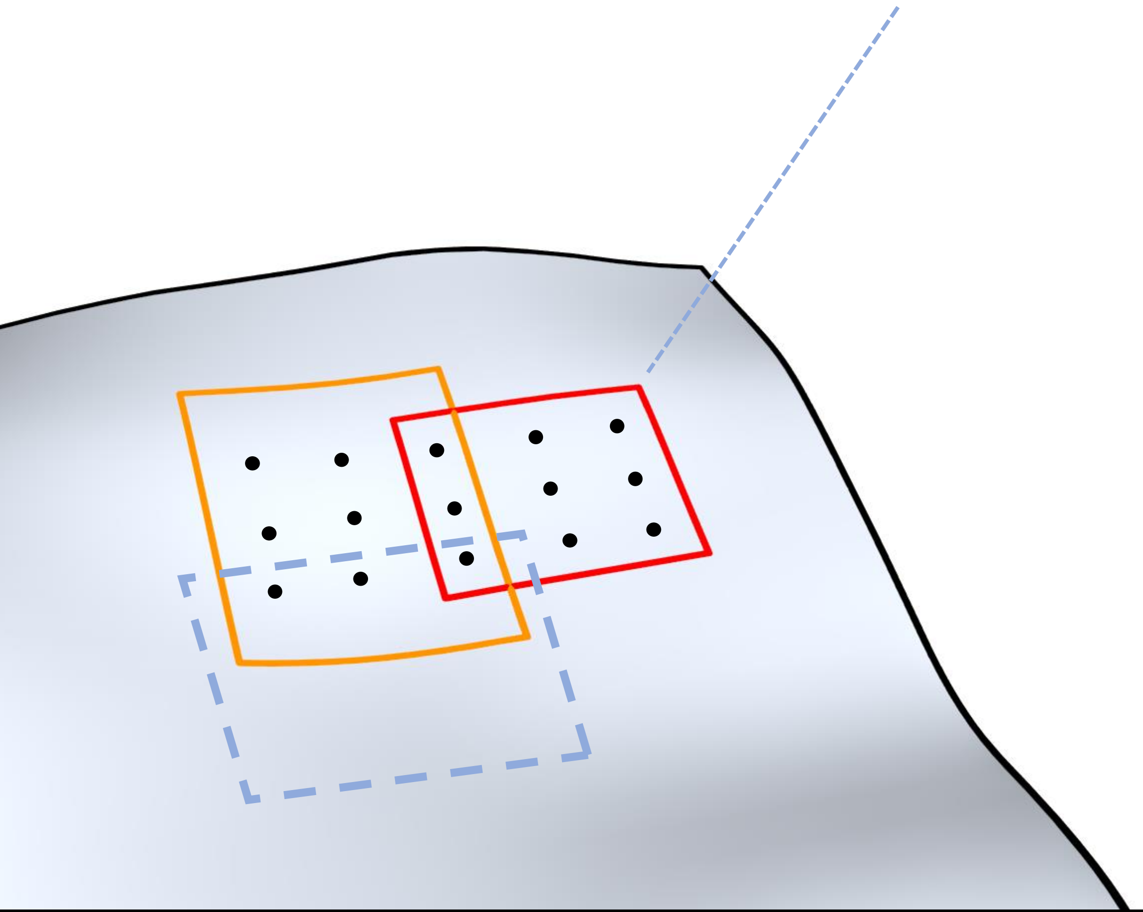

Methodology

sample points $\mathbf{p}_i$

group $\mathbf{p}_i$ to P_j

compute normals $\mathbf{n}_i$

optimize for planarity of $\mathbf{n}_i$ per P_j

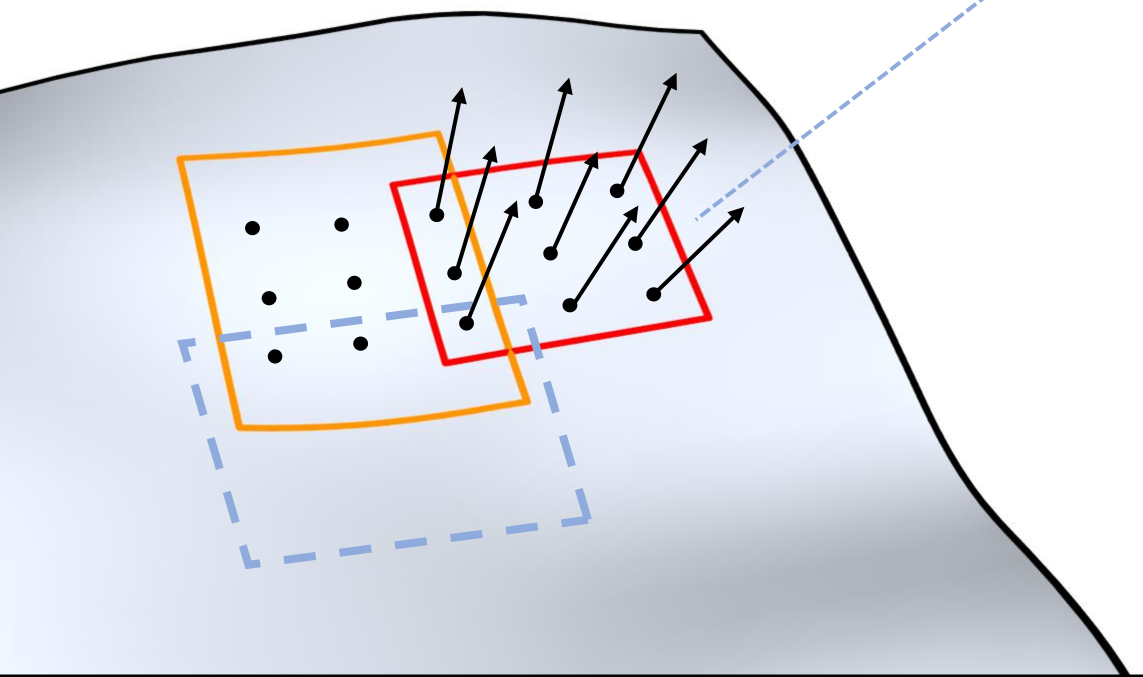

Methodology

sample points $\mathbf{p}_i$

group $\mathbf{p}_i$ to P_j

compute normals $\mathbf{n}_i$

optimize for planarity of $\mathbf{n}_i$ per P_j

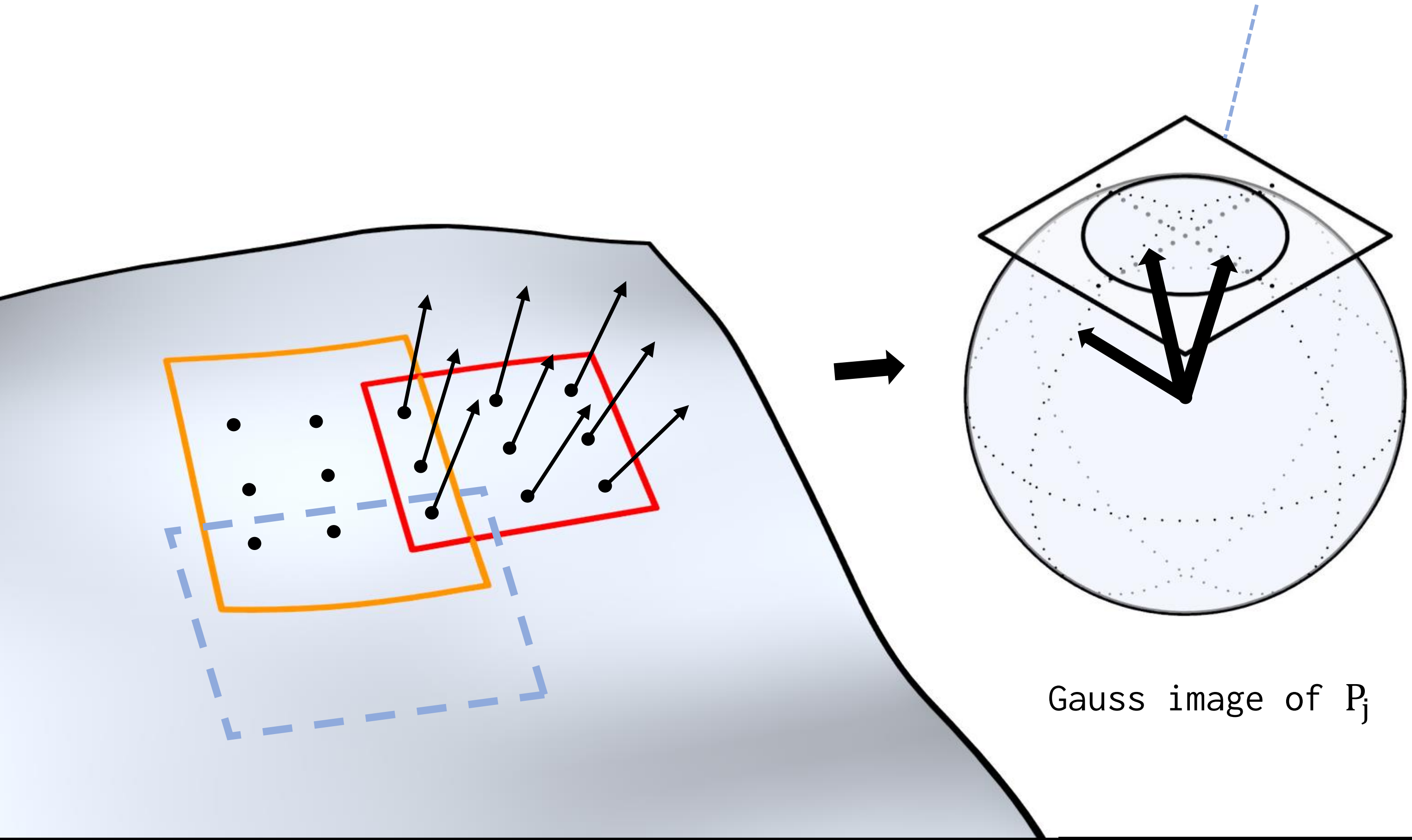

Gauss image of P_j

Methodology

sample points $\mathbf{p}_i$

group $\mathbf{p}_i$ to P_j

compute normals $\mathbf{n}_i$

optimize for planarity of $\mathbf{n}_i$ per P_j

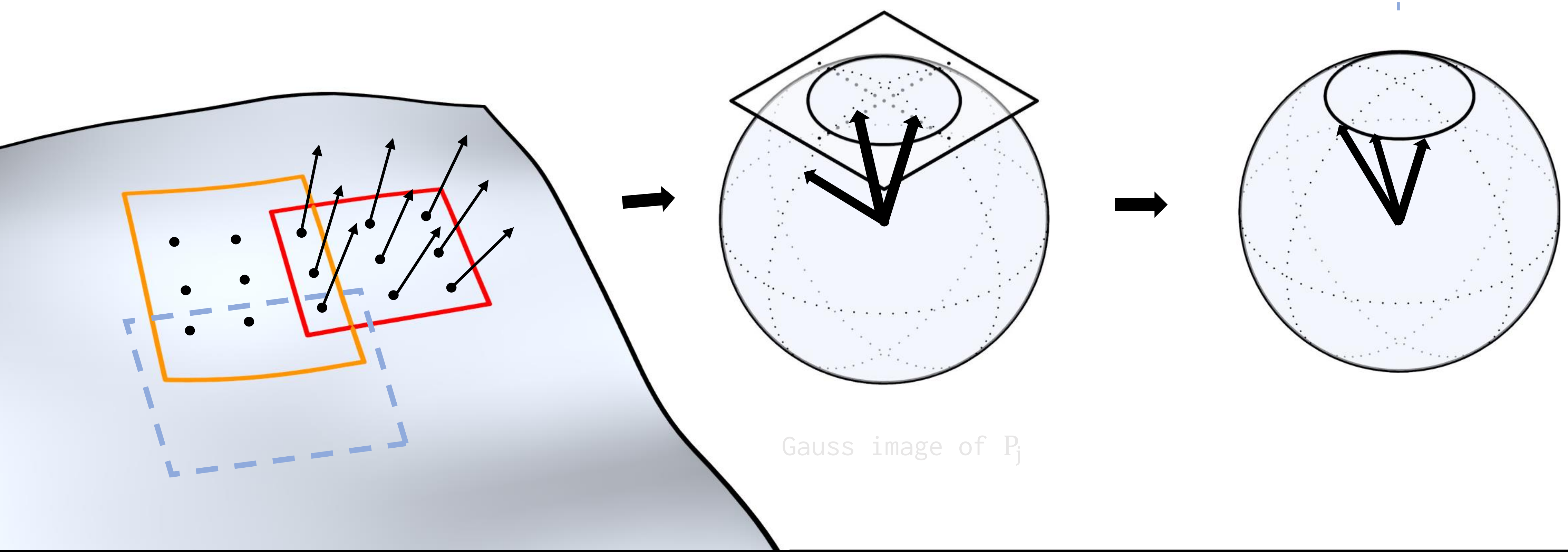

Gauss image of P_j

Energies

Developability. $\mathcal{E}_{\text{developable}} = \sum_{j} \sum_{\mathbf{p}_i \in P_j} (\mathbf{n}_i \cdot \mathbf{u}_j + d_j)^2$ where $\mathbf{n}_i^{\,2} = 1,\ \mathbf{u}_j^{\,2} = 1$

Rotationality. $\mathcal{E}_{\text{rotational}} = \sum_{j} \sum_{\mathbf{p}_i \in P_j} (\bar{\mathbf{a}}_j \cdot \mathbf{n}_i + \mathbf{a}_j \cdot \bar{\mathbf{n}}_i)^2$ where $\mathbf{a}_j^{\,2} = 1,$ $\mathbf{a}_j \cdot \bar{\mathbf{a}}_j = 0$

Closeness. $\mathcal{E}_{\text{closeness}}$

Fairness. $\mathcal{E}_{\text{fairness}}$

Energies

Developability. $\mathcal{E}_{\text{developable}} = \sum_{j} \sum_{\mathbf{p}_i \in P_j} (\mathbf{n}_i \cdot \mathbf{u}_j + d_j)^2$ where $\mathbf{n}_i{}^2 = 1,\ \mathbf{u}_j{}^2 = 1$

Rotationality. $\mathcal{E}_{\text{rotational}} = \sum_{j} \sum_{\mathbf{p}_i \in P_j} (\bar{\mathbf{a}}_j \cdot \mathbf{n}_i + \mathbf{a}_j \cdot \bar{\mathbf{n}}_i)^2$ where $\mathbf{a}_j{}^2 = 1,$ $\mathbf{a}_j \cdot \bar{\mathbf{a}}_j = 0$

Closeness. $\mathcal{E}_{\text{closeness}}$

Fairness. $\mathcal{E}_{\text{fairness}}$

Energies

Developability. $$\mathcal{E}_{\text{developable}} = \sum_{j} \sum_{\mathbf{p}_i \in P_j} (\mathbf{n}_i \cdot \mathbf{u}_j + d_j)^2 \quad \text{where} \quad \mathbf{n}_i^2 = 1,\ \mathbf{u}_j^2 = 1$$

Rotationality. $$\mathcal{E}_{\text{rotational}} = \sum_{j} \sum_{\mathbf{p}_i \in P_j} (\bar{\mathbf{a}}_j \cdot \mathbf{n}_i + \mathbf{a}_j \cdot \overline{\mathbf{n}}_i)^2 \quad \text{where} \quad \mathbf{a}_j^2 = 1,\ \mathbf{a}_j \cdot \bar{\mathbf{a}}_j = 0$$

Closeness. $\mathcal{E}_{\text{closeness}}$

Fairness. $\mathcal{E}_{\text{fairness}}$

Increasing developability

$$\text{minimize } \mathcal{E} = w_1 \mathcal{E}_{\text{developable}} + w_2 \mathcal{E}_{\text{rotational}} + w_3 \mathcal{E}_{\text{fairness}} + w_4 \mathcal{E}_{\text{closeness}}$$

Solve using standard **Gauss-Newton algorithm** for nonlinear least squares problems.

Variables:

- Control points.
- Cutting planes.
- Rotation axes.

Initialize by appropriate fitting of the cutting planes (generalized eigenvalue problem) and of the rotation axis (linear system).

Increasing developability

$$\text{minimize } \mathcal{E} = w_1\mathcal{E}_{\text{developable}} + w_2\mathcal{E}_{\text{rotational}} + w_3\mathcal{E}_{\text{fairness}} + w_4\mathcal{E}_{\text{closeness}}$$

Solve using standard **Gauss-Newton algorithm** for nonlinear least squares problems.

Variables:

- Control points.
- Cutting planes.
- Rotation axes.

Initialize by appropriate fitting of the cutting planes (generalized eigenvalue problem) and of the rotation axis (linear system).

Increasing developability

$$\text{minimize } \mathcal{E} = w_1\mathcal{E}_{\text{developable}} + w_2\mathcal{E}_{\text{rotational}} + w_3\mathcal{E}_{\text{fairness}} + w_4\mathcal{E}_{\text{closeness}}$$

Solve using standard **Gauss-Newton algorithm** for nonlinear least squares problems.

Variables:

- Control points.
- Cutting planes.
- Rotation axes.

Initialize by appropriate fitting of the cutting planes (generalized eigenvalue problem) and of the rotation axis (linear system).

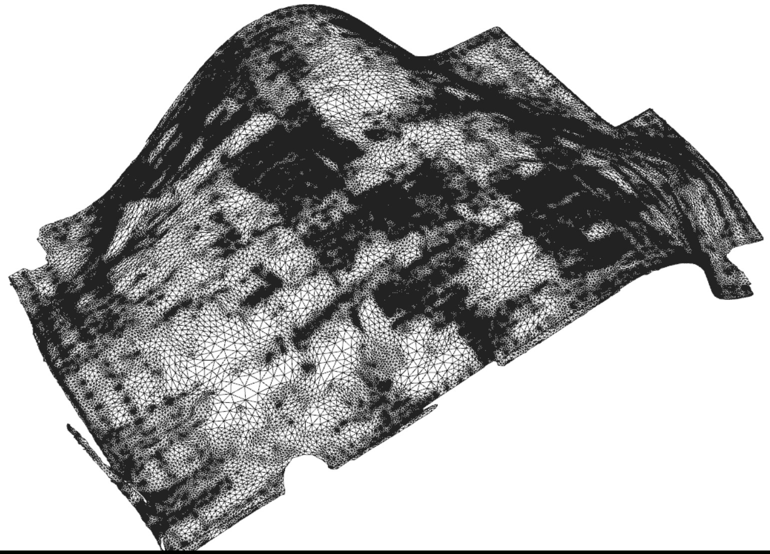

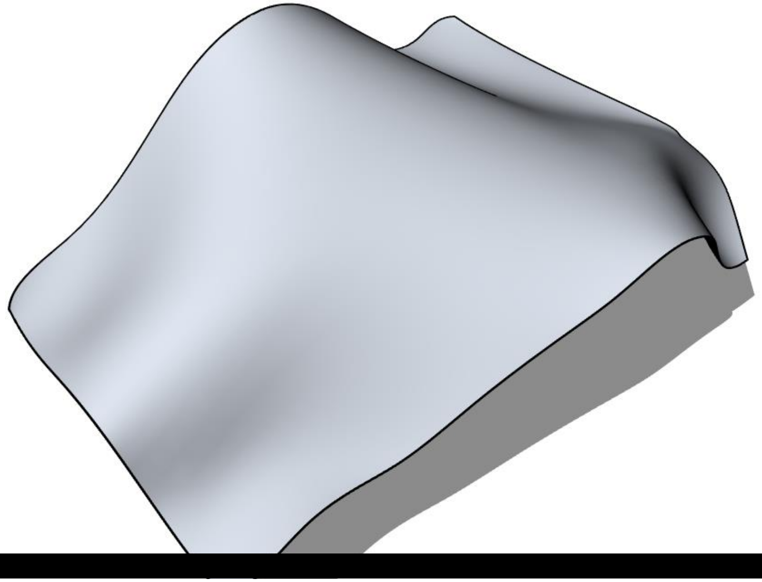


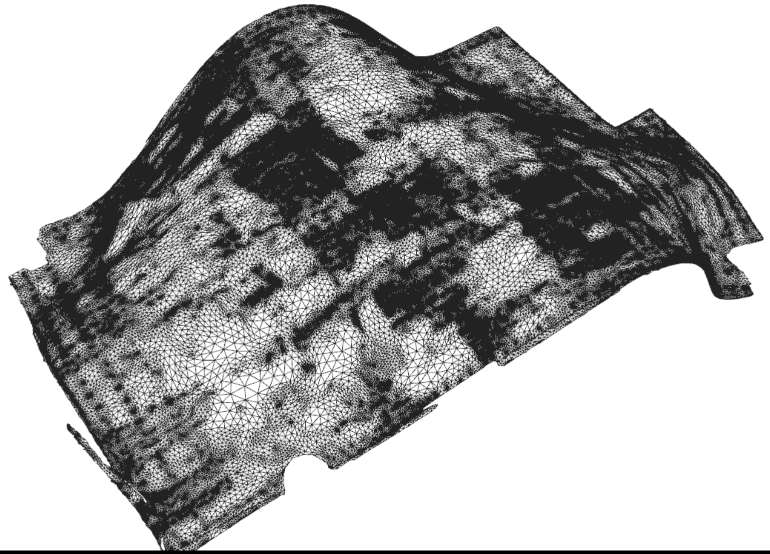
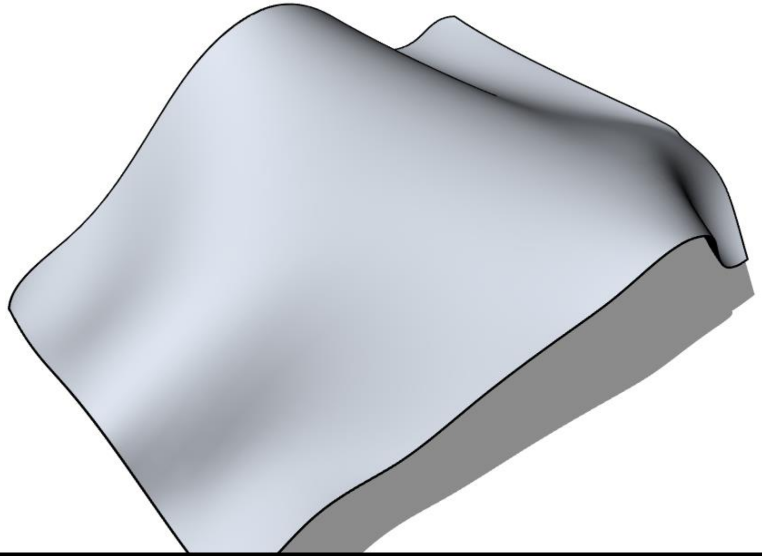
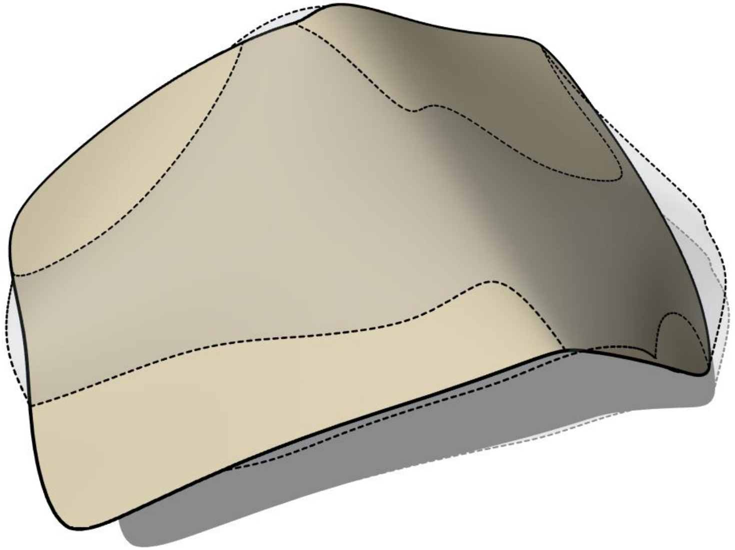



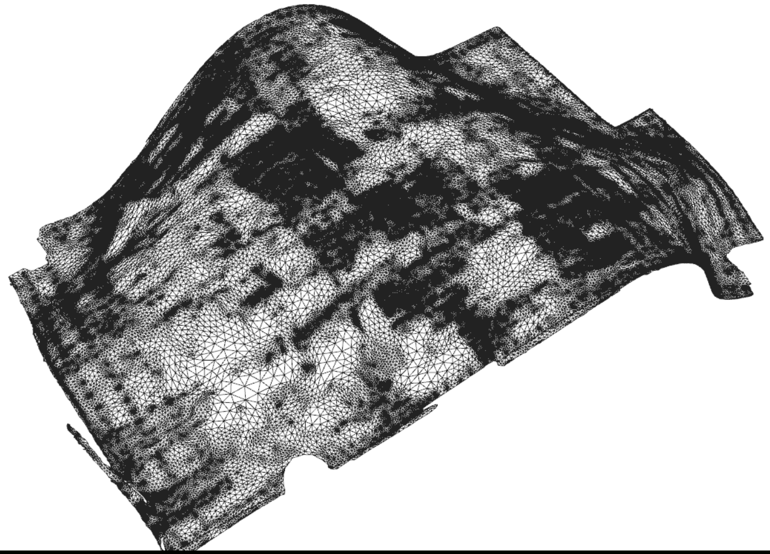
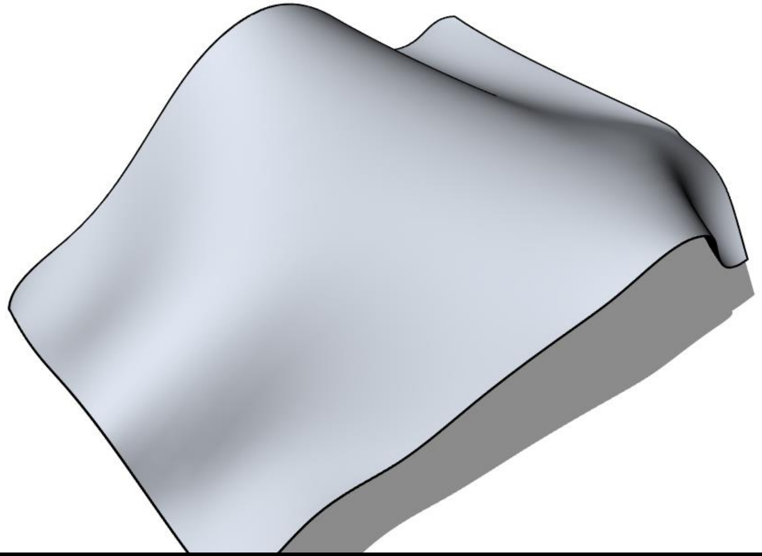
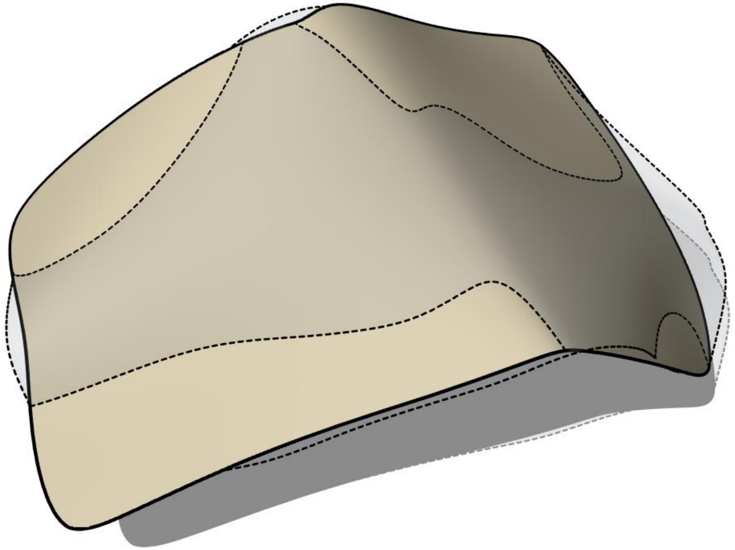
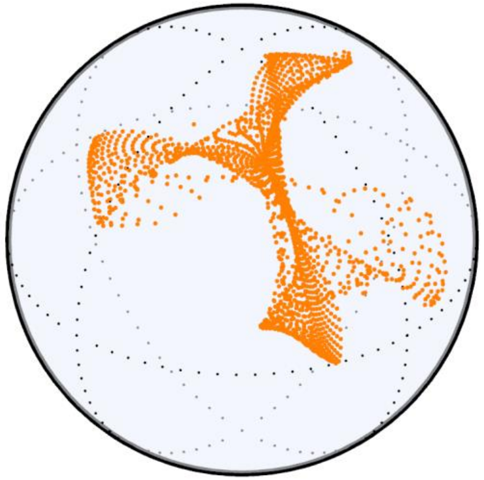
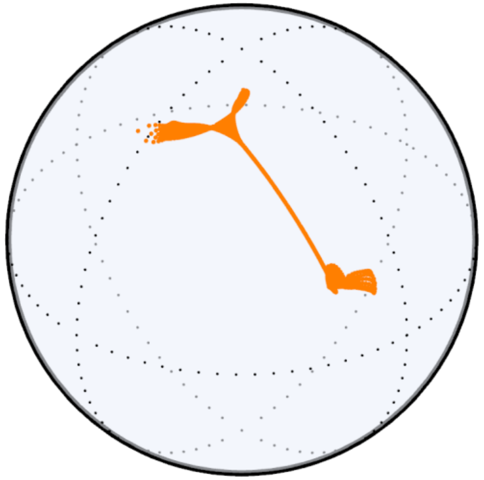

Principal curvature lines

The **straightening effect** on one family of principal curvature lines also confirms the increase of developability.

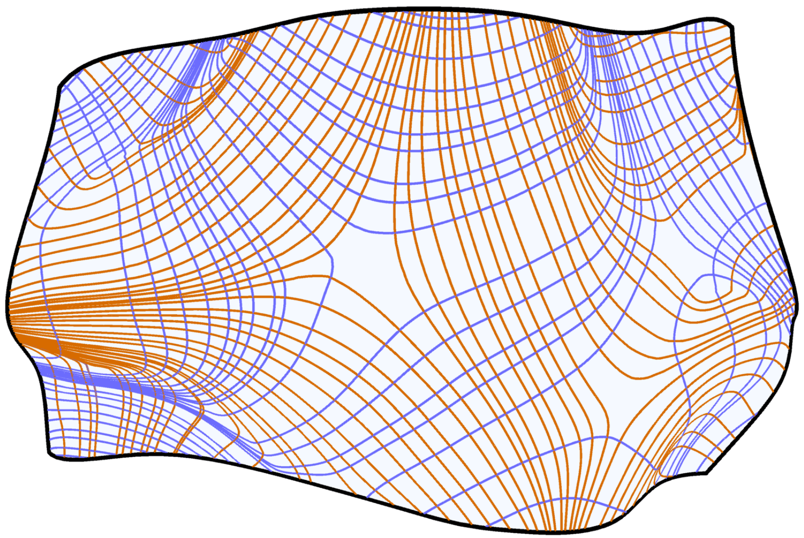

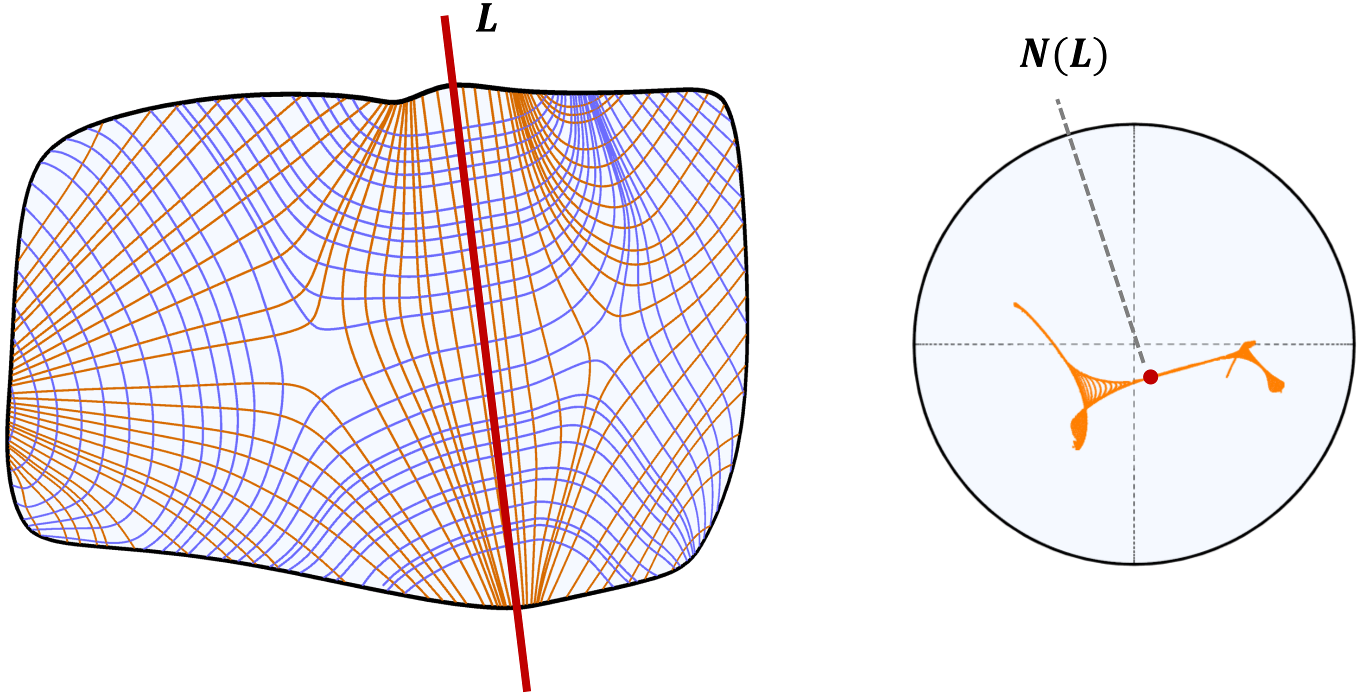

Gaussian curvature

The **Gaussian curvature** is zero at every point of a developable surface.

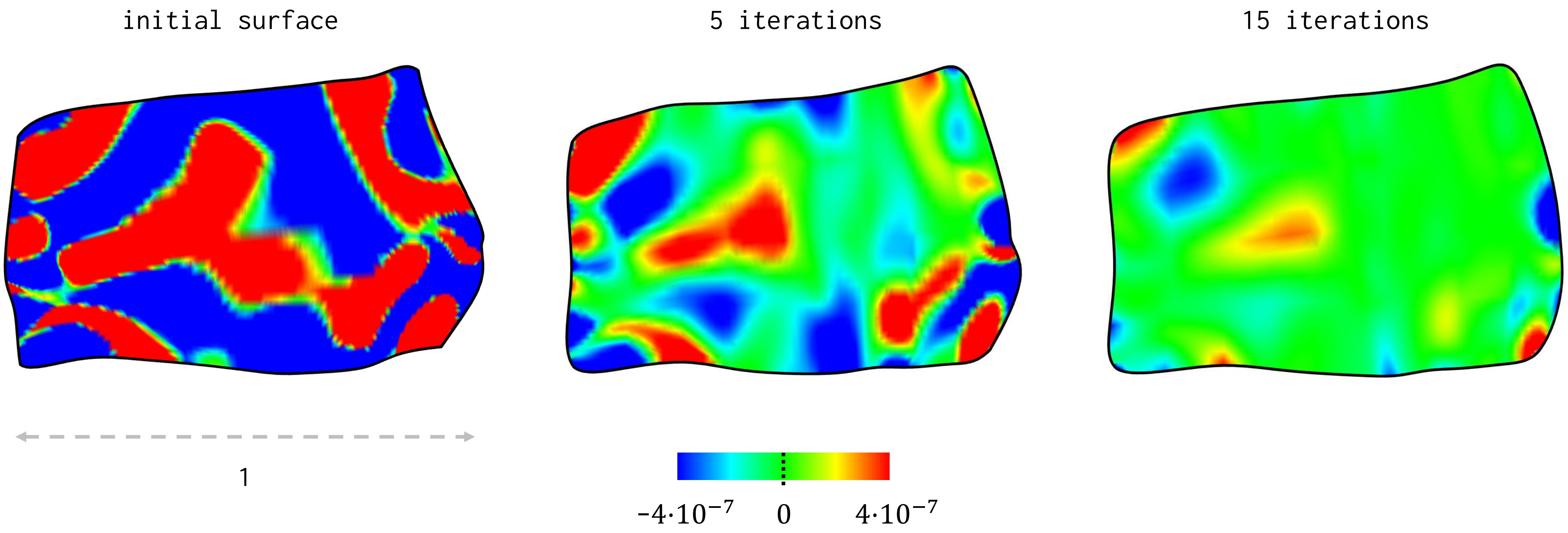

Paneling

with nearly developables

Konstantinos Gavriil

Methodology

sample points $\mathbf{p}_i$

group $\mathbf{p}_i$ to P_j

compute normals $\mathbf{n}_i$

optimize for planarity of $\mathbf{n}_i$ per P_j

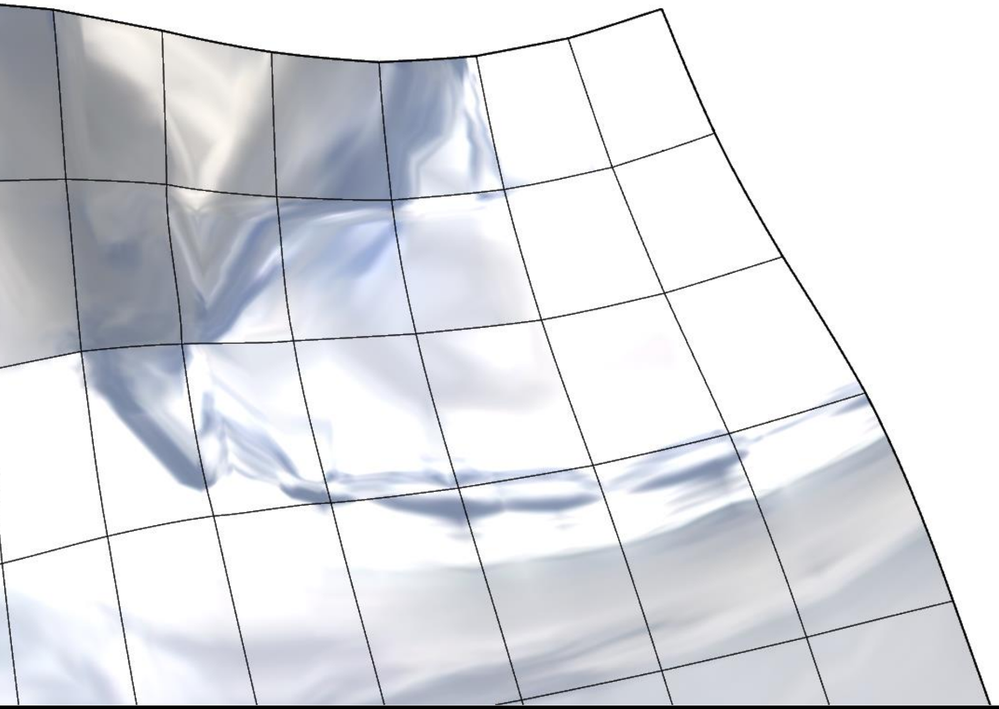

Methodology

sample points $\mathbf{p}_i$

group $\mathbf{p}_i$ to P_j

compute normals $\mathbf{n}_i$

optimize for planarity of $\mathbf{n}_i$ per P_j

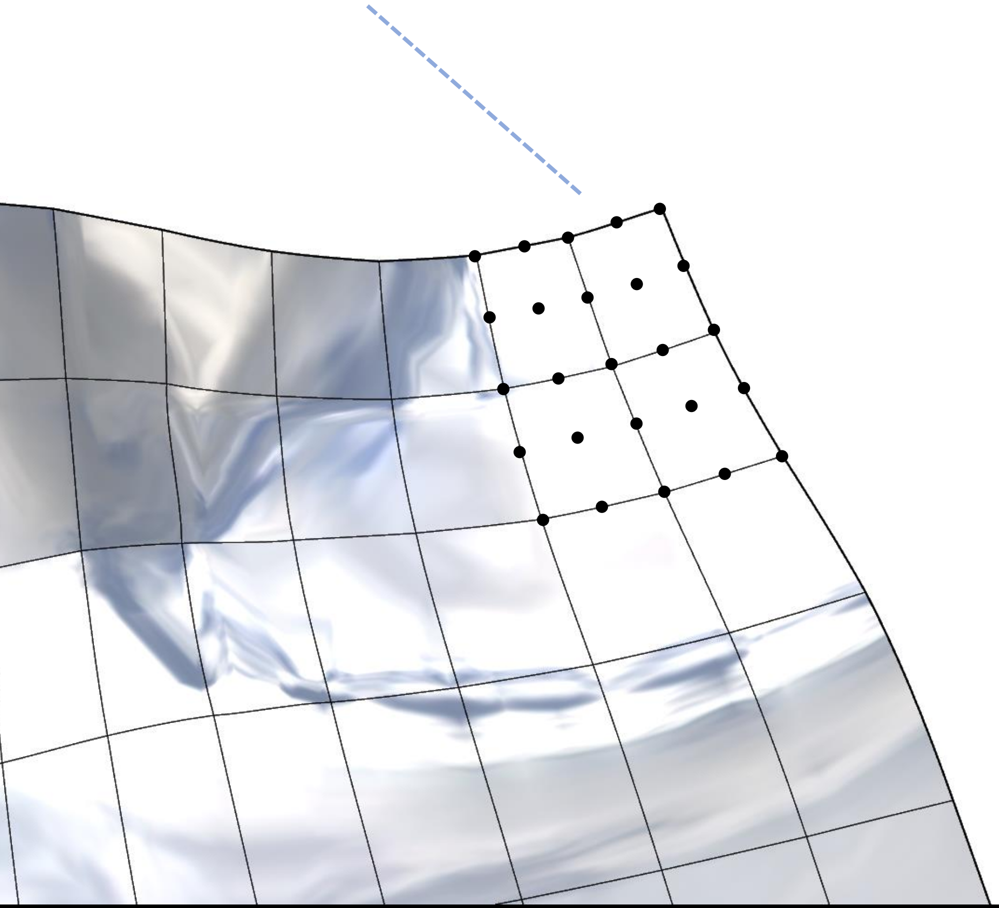

Methodology

sample points $\mathbf{p}_i$

group $\mathbf{p}_i$ to P_j

compute normals $\mathbf{n}_i$

optimize for planarity of $\mathbf{n}_i$ per P_j

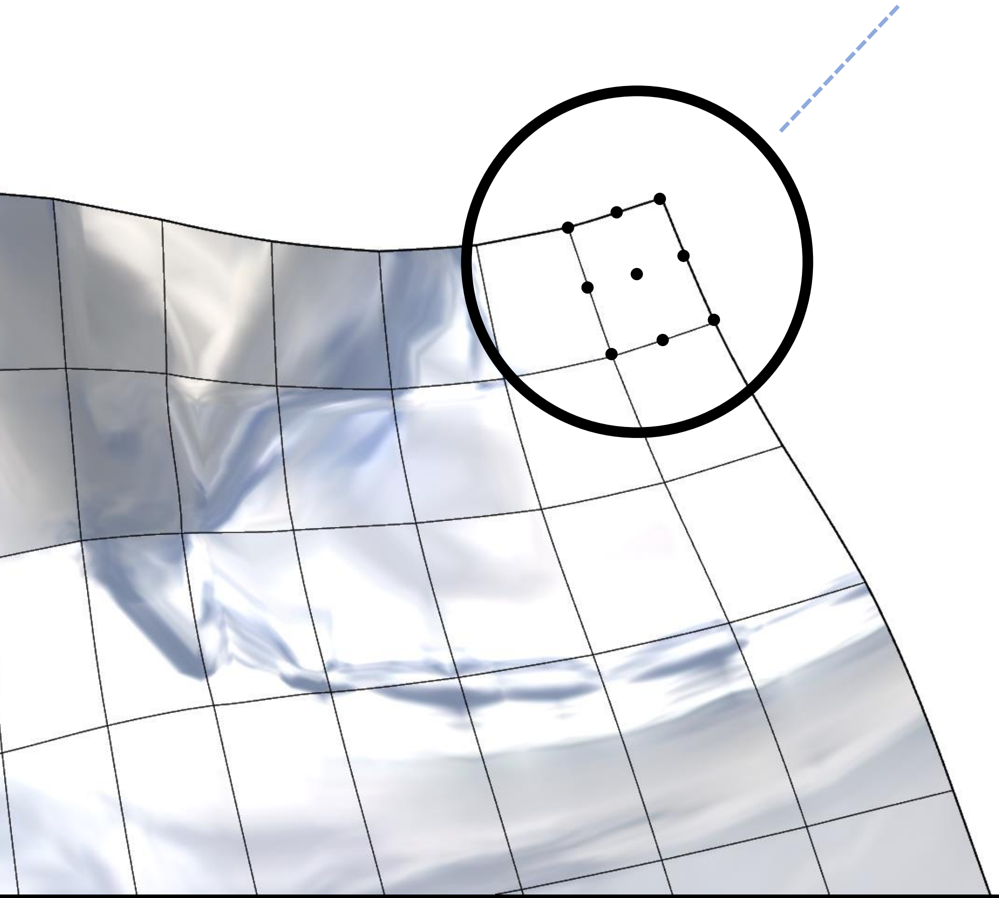

Methodology

sample points $\mathbf{p}_i$

group $\mathbf{p}_i$ to P_j

compute normals $\mathbf{n}_i$

optimize for planarity of $\mathbf{n}_i$ per P_j

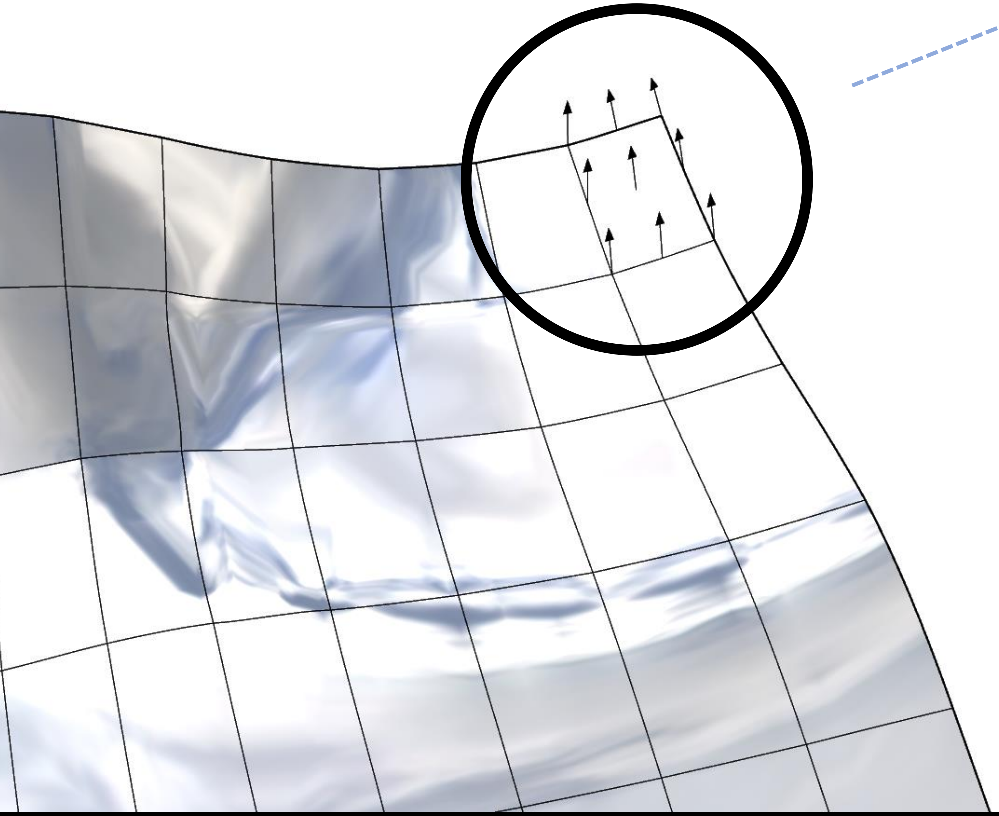

Methodology

sample points $\mathbf{p}_i$

group $\mathbf{p}_i$ to P_j

compute normals $\mathbf{n}_i$

optimize for planarity of $\mathbf{n}_i$ per P_j

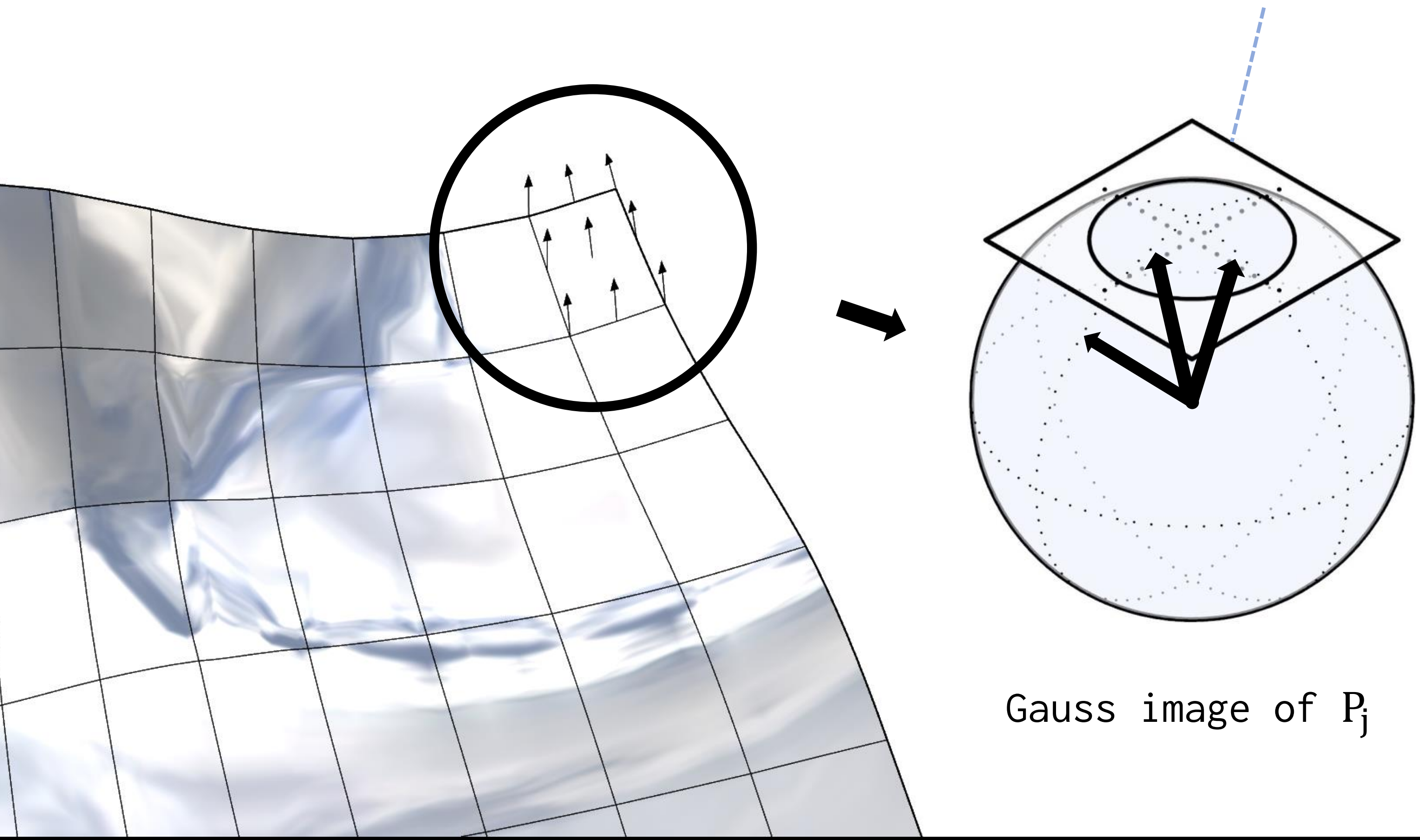

Gauss image of P_j

Methodology

sample points $\mathbf{p}_i$ group $\mathbf{p}_i$ to P_j compute normals $\mathbf{n}_i$ optimize for planarity of $\mathbf{n}_i$ per P_j

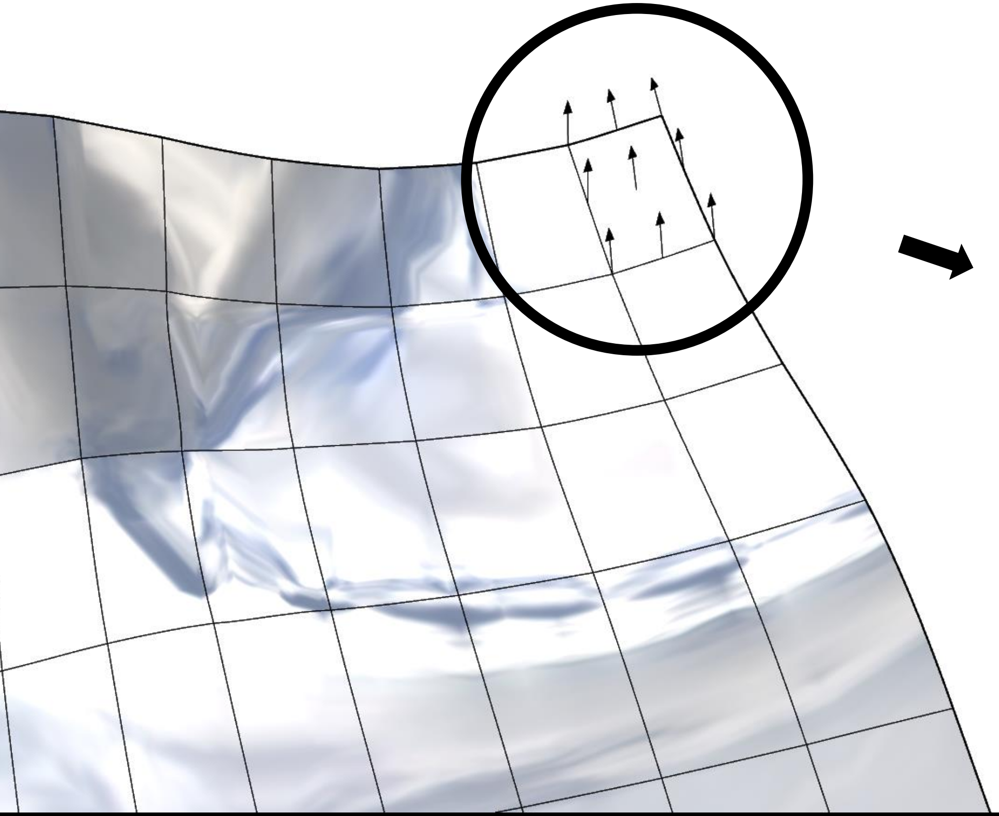

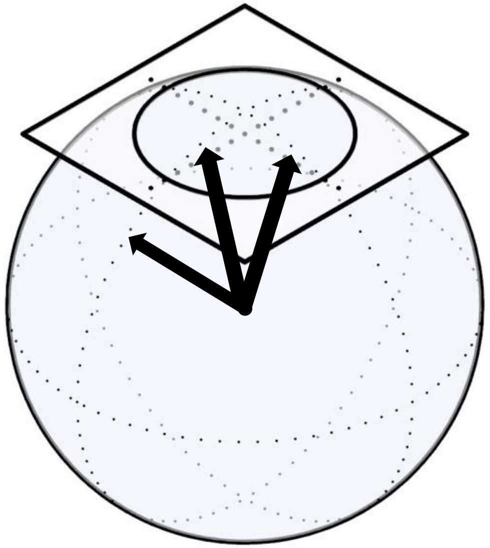

Gauss image of P_j

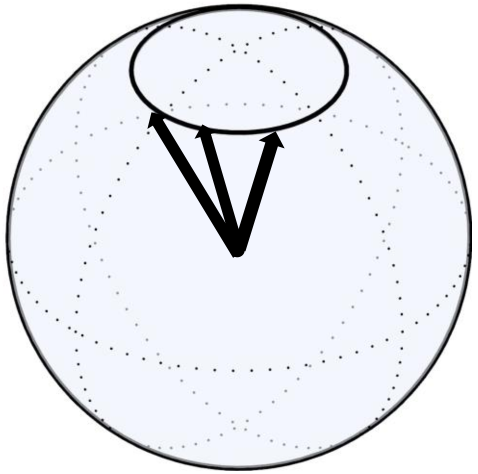

Panelization examples

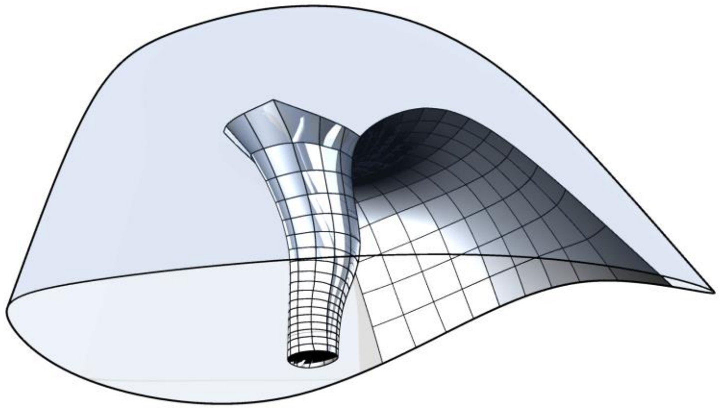

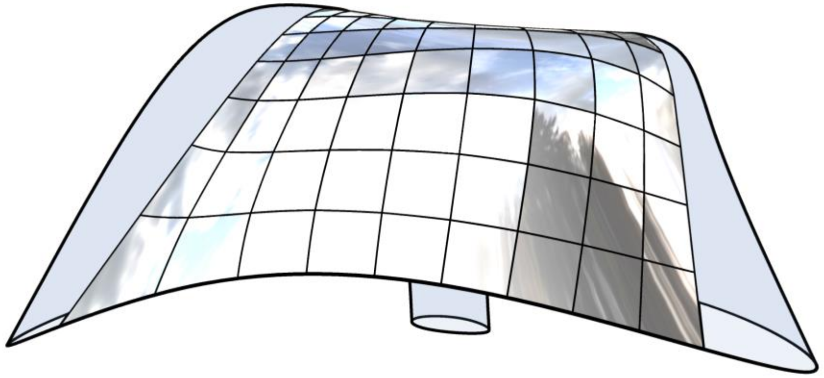

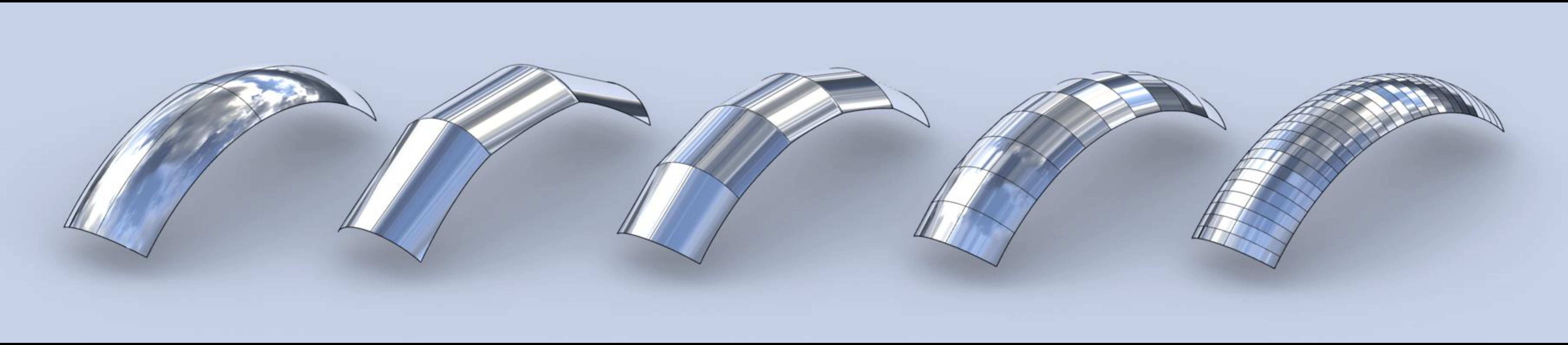

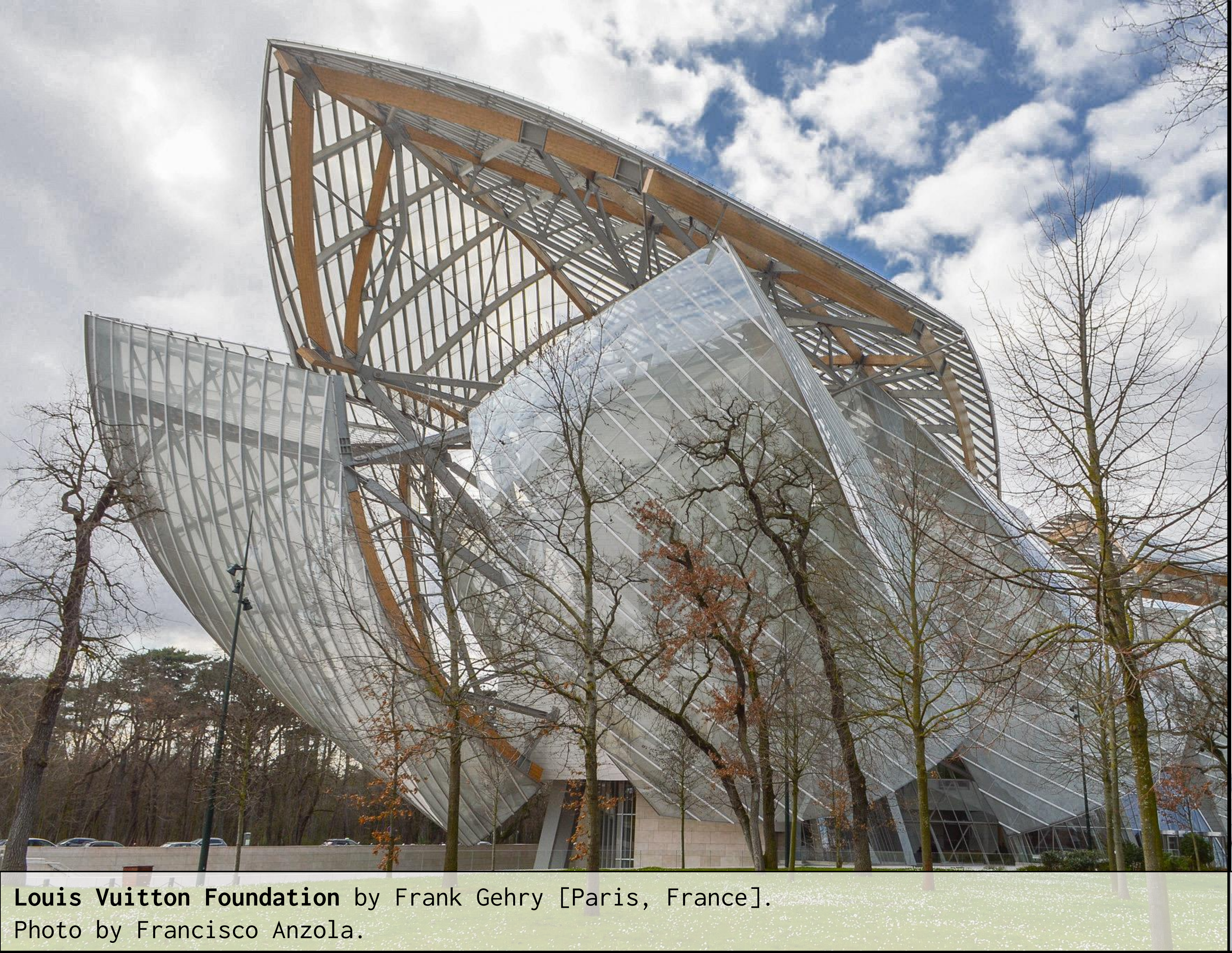

Louis Vuitton Foundation by Frank Gehry [Paris, France].
Photo by Francisco Anzola.

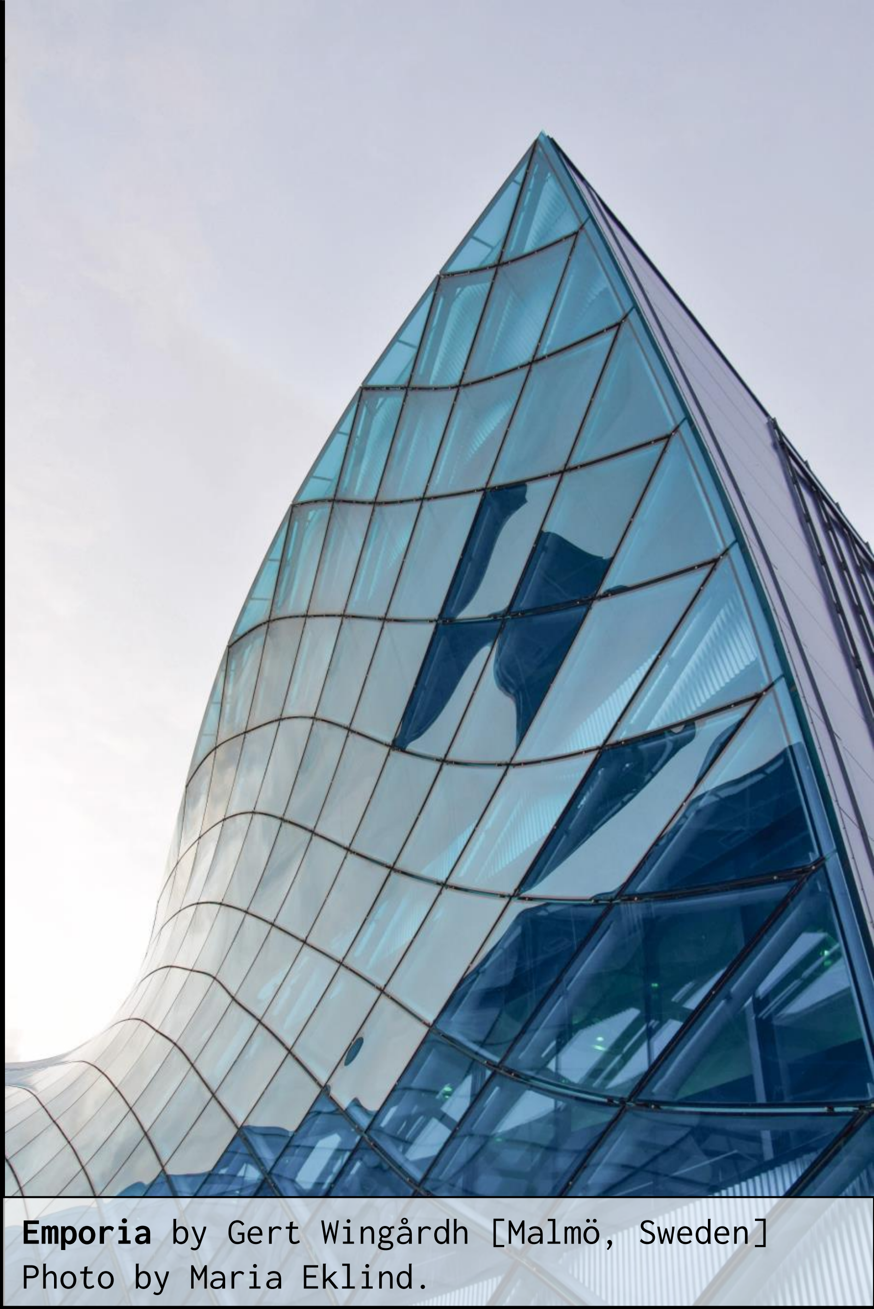

Emporia by Gert Wingårdh [Malmö, Sweden]
Photo by Maria Eklind.

Hot bending

Roller bending & **Static bending**

- High energy requirements.
- High transportation costs.
- Poor optical quality (roller bending).
- Multiple molds (static bending).
  High cost and material waste.

Cold bending

- Bend flat panel to frame with clamps/presses.
- Fix with mechanical fixings or structural adhesives.

- Low-cost & energy-efficient alternative.
  - No need for furnaces or molds.
  - Transportation of flat panels.

- Constrained design space.

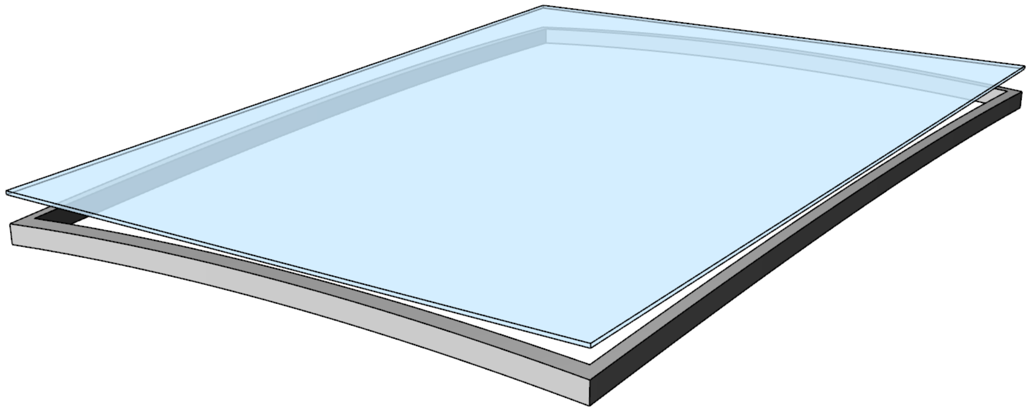

Cold bending

- Bend flat panel to frame with clamps/presses.
- Fix with mechanical fixings or structural adhesives.
- Low-cost & energy-efficient alternative.
  - No need for furnaces or molds.
  - Transportation of flat panels.
- Constrained design space.

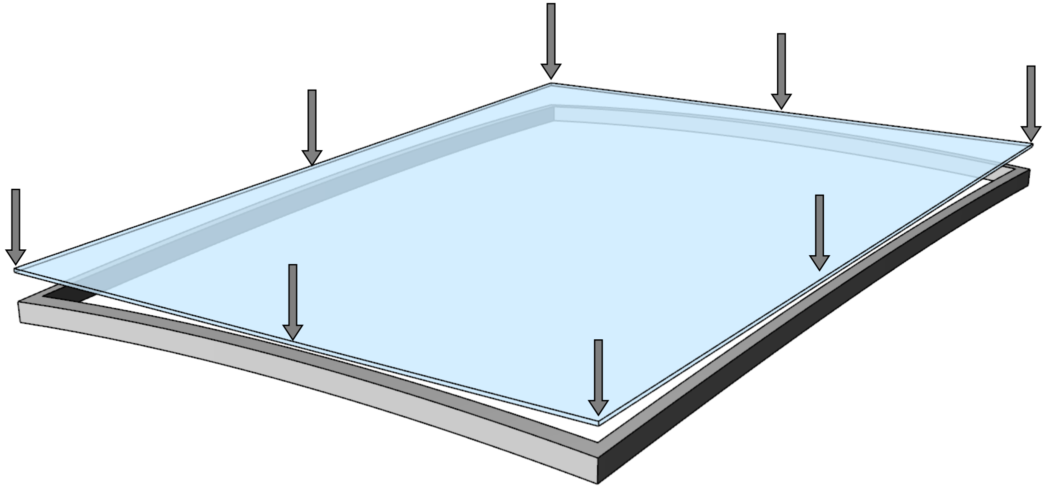

Cold bending

- Bend flat panel to frame with clamps/presses.
- Fix with mechanical fixings or structural adhesives.

- Low-cost & energy-efficient alternative.
  - No need for furnaces or molds.
  - Transportation of flat panels.

- Constrained design space.

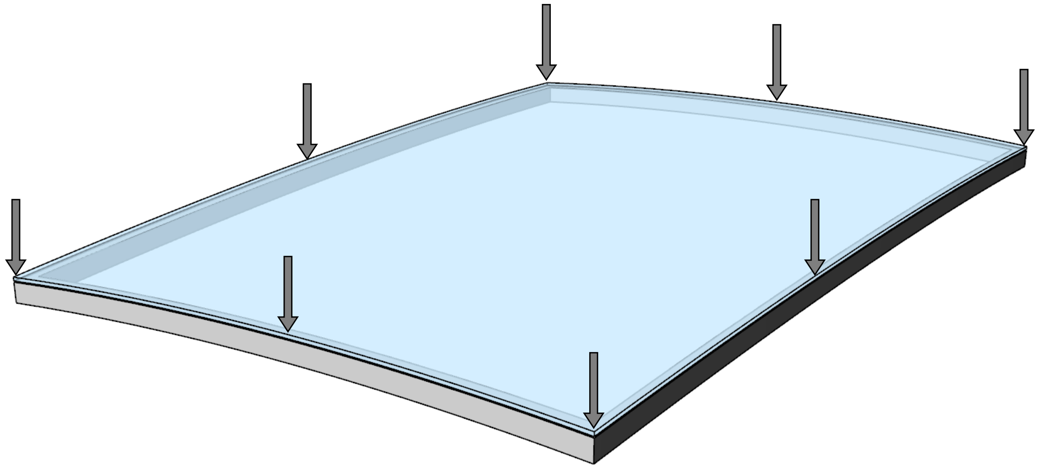

Cold bending

- Bend flat panel to frame with clamps/presses.
- Fix with mechanical fixings or structural adhesives.

- Low-cost & energy-efficient alternative.
    - No need for furnaces or molds.
    - Transportation of flat panels.

- Constrained design space.

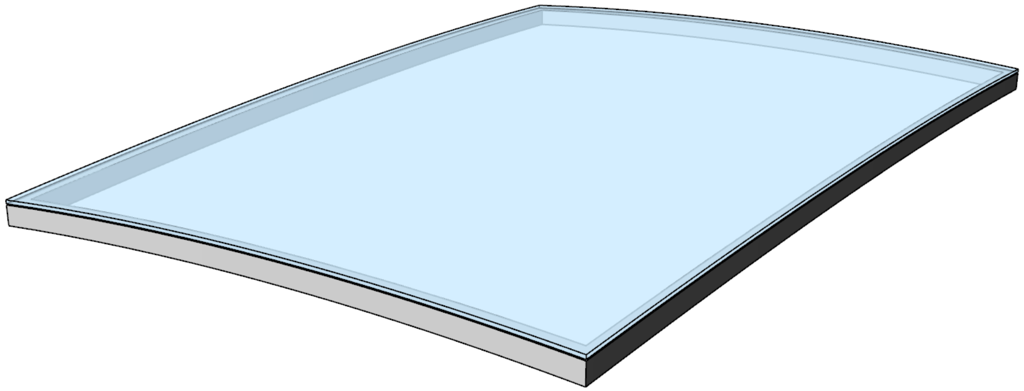

Cold bending

- Bend flat panel to frame with clamps/presses.
- Fix with mechanical fixings or structural adhesives.

- Low-cost & energy-efficient alternative.
  - No need for furnaces or molds.
  - Transportation of flat panels.

- Constrained design space.

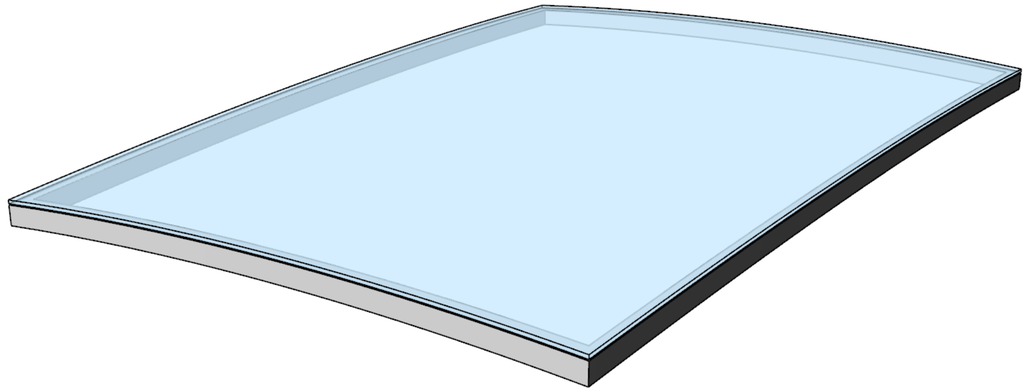

Cold bending

- Bend flat panel to frame with clamps/presses.
- Fix with mechanical fixings or structural adhesives.

- Low-cost & energy-efficient alternative.
  - No need for furnaces or molds.
  - Transportation of flat panels.

- Constrained design space.

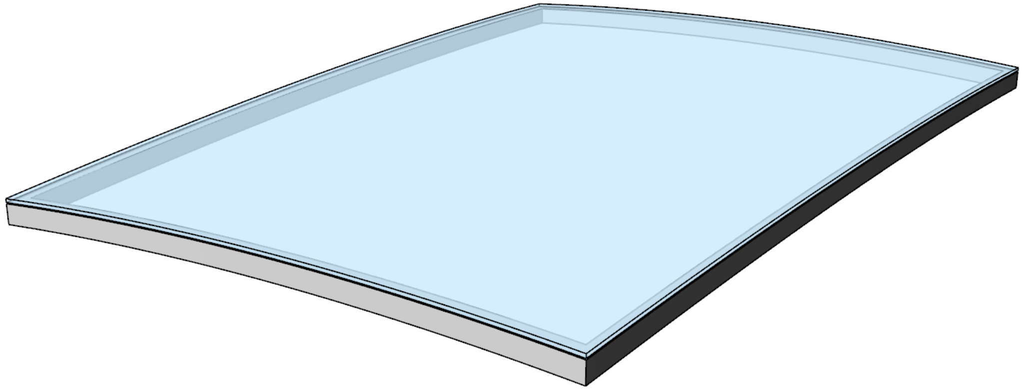

Method overview

- Build dataset of multiple simulations of cold bent glass panels.
- Fit regression model to the dataset.
- Use the model to interactively navigate the design space and provide immediate feedback on cold bent glass panelizations.

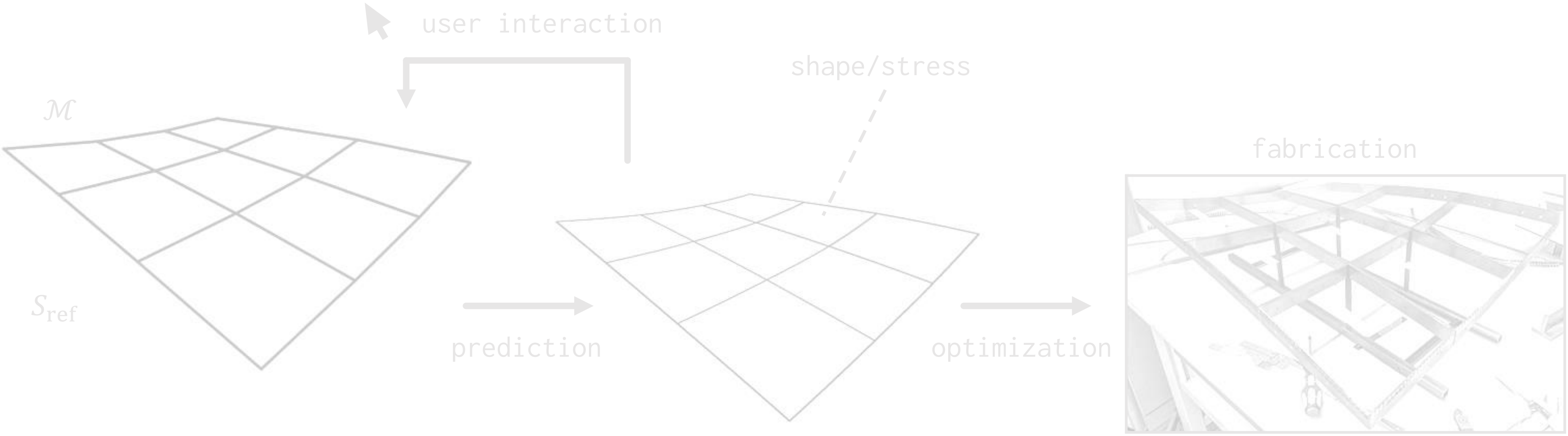

Method overview

- Build dataset of multiple simulations of cold bent glass panels.
- Fit regression model to the dataset.
- Use the model to interactively navigate the design space and provide immediate feedback on cold bent glass panelizations.

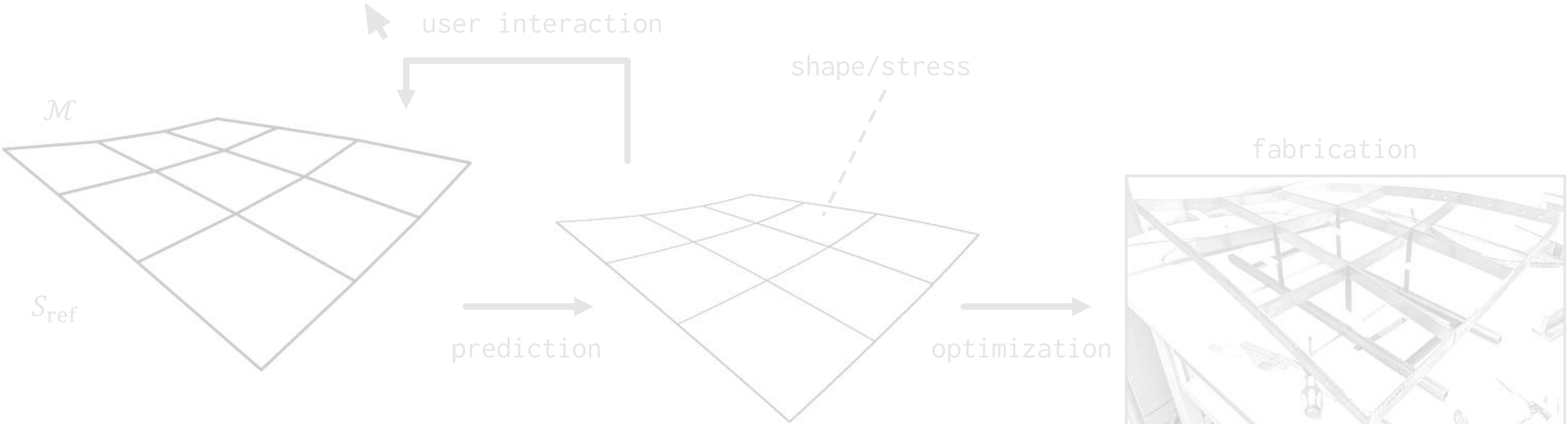

Method overview

- Build dataset of multiple simulations of cold bent glass panels.
- Fit regression model to the dataset.
- Use the model to interactively navigate the design space and provide immediate feedback on cold bent glass panelizations.

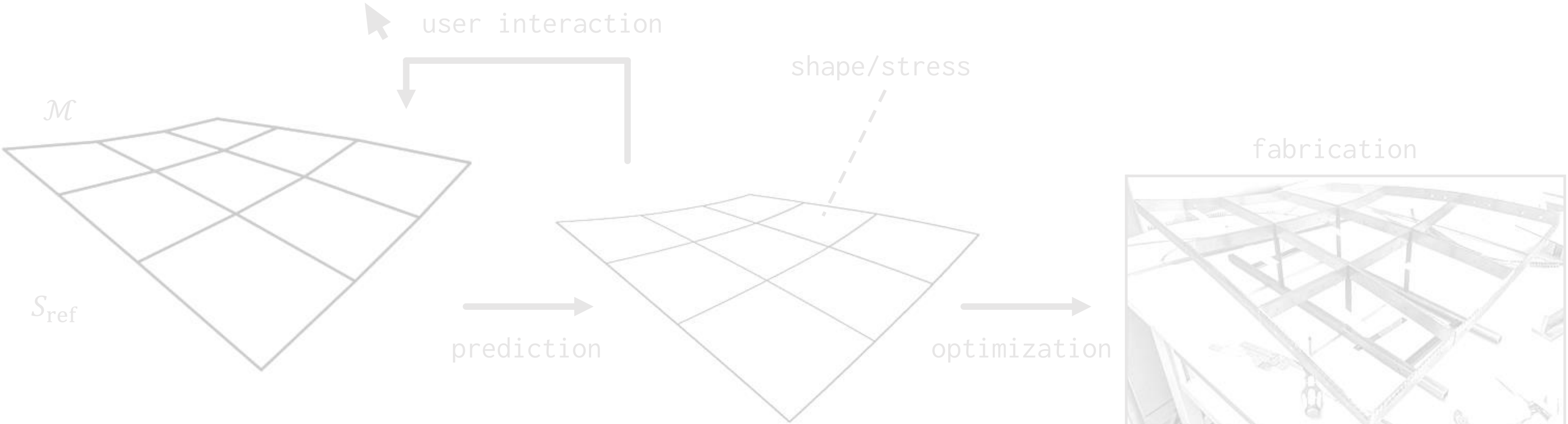

Method overview

- Build dataset of multiple simulations of cold bent glass panels.
- Fit regression model to the dataset.
- Use the model to interactively navigate the design space and provide immediate feedback on cold bent glass panelizations.

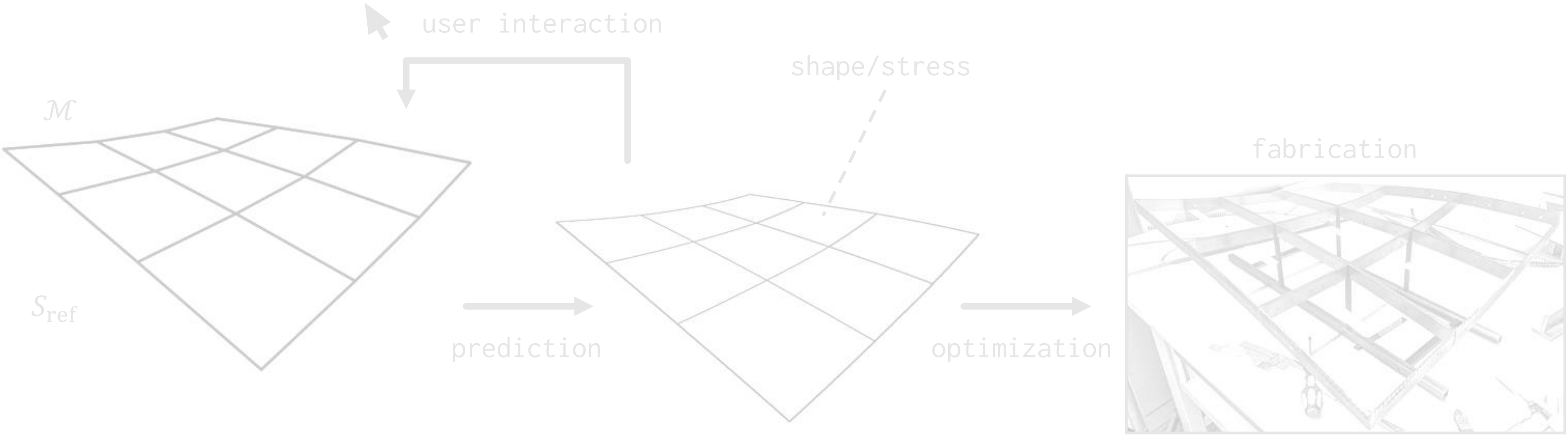

Method overview

- Build dataset of multiple simulations of cold bent glass panels.
- Fit regression model to the dataset.
- Use the model to interactively navigate the design space and provide immediate feedback on cold bent glass panelizations.

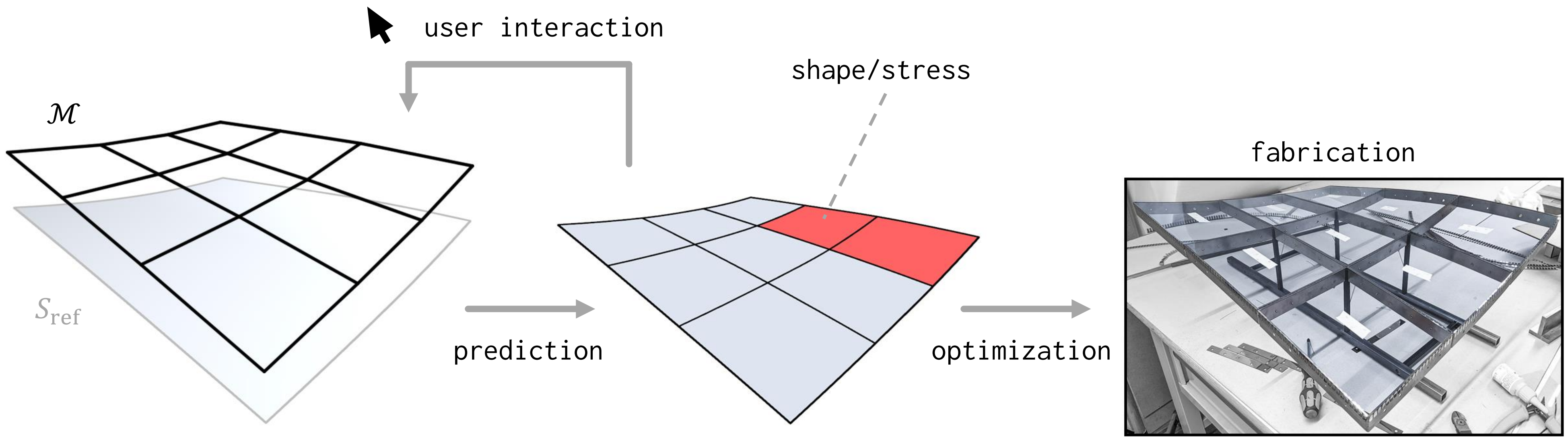

Geometry representation

of cold bent glass panelizations

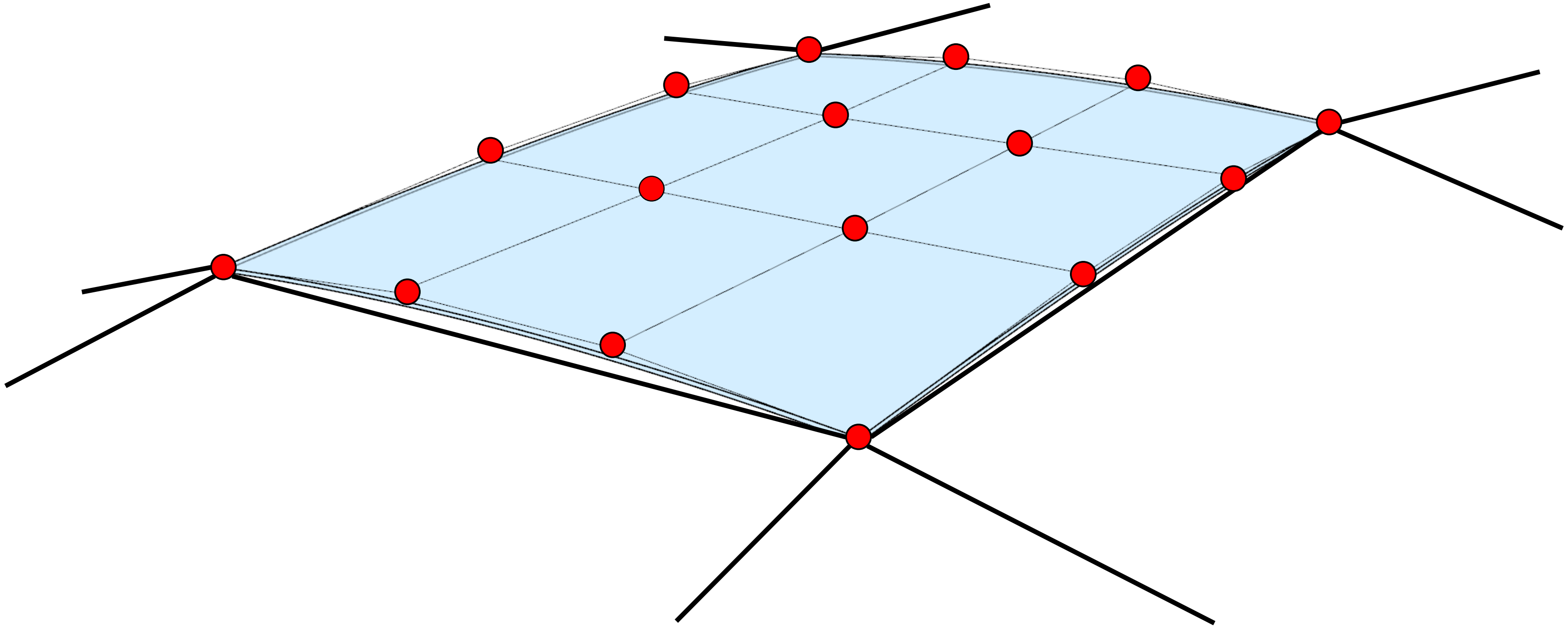

Optimized geometric Hermite curve [Yong & Cheng, 2004]

- Planar cubic curve $C\colon [0,1] \to \mathbb{R}^3$ of minimum strain energy $\int_0^1 [C''(t)]^2\,dt$.
- Defined by the two endpoints $\mathbf{v}_1$, $\mathbf{v}_2 \in \mathbb{R}^3$ and two tangent directions $\mathbf{t}_1$, $\mathbf{t}_2 \in \mathbb{R}^3$.
- Inner control points $\mathbf{v}_i + m_i \mathbf{t}_i$, $i = 1,2$ are given by

$$m_1 = \frac{(\mathbf{v}_2 - \mathbf{v}_1)\cdot[2\mathbf{t}_1 - (\mathbf{t}_1\cdot\mathbf{t}_2)\mathbf{t}_2]}{4 - (\mathbf{t}_1\cdot\mathbf{t}_2)^2},$$

and m_2 by switching indices $1 \leftrightarrow 2$.

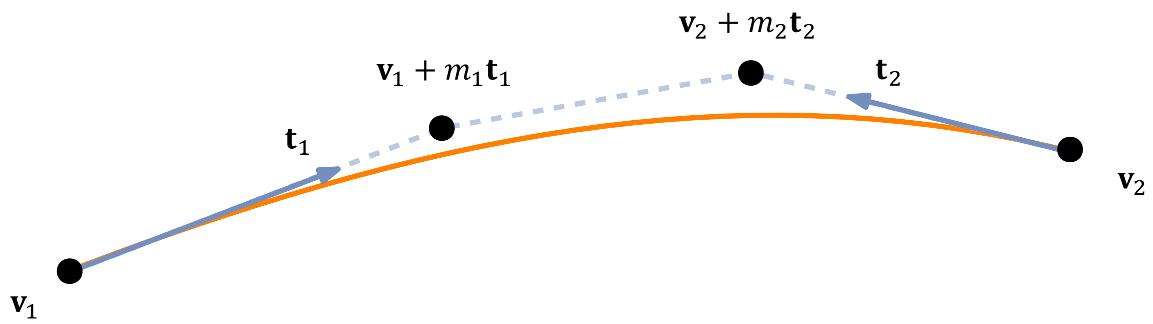

Optimized geometric Hermite curve [Yong & Cheng, 2004]

- Planar cubic curve $C: [0,1] \to \mathbb{R}^3$ of minimum strain energy $\int_0^1 [C''(t)]^2\, dt$.
- Defined by the two endpoints $\mathbf{v}_1$, $\mathbf{v}_2 \in \mathbb{R}^3$ and two tangent directions $\mathbf{t}_1$, $\mathbf{t}_2 \in \mathbb{R}^3$.
- Inner control points $\mathbf{v}_i + m_i \mathbf{t}_i$, $i = 1{,}2$ are given by

$$m_1 = \frac{(\mathbf{v}_2 - \mathbf{v}_1) \cdot [2\mathbf{t}_1 - (\mathbf{t}_1 \cdot \mathbf{t}_2)\mathbf{t}_2]}{4 - (\mathbf{t}_1 \cdot \mathbf{t}_2)^2},$$

and m_2 by switching indices $1 \leftrightarrow 2$.

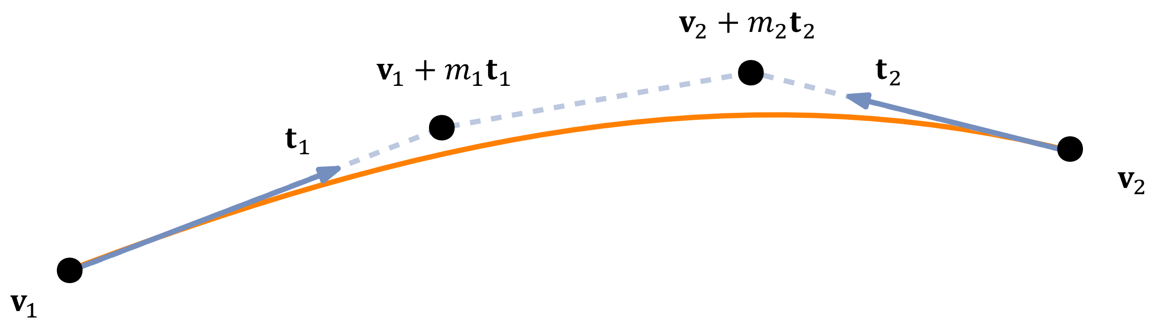

Optimized geometric Hermite curve [Yong & Cheng, 2004]

- Planar cubic curve $C: [0,1] \to \mathbb{R}^3$ of minimum strain energy $\int_0^1 [C''(t)]^2\, dt$.
- Defined by the two endpoints $\mathbf{v}_1,\ \mathbf{v}_2 \in \mathbb{R}^3$ and two tangent directions $\mathbf{t}_1,\ \mathbf{t}_2 \in \mathbb{R}^3$.
- Inner control points $\mathbf{v}_i + m_i \mathbf{t}_i,\ i = 1,2$ are given by

$$m_1 = \frac{(\mathbf{v}_2 - \mathbf{v}_1) \cdot [2\mathbf{t}_1 - (\mathbf{t}_1 \cdot \mathbf{t}_2)\mathbf{t}_2]}{4 - (\mathbf{t}_1 \cdot \mathbf{t}_2)^2},$$

and m_2 by switching indices $1 \leftrightarrow 2$.

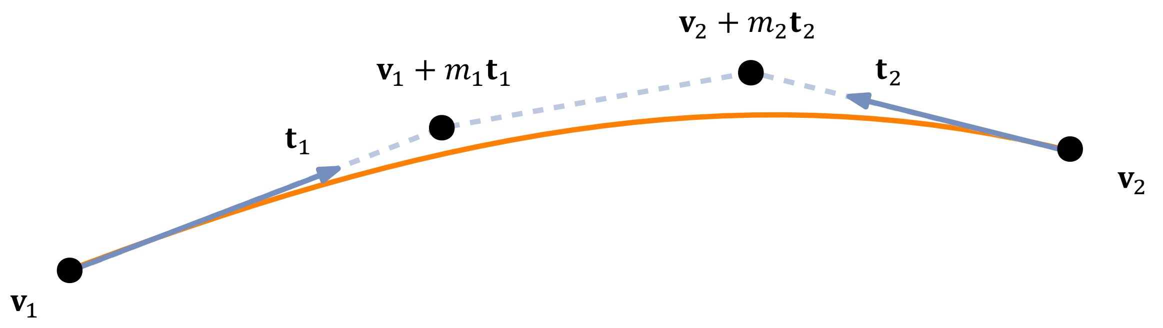

Edge curve C_e

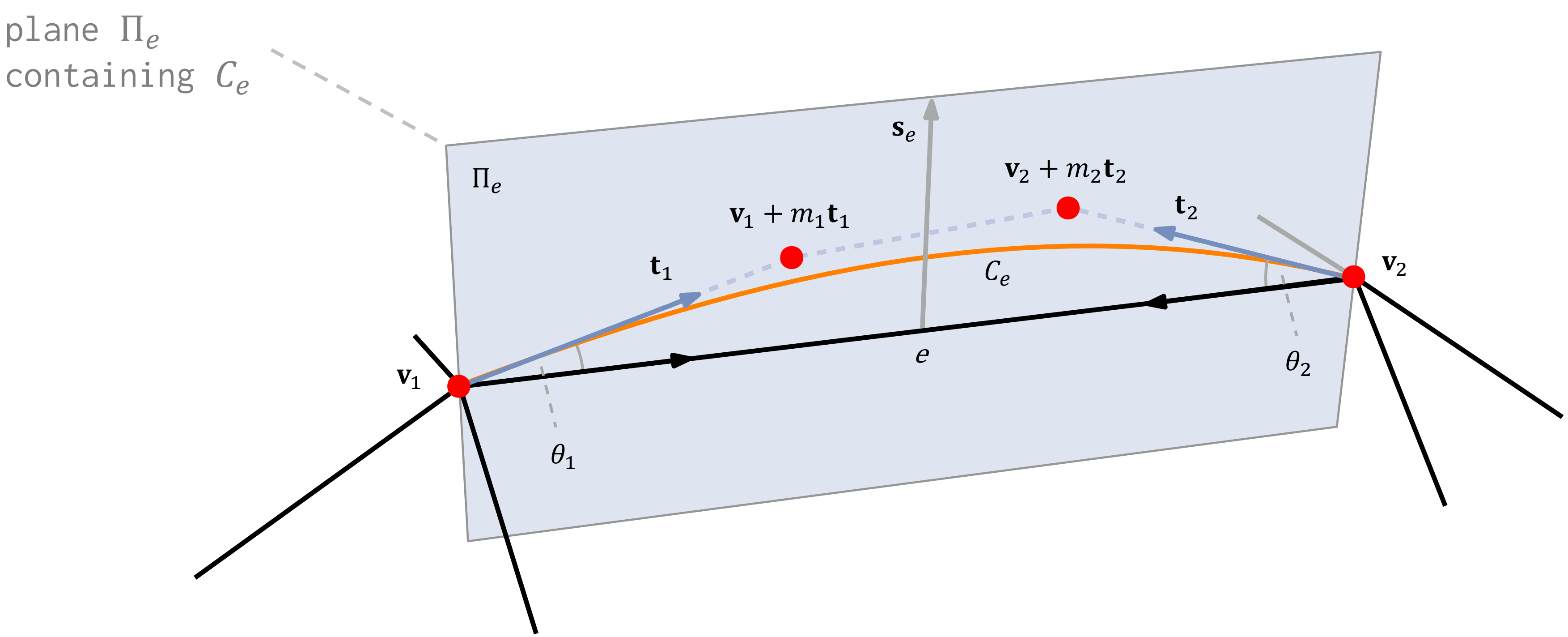

Panel boundary

$\mathbf{p} \in \mathbb{R}^{18}$

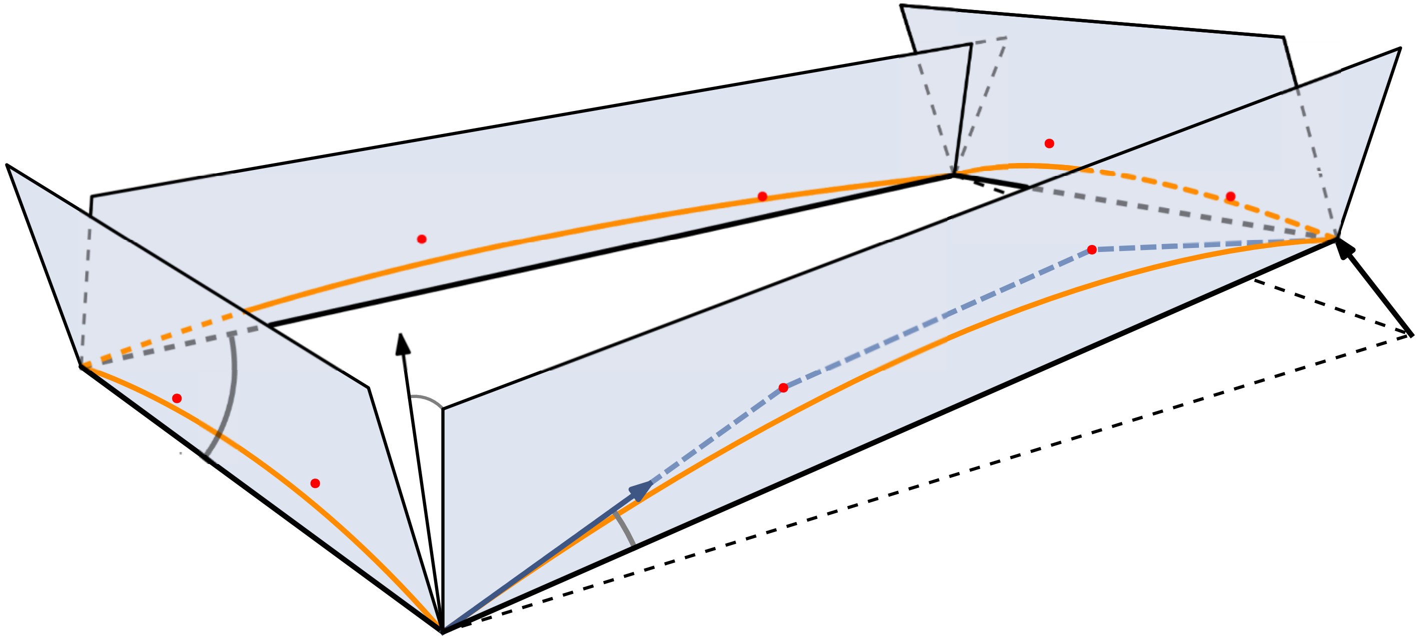

Simulation

Minimal energy panels

Simulation

Continuous formulation.

- Planar mid-surface orthogonally extruded by $h/2$ in both directions.
  [Gingold et al., 2004]

- Green's stress tensor.

  $$\mathbf{E}(\mathbf{x},\bar{\mathbf{x}},z) = \bar{\mathbf{E}}(\mathbf{x},\bar{\mathbf{x}}) + z\hat{\mathbf{E}}(\mathbf{x},\bar{\mathbf{x}})$$

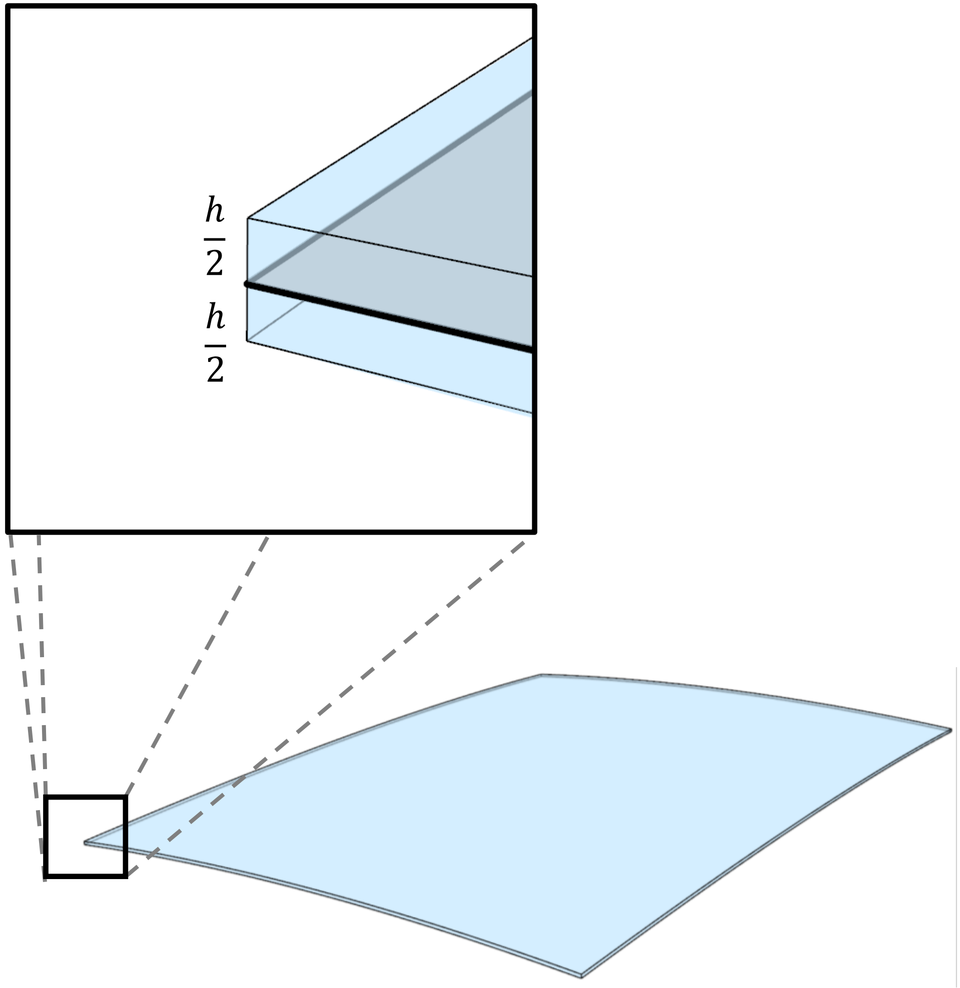

Simulation

Continuous formulation.

- Planar mid-surface orthogonally extruded by $h/2$ in both directions.
  [Gingold et al., 2004]

- Green's stress tensor.

  $$\mathbf{E}(\mathbf{x}, \bar{\mathbf{x}}, z) = \bar{\mathbf{E}}(\mathbf{x}, \bar{\mathbf{x}}) + z\hat{\mathbf{E}}(\mathbf{x}, \bar{\mathbf{x}})$$

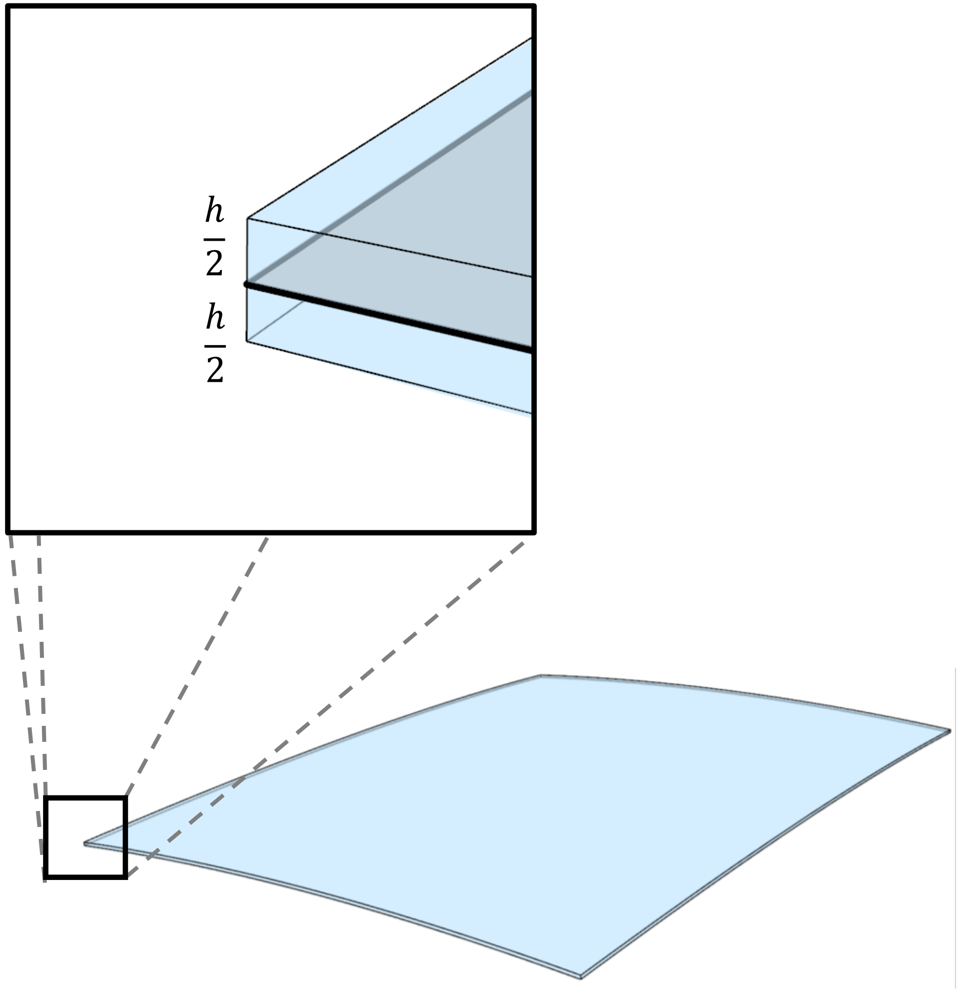

Simulation

Discrete formulation.

- **Membrane energy density.**
  - Triangle-based piecewise constant strains.
  - Integrated over panel thickness with the Saint Venant-Kirchhoff model.
- **Bending energy density.**
  - Triangle-based discrete approximation of the shape operator. [Grinspun et al., 2006]
  - Integrated over panel thickness using Koiter’s shell model.

[Pfaff et al., 2014]

[Grinspun et al., 2006]

Simulation

Discrete formulation.

- **Membrane energy density.**
  - Triangle-based piecewise constant strains.
  - Integrated over panel thickness with the Saint Venant-Kirchhoff model.

[Pfaff et al., 2014]

- **Bending energy density.**
  - Triangle-based discrete approximation of the shape operator. [Grinspun et al., 2006]
  - Integrated over panel thickness using Koiter’s shell model.

[Grinspun et al., 2006]

Simulation

Discrete formulation.

- **Membrane energy density.**
  - Triangle-based piecewise constant strains.
  - Integrated over panel thickness with the Saint Venant-Kirchhoff model.
- **Bending energy density.**
  - Triangle-based discrete approximation of the shape operator. [Grinspun et al., 2006]
  - Integrated over panel thickness using Koiter's shell model.

[Pfaff et al., 2014]

[Grinspun et al., 2006]

Simulation

Discrete formulation.

- **Membrane energy density.**
  - Triangle-based piecewise constant strains.
  - Integrated over panel thickness with the Saint Venant-Kirchhoff model.
- **Bending energy density.**
  - Triangle-based discrete approximation of the shape operator. [Grinspun et al., 2006]
  - Integrated over panel thickness using Koiter's shell model.

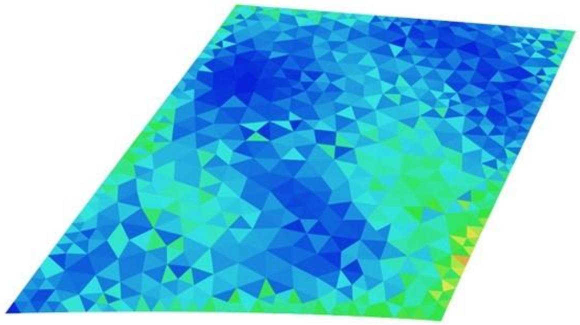

[Pfaff et al., 2014]

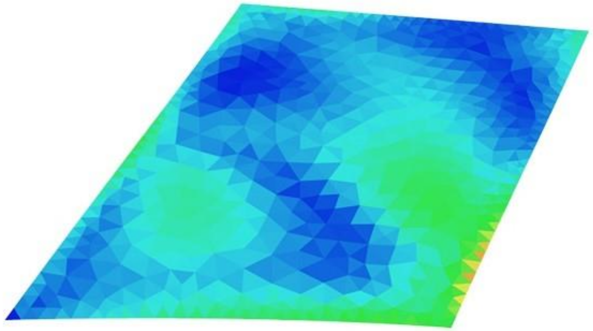

[Grinspun et al., 2006]

Simulation

Minimal energy panels. Minimize total strain energy of the panel given C^0 boundary conditions.

Initialization.

- Zero-twist Hermite interpolant of the boundary.
- Delaunay triangulation of the interior given number of boundary edges.
- Minimum distortion conformal flattening of the mesh.

Minimization.

- Both deformed and undeformed configurations are variable.
- Internal nodes of rest configuration are computed through Laplacian smoothing of boundary nodes.

Simulation

Minimal energy panels. Minimize total strain energy of the panel given C^0 boundary conditions.

Initialization.

- Zero-twist Hermite interpolant of the boundary.
- Delaunay triangulation of the interior given number of boundary edges.
- Minimum distortion conformal flattening of the mesh.

Minimization.

- Both deformed and undeformed configurations are variable.
- Internal nodes of rest configuration are computed through Laplacian smoothing of boundary nodes.

Simulation

Minimal energy panels. Minimize total strain energy of the panel given C^0 boundary conditions.

Initialization.

- Zero-twist Hermite interpolant of the boundary.
- Delaunay triangulation of the interior given number of boundary edges.
- Minimum distortion conformal flattening of the mesh.

Minimization.

- Both deformed and undeformed configurations are variable.
- Internal nodes of rest configuration are computed through Laplacian smoothing of boundary nodes.

Simulation

Failure criterion.

- Compute principal stress as the maximum absolute singular value of the first Piola-Kirchhoff stress tensor for each element at offset $\pm h/2$.
- Maximal stress is defined as the L_{12}-norm of the principal stresses.

Multiple stable equilibria.

Simulation

Failure criterion.

- Compute principal stress as the maximum absolute singular value of the first Piola-Kirchhoff stress tensor for each element at offset $\pm h/2$.
- Maximal stress is defined as the L_{12}-norm of the principal stresses.

Multiple stable equilibria.

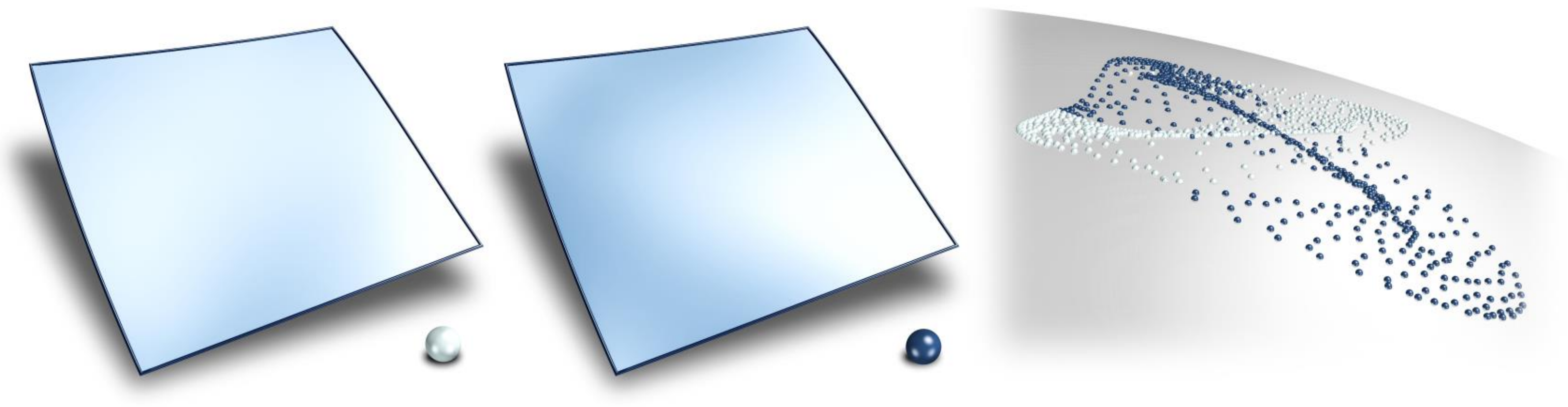

Data-driven model

Mixture density network

Model architecture

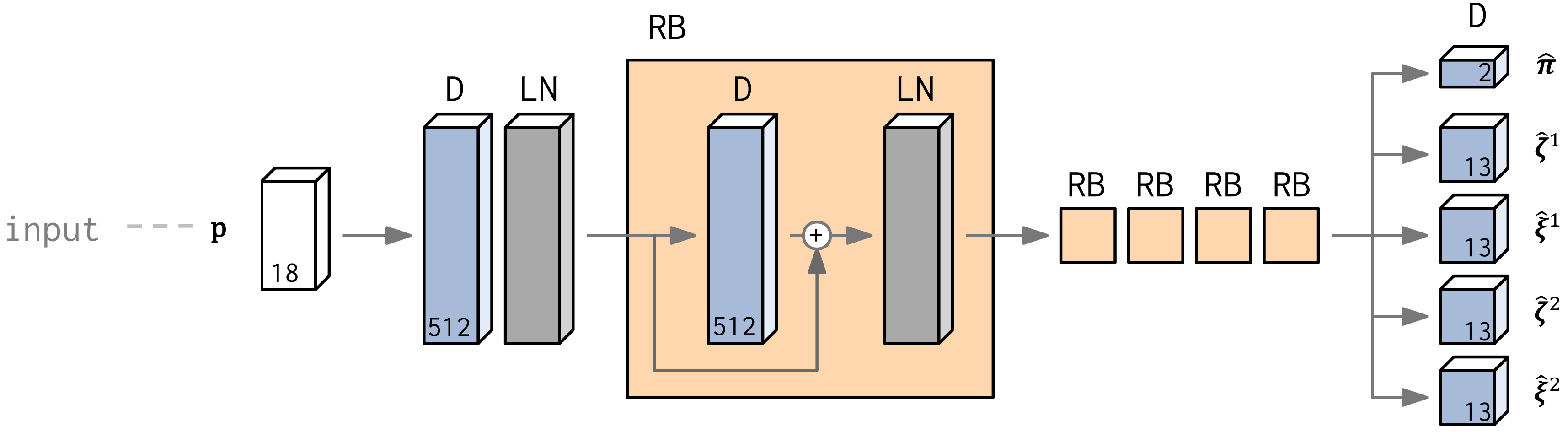

D: dense layer
LN: layer normalization
RB: residual block

Model architecture

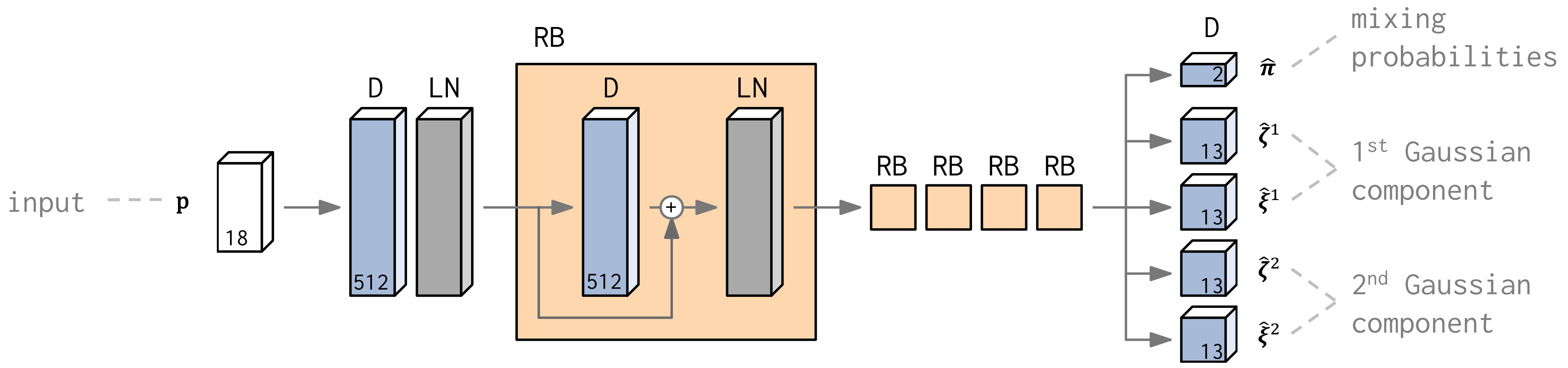

D: dense layer
LN: layer normalization
RB: residual block

Model architecture

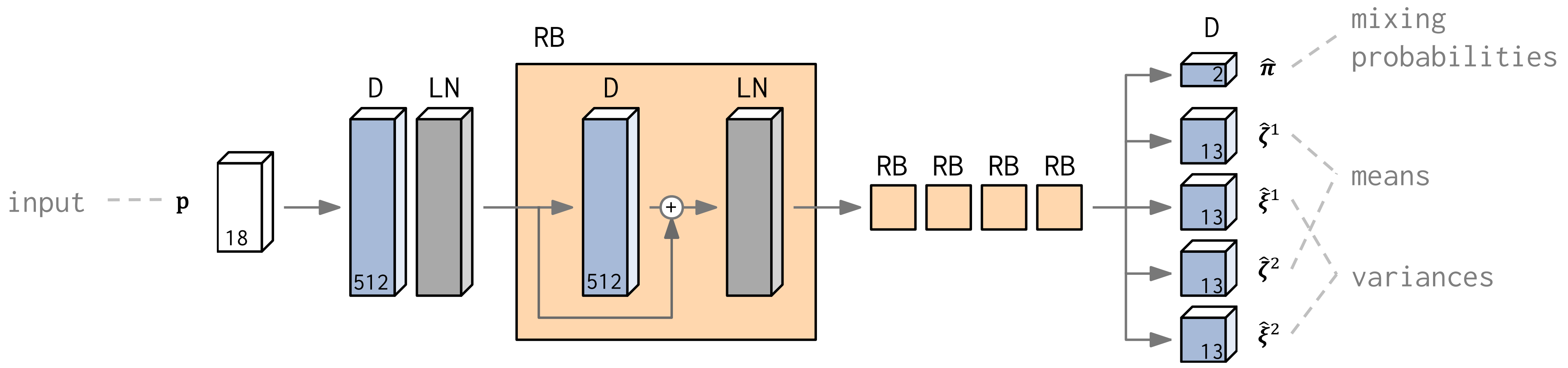

D: dense layer
LN: layer normalization
RB: residual block

Model output

$$\hat{\boldsymbol{\zeta}}^k = \left(\hat{\mathbf{S}}_{\mathbf{p}}^k ; \hat{\sigma}_{\mathbf{p}}^k\right)$$

$$\hat{\pi}^k$$

Model training

Minimize negative log-likelihood of the training set $\mathcal{T}$ under the Gaussian mixture model

$$\mathcal{L}(\mathcal{T};\mathbf{w}) = -\sum_{(\mathbf{p},\boldsymbol{\zeta})\in\mathcal{T}} \log\left\{\sum_{k=1}^{2} \hat{\pi}^k(\mathbf{p};\mathbf{w})\,\mathcal{N}\left(\boldsymbol{\zeta}|\hat{\boldsymbol{\zeta}}^k(\mathbf{p};\mathbf{w}),\hat{\boldsymbol{\xi}}^k(\mathbf{p};\mathbf{w})\right)\right\}$$

where

$\mathbf{p}$: (input) panel boundary

$\boldsymbol{\zeta}$: true output

$\mathbf{w}$: network weights

$\hat{\boldsymbol{\zeta}}^k$: mean of k^{th} component (output)

$\hat{\boldsymbol{\xi}}^k$: variance of k^{th} component

Model training

Best model determined by random sampling of hyperparameters:

- Stochastic gradient descent method **Adam** [Kingma & Ba, 2014].
- Learning rate of 1e-4.
- Batch size of 2048 samples.
- Early stopping with patience of 400 epochs.
- Validation set of 10%.

Training time on an NVIDIA TITAN X: ~20 hours (~30 seconds / epoch).

Interactive design

of cold bent glass panelizations

Interactive design

Cold bent glass panelization as an **optimization problem**.

$$\text{minimize } \mathcal{E} = w_\sigma \mathcal{E}_\sigma + w_\mathrm{s} \mathcal{E}_\mathrm{s} + w_\mathrm{f} \mathcal{E}_\mathrm{f} + w_\mathrm{p} \mathcal{E}_\mathrm{p} + w_\mathrm{c} \mathcal{E}_\mathrm{c}$$

$\mathcal{E}_\sigma$: panel stress

$\mathcal{E}_\mathrm{s}$: smoothness

$\mathcal{E}_\mathrm{f}$: mesh fairness

$\mathcal{E}_\mathrm{p}$: proximity to reference mesh

$\mathcal{E}_\mathrm{c}$: design space constraints

Panel stress $\mathcal{E}_\sigma$

$$\mathcal{E}_\sigma = \sum_{\mathbf{p}} \left(\hat{\sigma}_{\mathbf{p}} - \sigma_{\max} + u_{\mathbf{p}}^2\right)^2$$

- Penalize stress values exceeding maximum allowed. $\boxed{\hat{\sigma}_{\mathbf{p}} \leq \sigma_{\max}}$
- We use 65 MPa for $\sigma_{\max}$.

Panel stress $\mathcal{E}_{\sigma}$

[NHHQ, ZHA]

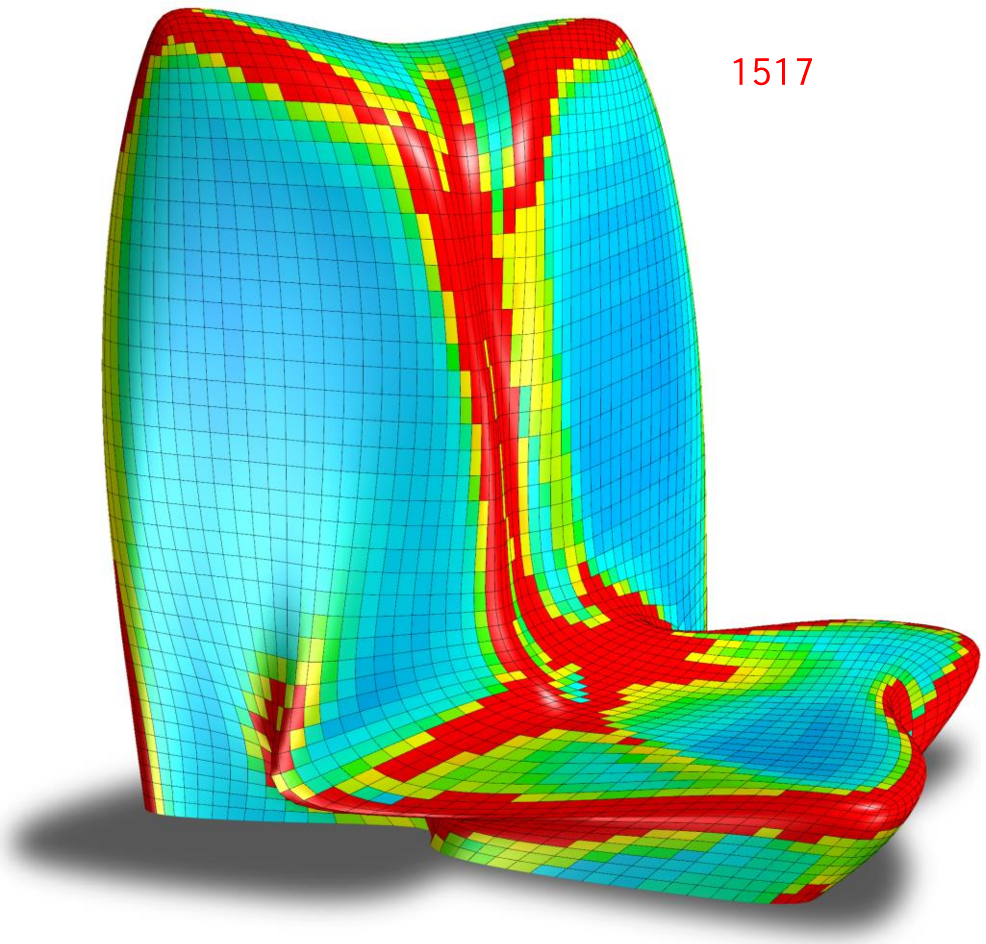

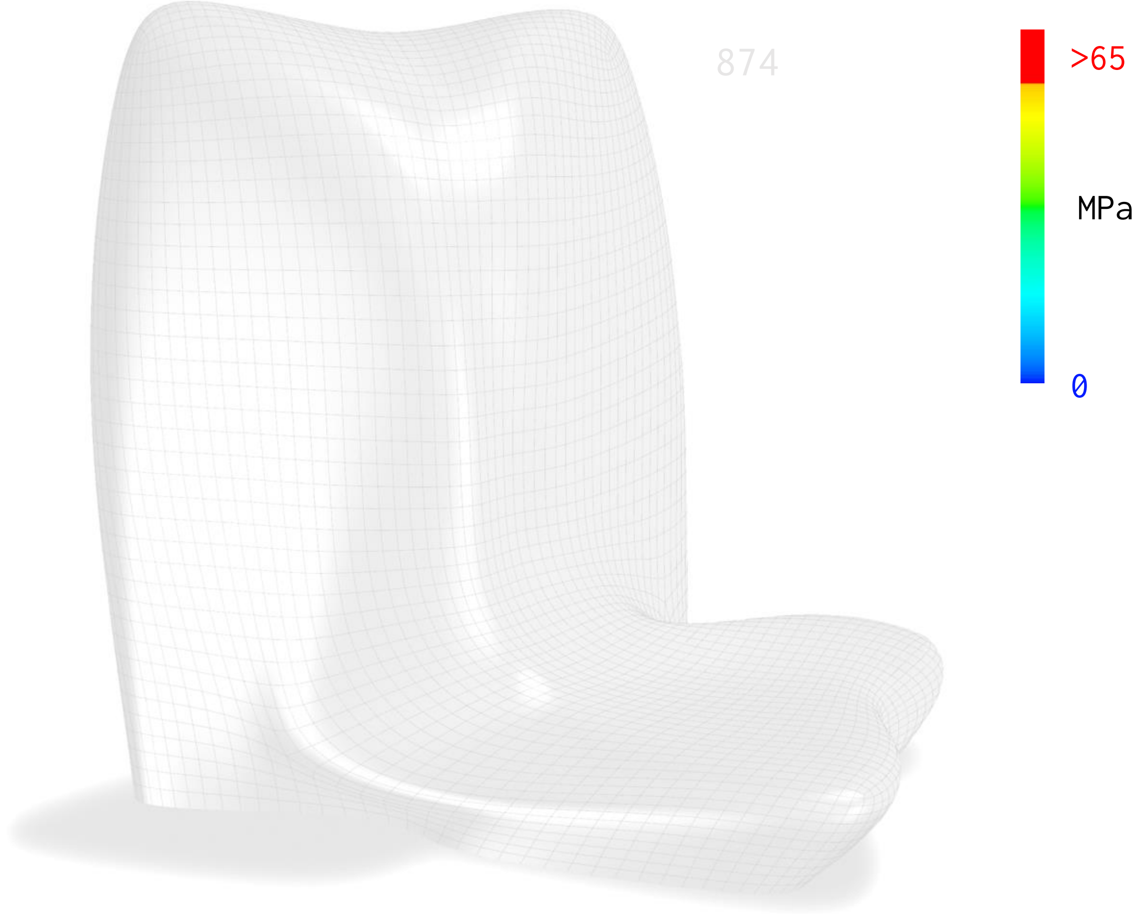

Panel stress $\mathcal{E}_\sigma$

[NHHQ, ZHA]

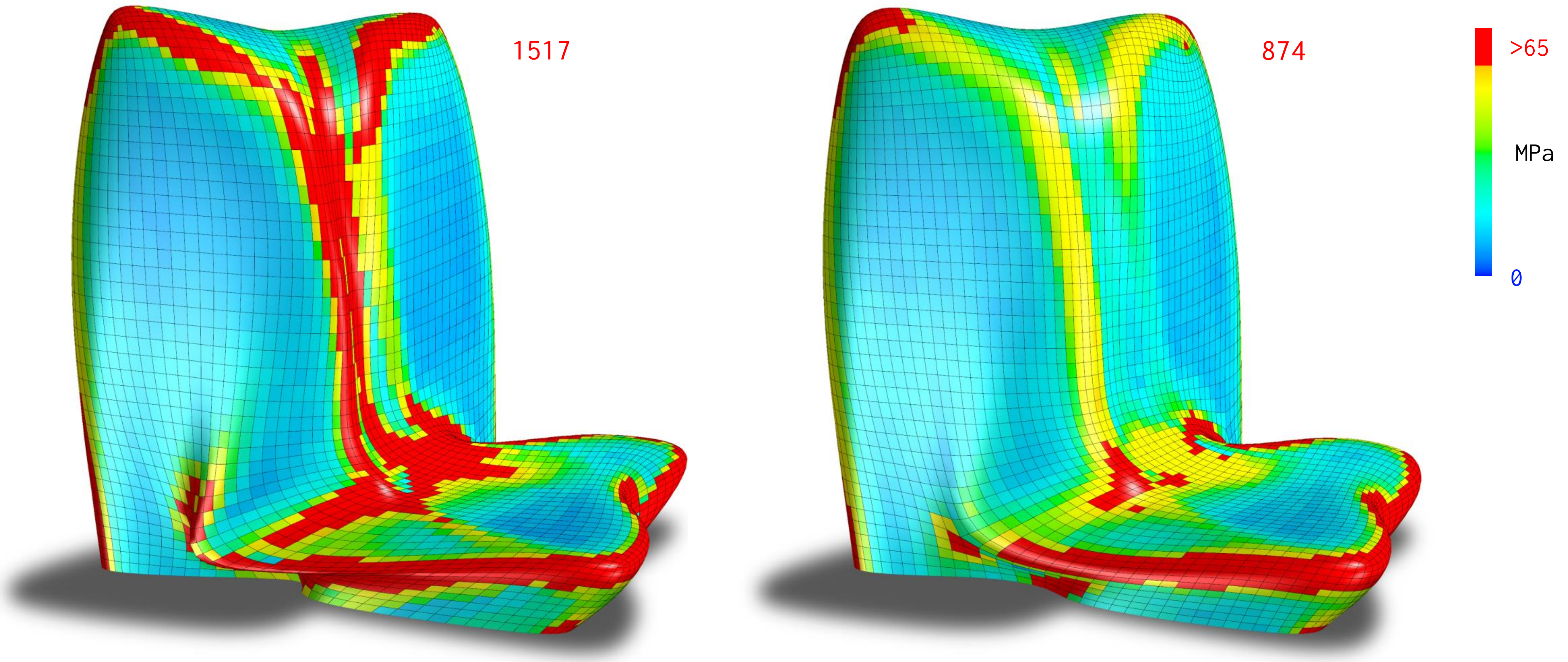

Smoothness $\mathcal{E}_s = \mathcal{E}_1 + \mathcal{E}_2$

- **King angle smoothness $\mathcal{E}_1$.** Smooth connections for panels sharing an edge.

$$\mathcal{E}_1 = \frac{1}{10} \sum_{e \in E_I} \left(1 - \mathbf{n}_i \cdot \mathbf{n}_j\right)^2$$

- **Curve network smoothness $\mathcal{E}_2$.** Smooth connections for consecutive edge curves.

$$\mathcal{E}_2 = \sum \left(\mathbf{t}_i \cdot \mathbf{t}_j + 1\right)^2 + \sum [\mathbf{s}_e \cdot (\mathbf{n}_i + \mathbf{n}_{i+1})]^2$$

Smoothness $\mathcal{E}_\text{s} = \mathcal{E}_1 + \mathcal{E}_2$

- **King angle smoothness $\mathcal{E}_1$.** Smooth connections for panels sharing an edge.

$$\mathcal{E}_1 = \frac{1}{10}\sum_{e\in E_I}\left(1-\mathbf{n}_i\cdot\mathbf{n}_j\right)^2$$

- **Curve network smoothness $\mathcal{E}_2$.** Smooth connections for consecutive edge curves.

$$\mathcal{E}_2 = \sum\left(\mathbf{t}_i\cdot\mathbf{t}_j+1\right)^2 + \sum[\mathbf{s}_e\cdot(\mathbf{n}_i+\mathbf{n}_{i+1})]^2$$

Smoothness $\mathcal{E}_s$

[NHHQ, ZHA]

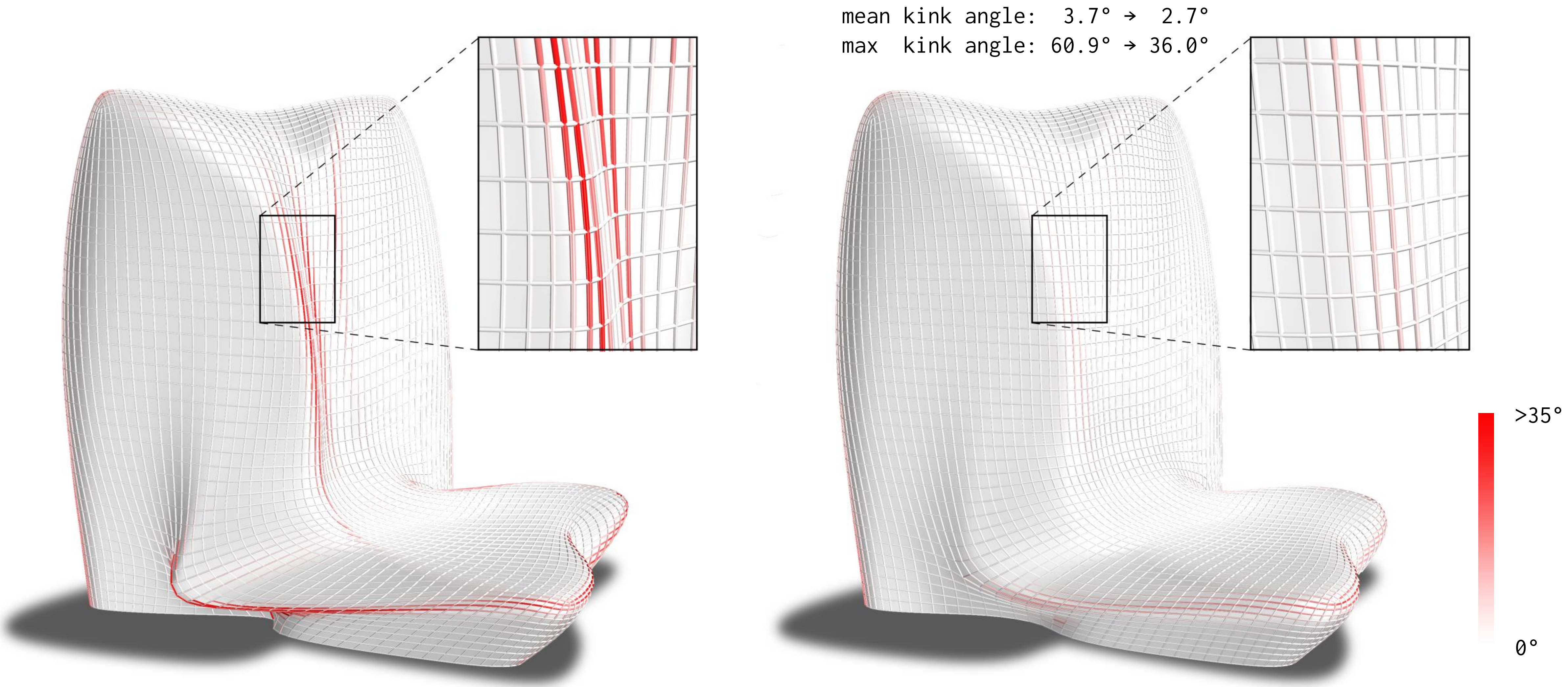

Smoothness $\mathcal{E}_s$

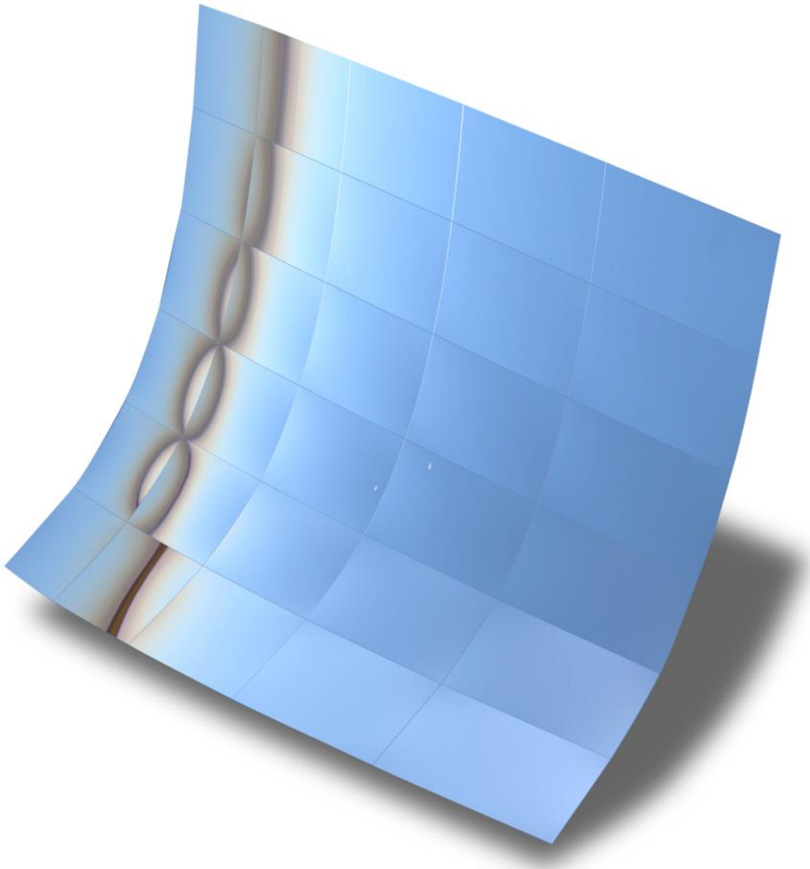

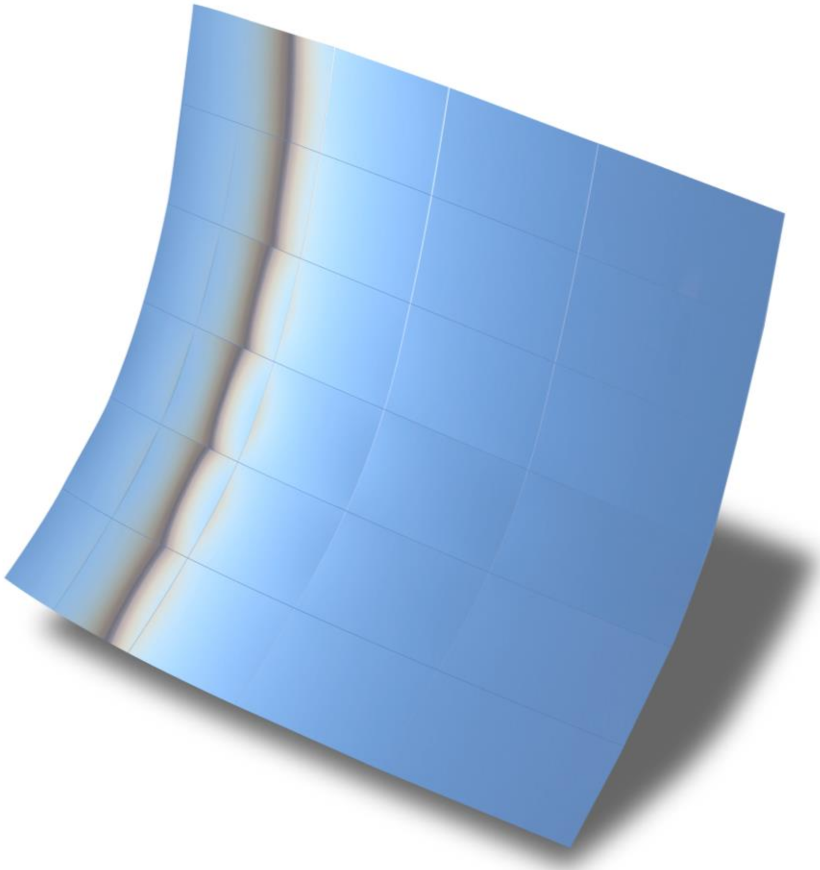

Mesh fairness $\mathcal{E}_\mathrm{f}$

- Summation of standard mesh fairness functionals, e.g. first-order and second-order differences of consecutive vertices along dominant mesh polylines.

- We mainly use second-order differences.

$$\mathcal{E}_\mathrm{f} = \sum (\mathbf{v}_{i-1} - 2\mathbf{v}_i + \mathbf{v}_{i+1})^2$$

Proximity to reference mesh $\mathcal{E}_{\mathrm{p}}$

- Use either the original mesh $\mathcal{M}$ or a different (usually finer) reference mesh $\mathcal{M}_{\mathrm{ref}}$.

- Use tangent distance minimization (TDM).

$$\mathcal{E}_{\mathrm{p}} = \sum_{\mathbf{v}_i \in V} [(\mathbf{v}_i - \mathbf{v}_i^*) \cdot \mathbf{n}_i^*]^2$$

where

$\mathbf{v}_i$: vertex of $\mathcal{M}$

$\mathbf{v}_i^*$: nearest neighbor of $\mathbf{v}_i$ in $\mathcal{M}_{\mathrm{ref}}$

$\mathbf{n}_i^*$: estimated normal of $\mathbf{v}_i^*$ in $\mathcal{M}_{\mathrm{ref}}$

Design space constraints $\mathcal{E}_\mathrm{c} = \mathcal{E}_3 + \mathcal{E}_4$

- Tangent angle constraint $\mathcal{E}_3$.

$$\mathcal{E}_3 = \sum\left(\theta_i^2 - (4.9°)^2 + u_i^2\right)^2 \qquad \boxed{|\theta_i| = \angle(\mathbf{t}_i, \boldsymbol{e}_i) \leq 4.9°}$$

- Unity & orthogonality of plane spanning vector $\mathcal{E}_4$.

$$\mathcal{E}_4 = \sum_e [(\mathbf{s}_e \cdot \mathbf{e})^2 + (\mathbf{s}_e^2 - 1)^2]$$

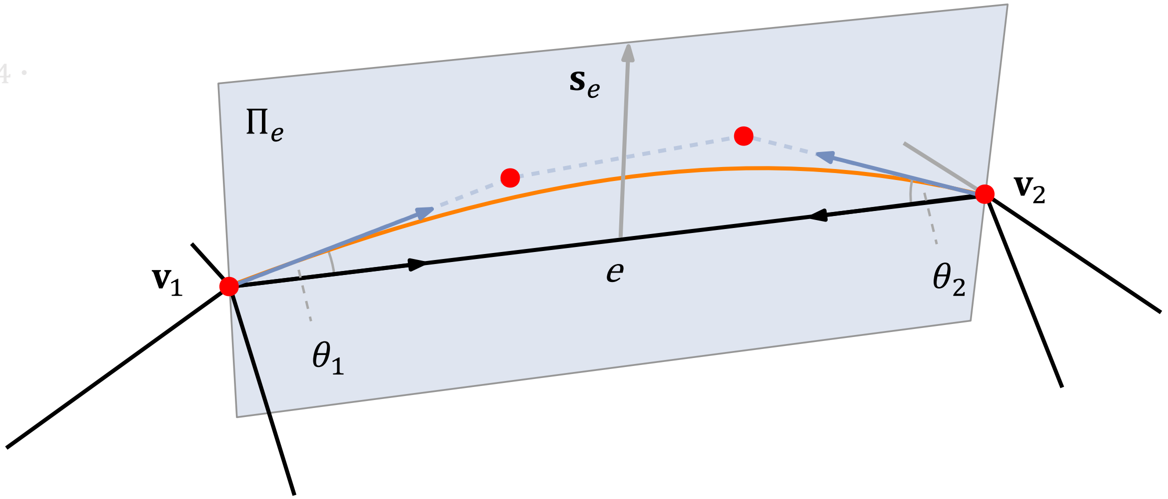

Design space constraints $\mathcal{E}_c = \mathcal{E}_3 + \mathcal{E}_4$

- Tangent angle constraint $\mathcal{E}_3$.

$$\mathcal{E}_3 = \sum \left(\theta_i^2 - (4.9°)^2 + u_i^2\right)^2$$

$$\boxed{|\theta_i| = \angle(\mathbf{t}_i, \boldsymbol{e}_i) \leq 4.9°}$$

- Unity & orthogonality of plane spanning vector $\mathcal{E}_4$.

$$\mathcal{E}_4 = \sum_e [(\mathbf{s}_e \cdot \mathbf{e})^2 + (\mathbf{s}_e^2 - 1)^2]$$

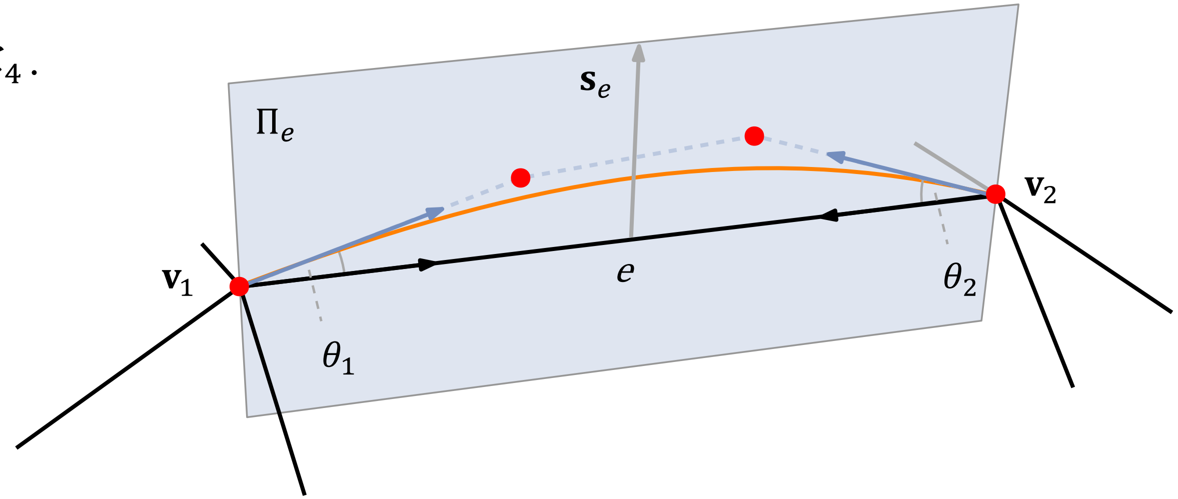

Optimization problem

Initialization.

- Initialize edge plane vectors $\mathbf{s}_e$ such that plane Π_e is the bisecting plane of the previous and next osculating planes.
- Initialize angles θ_i such that they are at most 4.9° and the tangents $\mathbf{t}_i$ lie as close as possible to the tangent plane of the corresponding vertex.
- Initialize a panel (shape $\mathbf{S}_\mathbf{p}$ & stress $\sigma_\mathbf{p}$) for each (quad) face boundary $\mathbf{p}$ using the MDN.
  In case multiple panels are valid, choose *best* one according to user-defined criterion:
  - Lowest stress.
  - Smoothest fit. According an angle deviation measure $\sum(1-\mathbf{n}_i \cdot \mathbf{n}_e)^2$.

Solution.

- Unconstrained nonlinear least-squares problem.
- Use standard Gauss-Newton method.

Optimization problem

Initialization.

- Initialize edge plane vectors $\mathbf{s}_e$ such that plane Π_e is the bisecting plane of the previous and next osculating planes.
- Initialize angles θ_i such that they are at most 4.9° and the tangents $\mathbf{t}_i$ lie as close as possible to the tangent plane of the corresponding vertex.
- Initialize a panel (shape $\mathbf{S}_\mathbf{p}$ & stress $\sigma_\mathbf{p}$) for each (quad) face boundary $\mathbf{p}$ using the MDN.
  In case multiple panels are valid, choose *best* one according to user-defined criterion:
  - Lowest stress.
  - Smoothest fit. According an angle deviation measure $\sum(1 - \mathbf{n}_i \cdot \mathbf{n}_e)^2$.

Solution.

- Unconstrained nonlinear least-squares problem.
- Use standard Gauss-Newton method.

Optimization problem

Initialization.

- Initialize edge plane vectors $\mathbf{s}_e$ such that plane Π_e is the bisecting plane of the previous and next osculating planes.
- Initialize angles θ_i such that they are at most 4.9° and the tangents $\mathbf{t}_i$ lie as close as possible to the tangent plane of the corresponding vertex.
- Initialize a panel (shape $\mathbf{S}_\mathbf{p}$ & stress $\sigma_\mathbf{p}$) for each (quad) face boundary $\mathbf{p}$ using the MDN.
  In case multiple panels are valid, choose *best* one according to user-defined criterion:
  - Lowest stress.
  - Smoothest fit. According an angle deviation measure $\sum(1-\mathbf{n}_i \cdot \mathbf{n}_e)^2$.

Solution.

- Unconstrained nonlinear least-squares problem.
- Use standard Gauss-Newton method.

Optimization problem

Initialization.

- Initialize edge plane vectors $\mathbf{s}_e$ such that plane Π_e is the bisecting plane of the previous and next osculating planes.
- Initialize angles θ_i such that they are at most 4.9° and the tangents $\mathbf{t}_i$ lie as close as possible to the tangent plane of the corresponding vertex.
- Initialize a panel (shape $\mathbf{S}_\mathbf{p}$ & stress $\sigma_\mathbf{p}$) for each (quad) face boundary $\mathbf{p}$ using the MDN.
  In case multiple panels are valid, choose *best* one according to user-defined criterion:
  - Lowest stress.
  - Smoothest fit. According an angle deviation measure $\sum(1 - \mathbf{n}_i \cdot \mathbf{n}_e)^2$.

Solution.

- Unconstrained nonlinear least-squares problem.
- Use standard Gauss-Newton method.

Weight influence

[Lilium Tower, ZHA]

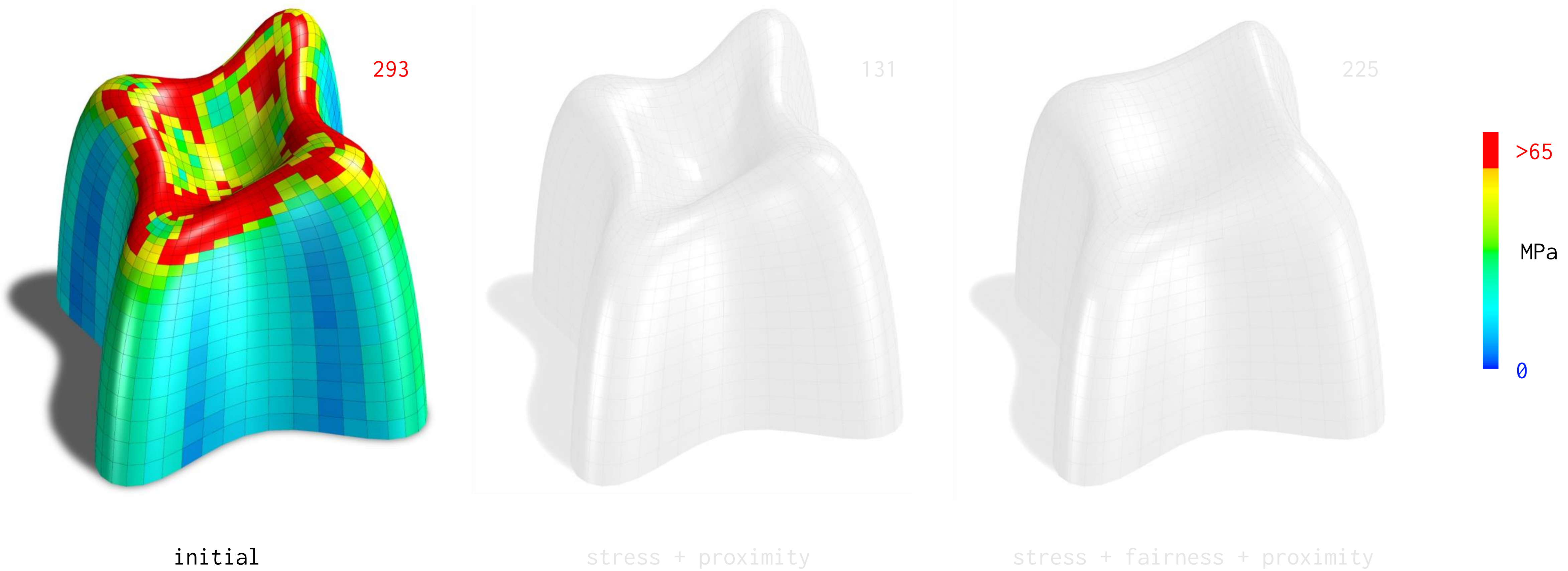

TU WIEN

Weight influence

[Lilium Tower, ZHA]

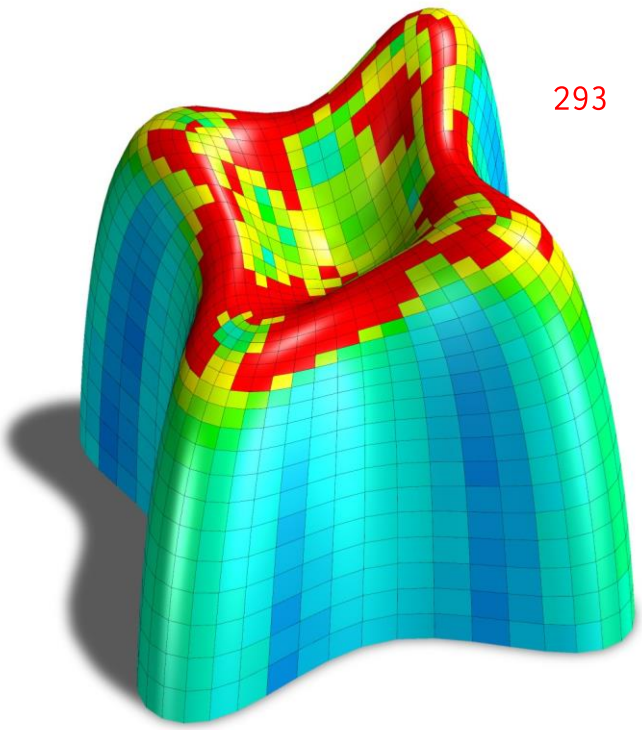

initial

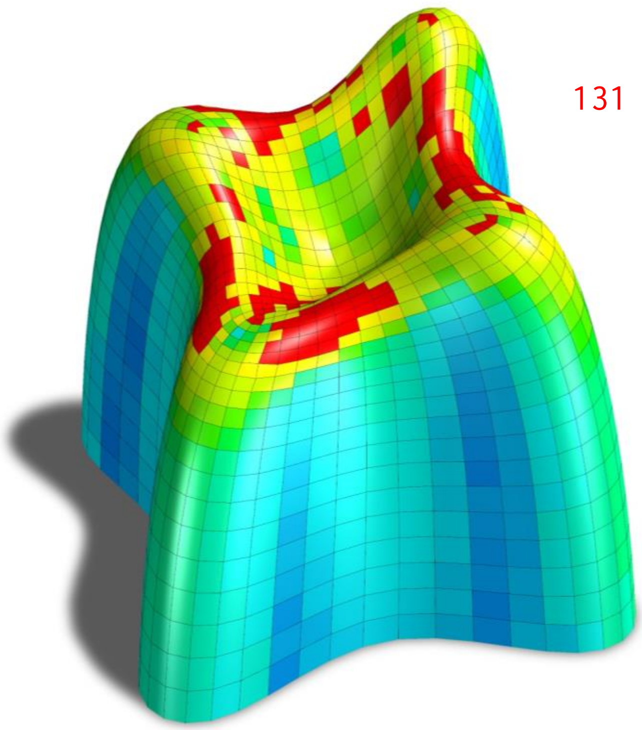

stress + proximity

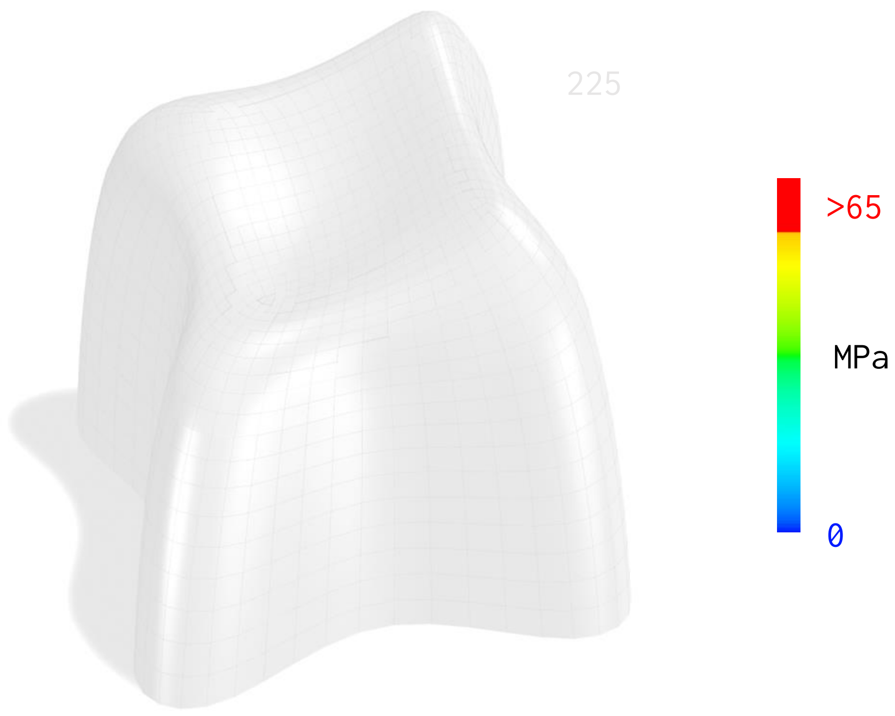

stress + fairness + proximity

Weight influence

[Lilium Tower, ZHA]

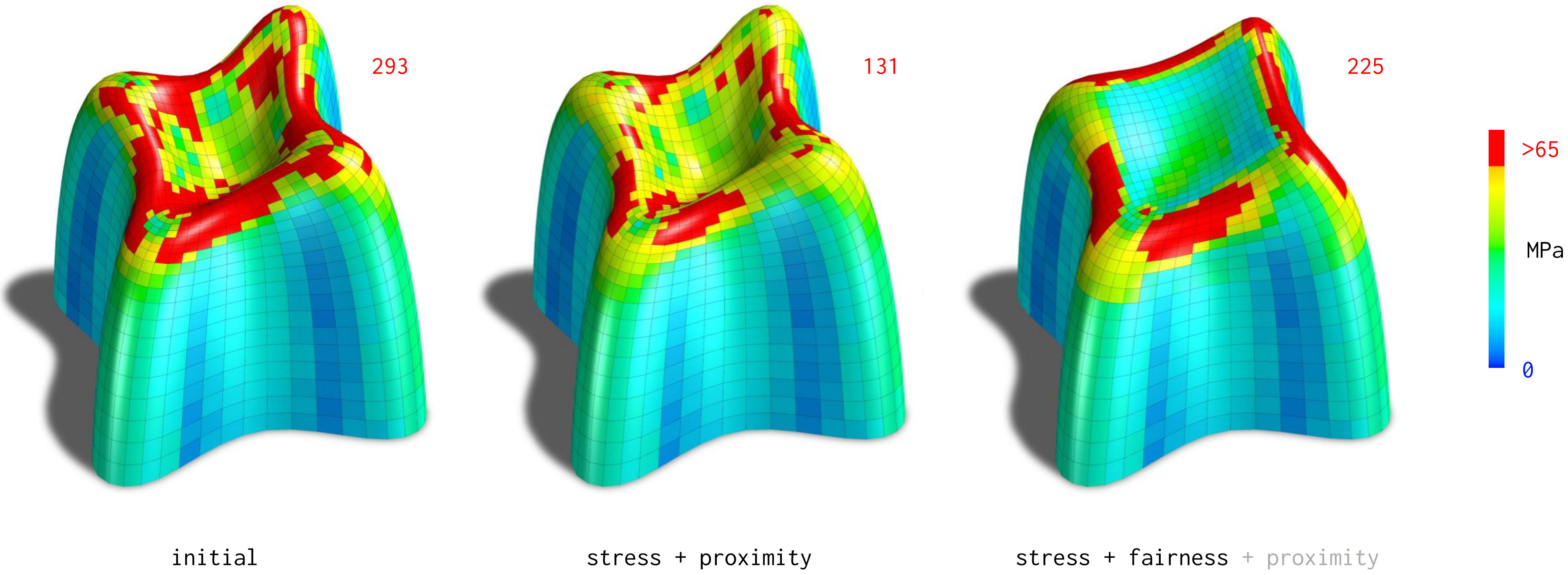

Validation

Experimental validation

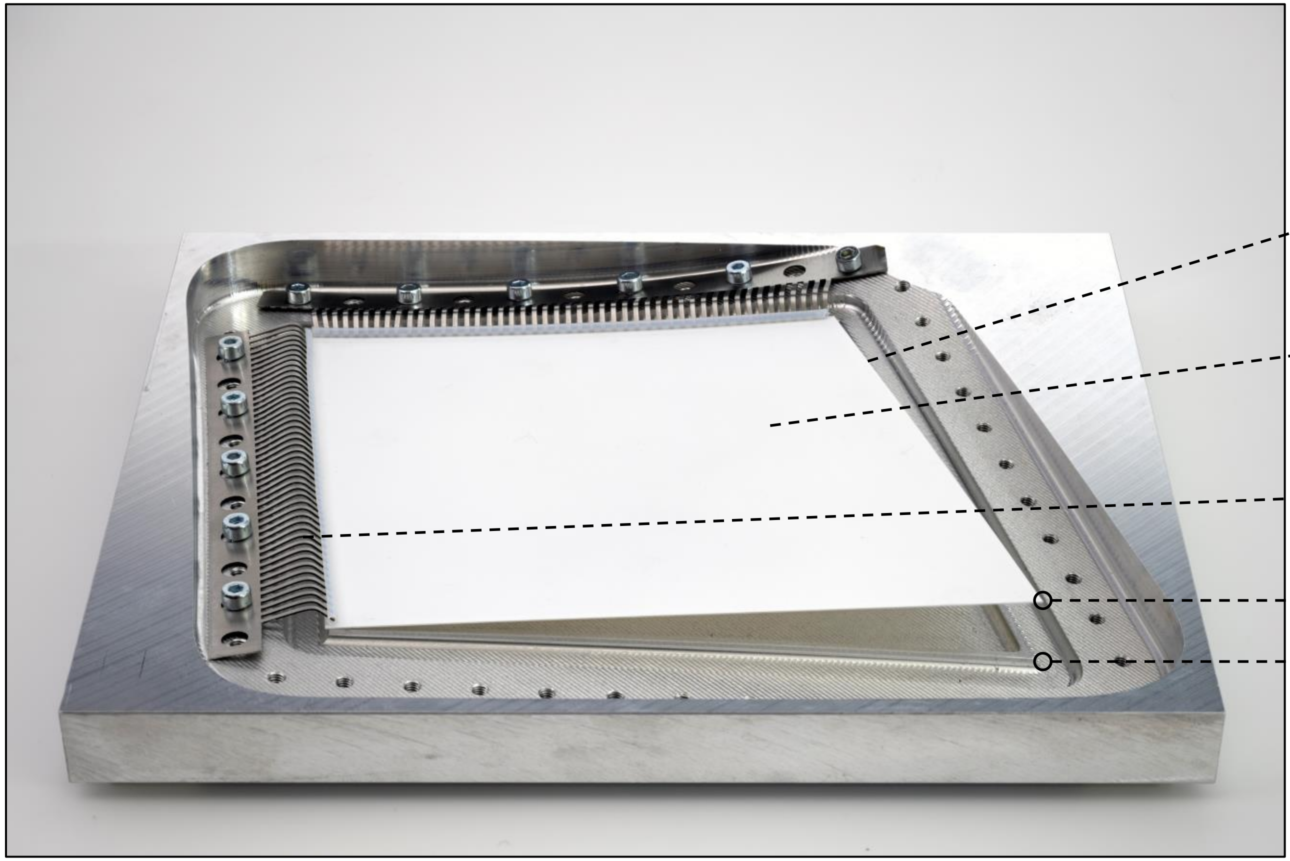

Experimental validation

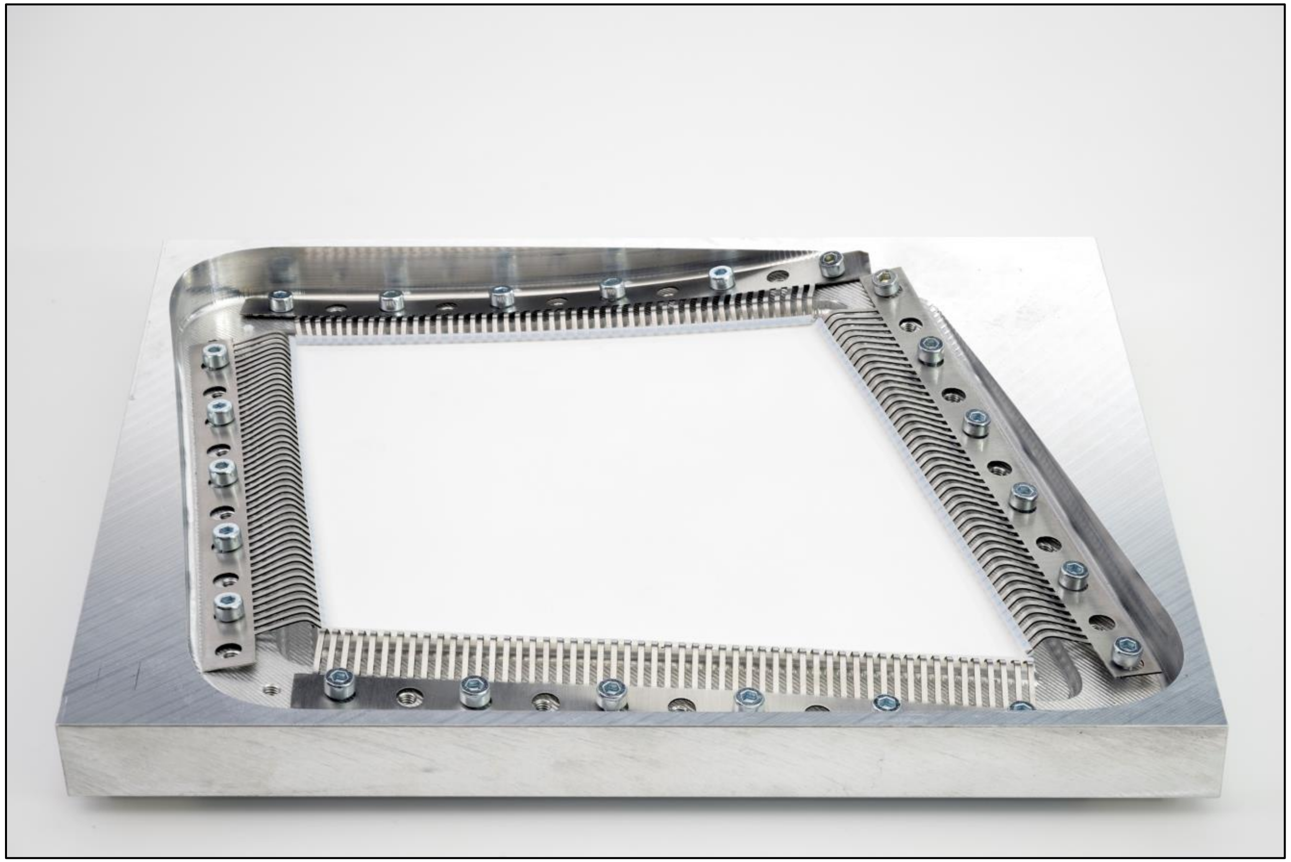

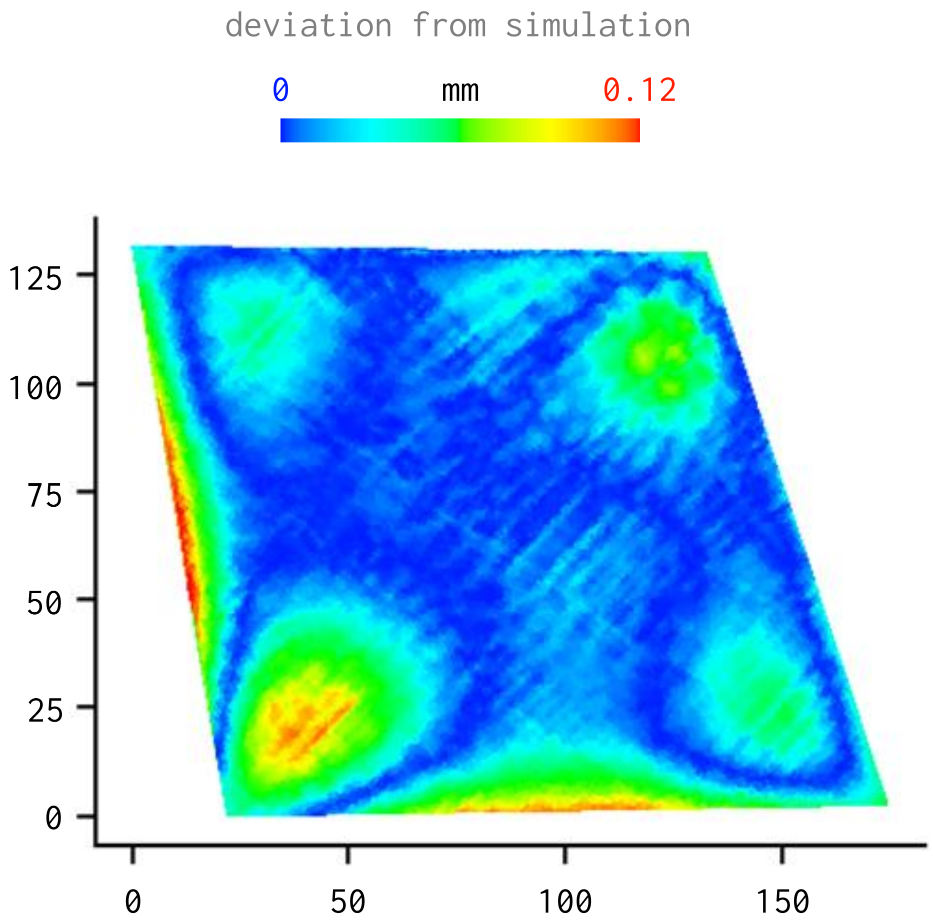

TU WIEN

Prototype

- Borosilicate thin glass.
  200 x 170 x 0.35 (mm)
- Frame from laser cut and welded stainless steel sheet metal.
  1.2 mm thick
- L-shaped fixtures press the (tape-cushioned) glass to the frame.
- Expected stress range:
  20 – 62 MPa

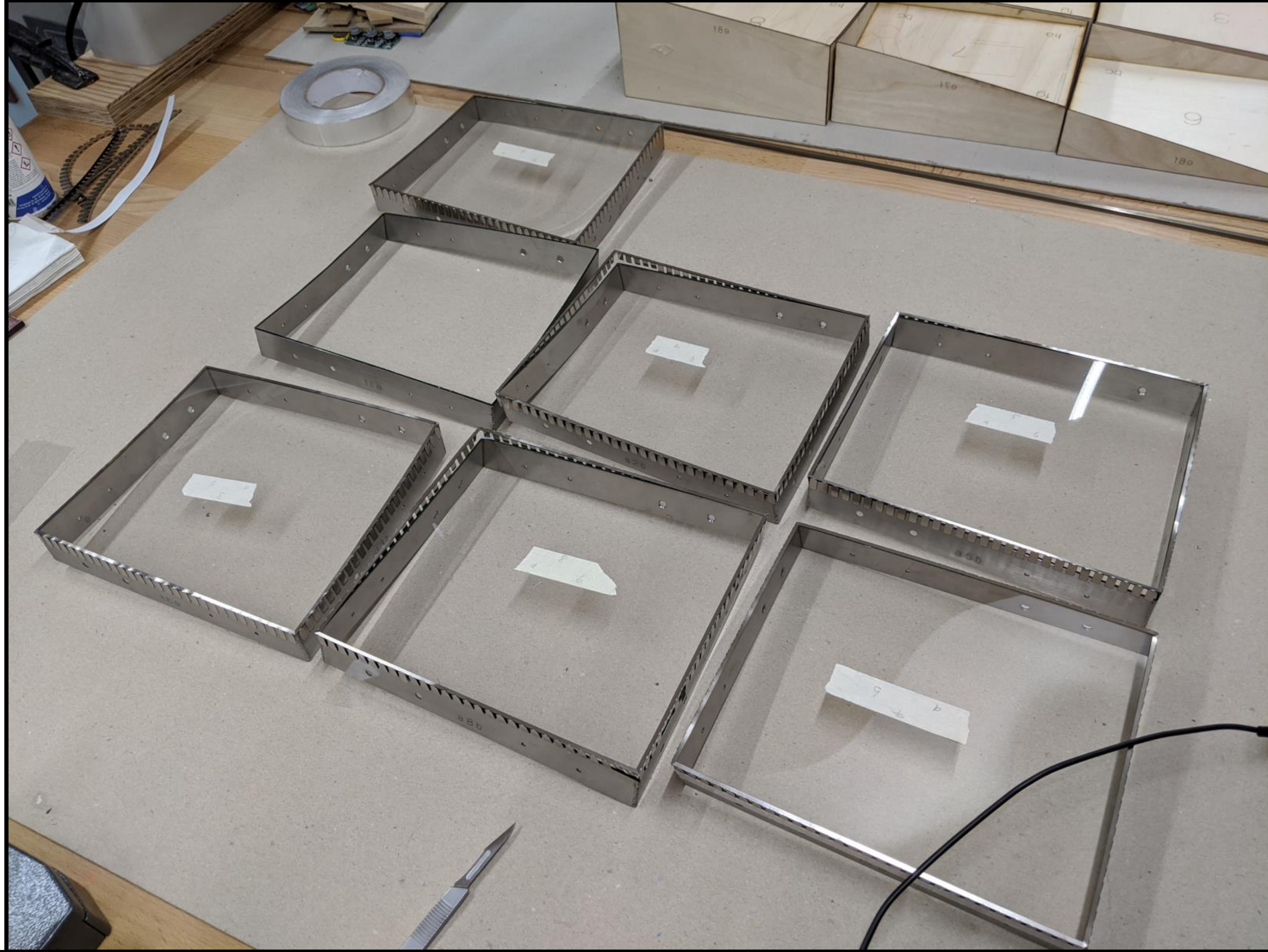

Prototype

- Borosilicate thin glass.
  200 x 170 x 0.35 (mm)
- Frame from laser cut and welded stainless steel sheet metal.
  1.2 mm thick
- L-shaped fixtures press the (tape-cushioned) glass to the frame.
- Expected stress range:
  20 - 62 MPa

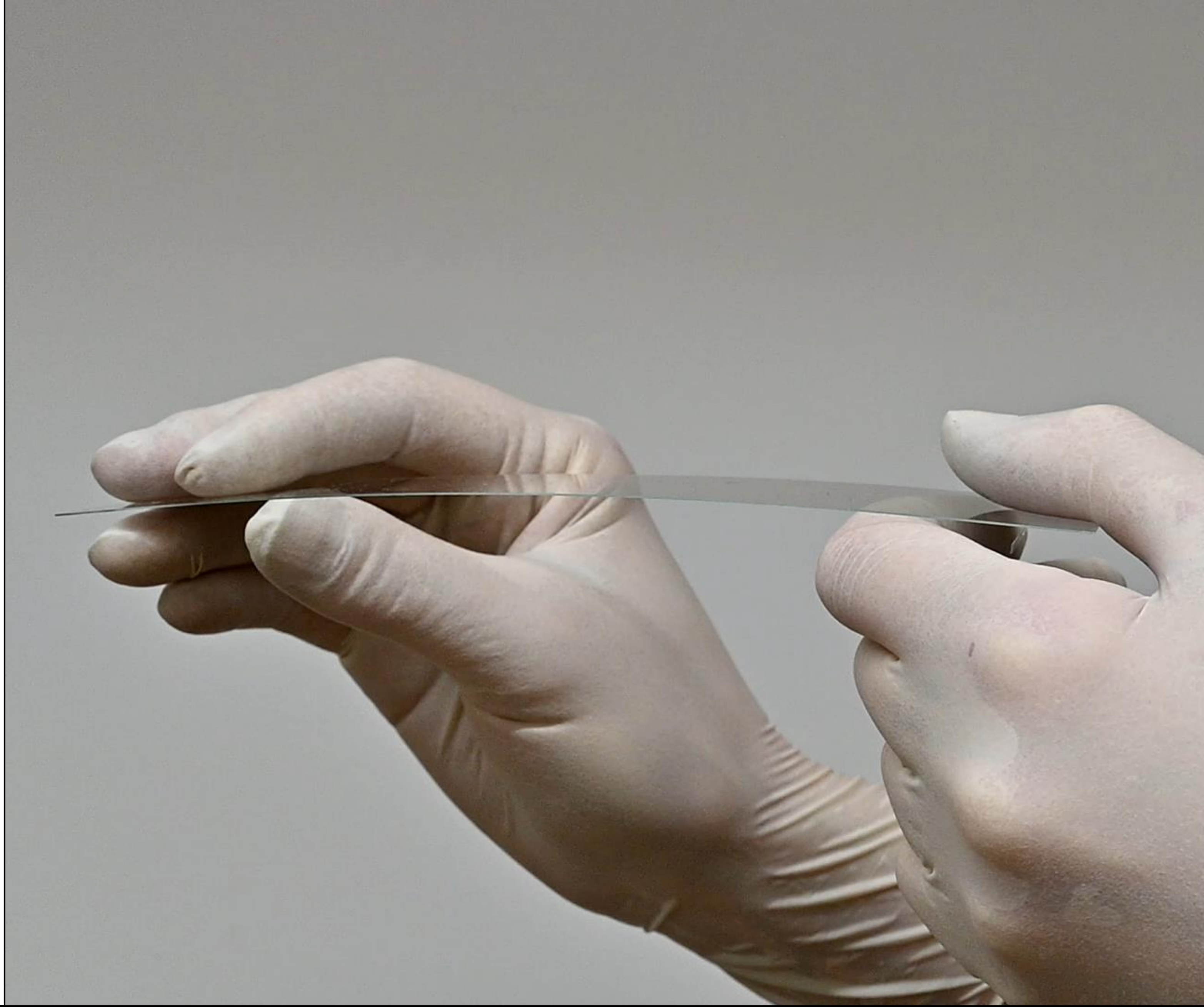

Prototype

- Borosilicate thin glass.
  200 x 170 x 0.35 (mm)
- Frame from laser cut and welded stainless steel sheet metal.
  1.2 mm thick
- L-shaped fixtures press the (tape-cushioned) glass to the frame.
- Expected stress range:
  20 - 62 MPa

Prototype

- Borosilicate thin glass.
  200 x 170 x 0.35 (mm)
- Frame from laser cut and welded stainless steel sheet metal.
  1.2 mm thick
- L-shaped fixtures press the (tape-cushioned) glass to the frame.
- Expected stress range:
  20 - 62 MPa

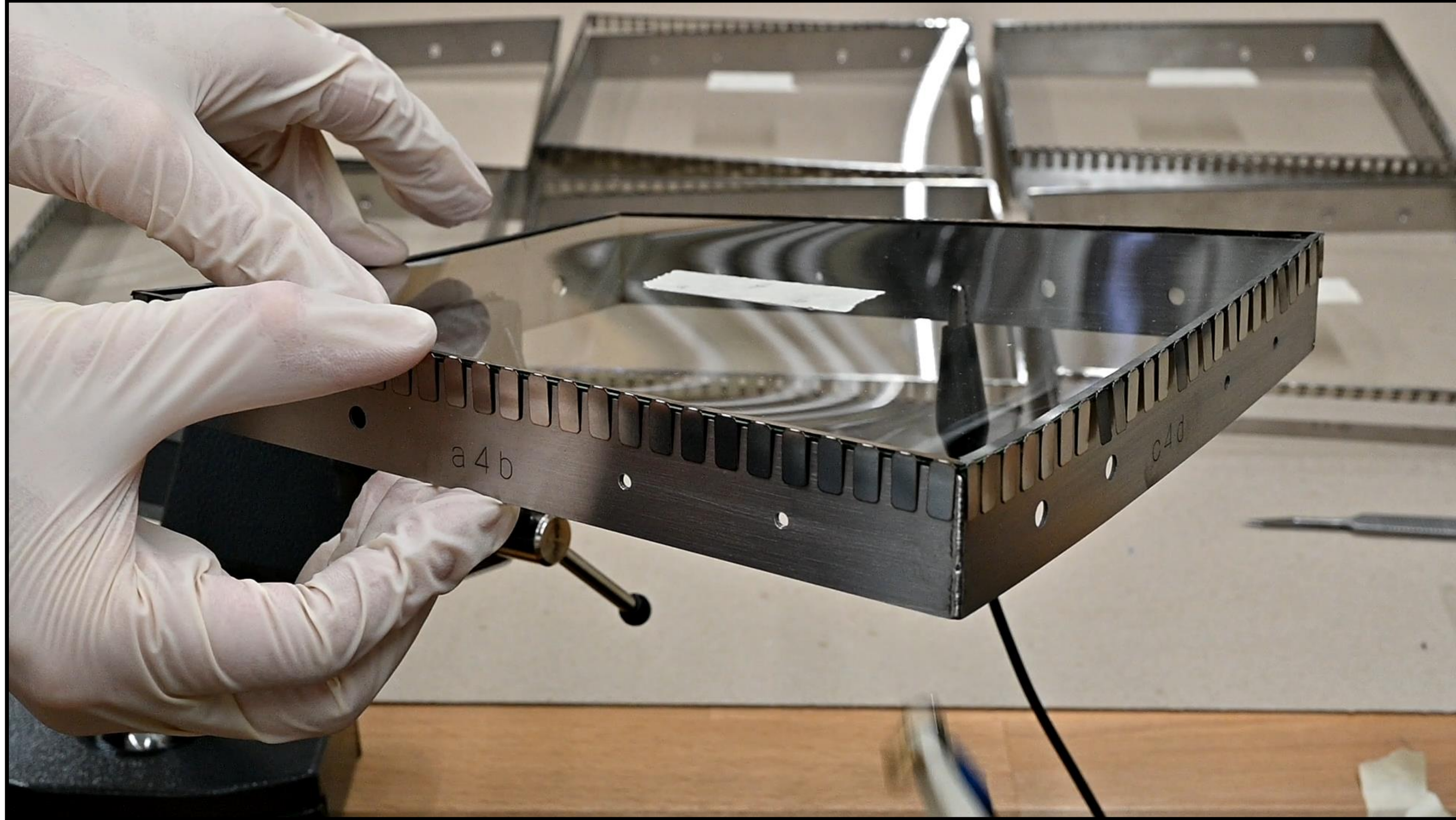

Prototype

- Borosilicate thin glass.
  200 x 170 x 0.35 (mm)
- Frame from laser cut and welded stainless steel sheet metal.
  1.2 mm thick
- L-shaped fixtures press the (tape-cushioned) glass to the frame.
- Expected stress range:
  20 - 62 MPa

Prototype

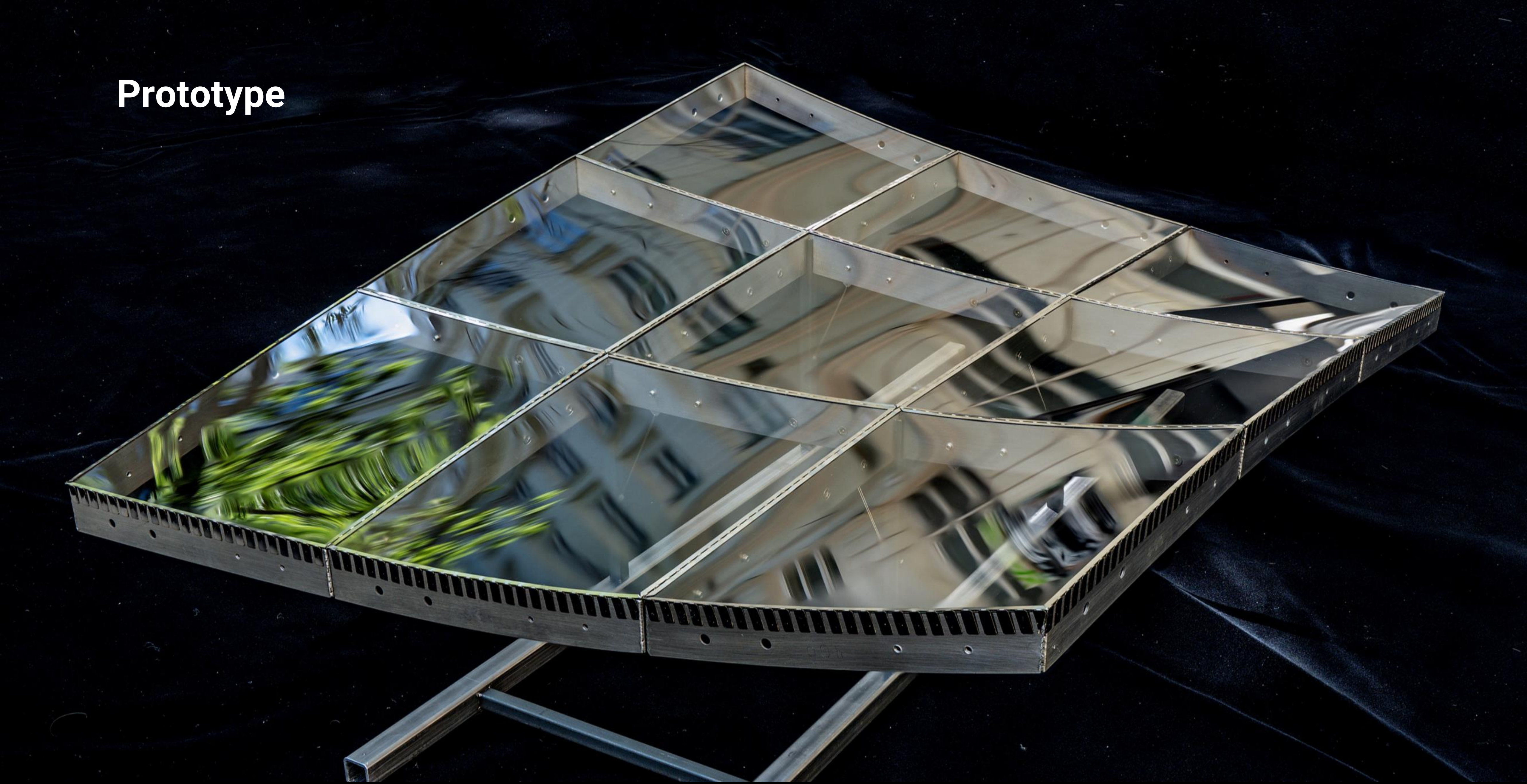

Validation of data-driven model

- Use test set of 10K panel boundaries.
- Predict shape $\hat{\mathbf{S}}_{\mathbf{p}}^k$ and stress $\hat{\sigma}_{\mathbf{p}}^k$. Consider only predictions with $\hat{\pi}_{\mathbf{p}}^k \geq 0.05$.
- Use shape prediction to initialize simulation and compare.
- Shape prediction for panels with $\sigma_{\mathbf{p}}^k \leq 65\,\mathrm{MPa}$ (manufacturable panels)
  $\mathrm{MAE} \approx 0.5\,\mathrm{mm} < 1\,\mathrm{mm}$ (glass thickness).
- Stress prediction for panels with $\sigma_{\mathbf{p}}^k \in [50, 65]\,\mathrm{MPa}$ (region of interest)
  $\mathrm{MAE} \approx 2.9\,\mathrm{MPa}$.

Validation of data-driven model

- Use test set of 10K panel boundaries.

- Predict shape $\hat{\mathbf{S}}_{\mathbf{p}}^{k}$ and stress $\hat{\sigma}_{\mathbf{p}}^{k}$. Consider only predictions with $\hat{\pi}_{\mathbf{p}}^{k} \geq 0.05$.

- Use shape prediction to initialize simulation and compare.

- Shape prediction for panels with $\sigma_{\mathbf{p}}^{k} \leq 65\,\mathrm{MPa}$ (manufacturable panels)
  $\mathrm{MAE} \approx 0.5\,\mathrm{mm} < 1\,\mathrm{mm}$ (glass thickness).

- Stress prediction for panels with $\sigma_{\mathbf{p}}^{k} \in [50, 65]\,\mathrm{MPa}$ (region of interest)
  $\mathrm{MAE} \approx 2.9\,\mathrm{MPa}$.

Validation of data-driven model

- Use test set of 10K panel boundaries.
- Predict shape $\hat{\mathbf{S}}_{\mathbf{p}}^k$ and stress $\hat{\sigma}_{\mathbf{p}}^k$. Consider only predictions with $\hat{\pi}_{\mathbf{p}}^k \geq 0.05$.
- Use shape prediction to initialize simulation and compare.
- Shape prediction for panels with $\sigma_{\mathbf{p}}^k \leq 65\,\mathrm{MPa}$ (manufacturable panels) $\mathrm{MAE} \approx 0.5\,\mathrm{mm} < 1\,\mathrm{mm}$ (glass thickness).
- Stress prediction for panels with $\sigma_{\mathbf{p}}^k \in [50, 65]\,\mathrm{MPa}$ (region of interest) $\mathrm{MAE} \approx 2.9\,\mathrm{MPa}$.

Validation of data-driven model

- Use test set of 10K panel boundaries.
- Predict shape $\hat{\mathbf{S}}_{\mathbf{p}}^{k}$ and stress $\hat{\sigma}_{\mathbf{p}}^{k}$. Consider only predictions with $\hat{\pi}_{\mathbf{p}}^{k} \geq 0.05$.
- Use shape prediction to initialize simulation and compare.
- Shape prediction for panels with $\sigma_{\mathbf{p}}^{k} \leq 65\,\mathrm{MPa}$ (manufacturable panels)
  $\mathrm{MAE} \approx 0.5\,\mathrm{mm} < 1\,\mathrm{mm}$ (glass thickness).
- Stress prediction for panels with $\sigma_{\mathbf{p}}^{k} \in [50, 65]\,\mathrm{MPa}$ (region of interest)
  $\mathrm{MAE} \approx 2.9\,\mathrm{MPa}$.

Validation of data-driven model

- Use test set of 10K panel boundaries.
- Predict shape $\hat{\mathbf{S}}_{\mathbf{p}}^k$ and stress $\hat{\sigma}_{\mathbf{p}}^k$. Consider only predictions with $\hat{\pi}_{\mathbf{p}}^k \geq 0.05$.
- Use shape prediction to initialize simulation and compare.
- Shape prediction for panels with $\sigma_{\mathbf{p}}^k \leq 65\,\mathrm{MPa}$ (manufacturable panels)
  $\mathrm{MAE} \approx 0.5\,\mathrm{mm} < 1\,\mathrm{mm}$ (glass thickness).
- Stress prediction for panels with $\sigma_{\mathbf{p}}^k \in [50, 65]\,\mathrm{MPa}$ (region of interest)
  $\mathrm{MAE} \approx 2.9\,\mathrm{MPa}$.

Validation of data-driven model

- Use test set of 10K panel boundaries.
- Predict shape $\hat{\mathbf{S}}_{\mathbf{p}}^k$ and stress $\hat{\sigma}_{\mathbf{p}}^k$. Consider only predictions with $\hat{\pi}_{\mathbf{p}}^k \geq 0.05$.
- Use shape prediction to initialize simulation and compare.
- Shape prediction for panels with $\sigma_{\mathbf{p}}^k \leq 65\,\mathrm{MPa}$ (manufacturable panels)
  $\mathrm{MAE} \approx 0.5\,\mathrm{mm} < 1\,\mathrm{mm}$ (glass thickness).
- Stress prediction for panels with $\sigma_{\mathbf{p}}^k \in [50, 65]\,\mathrm{MPa}$ (region of interest)
  $\mathrm{MAE} \approx 2.9\,\mathrm{MPa}$.

Results

Comparison to PQ panelization

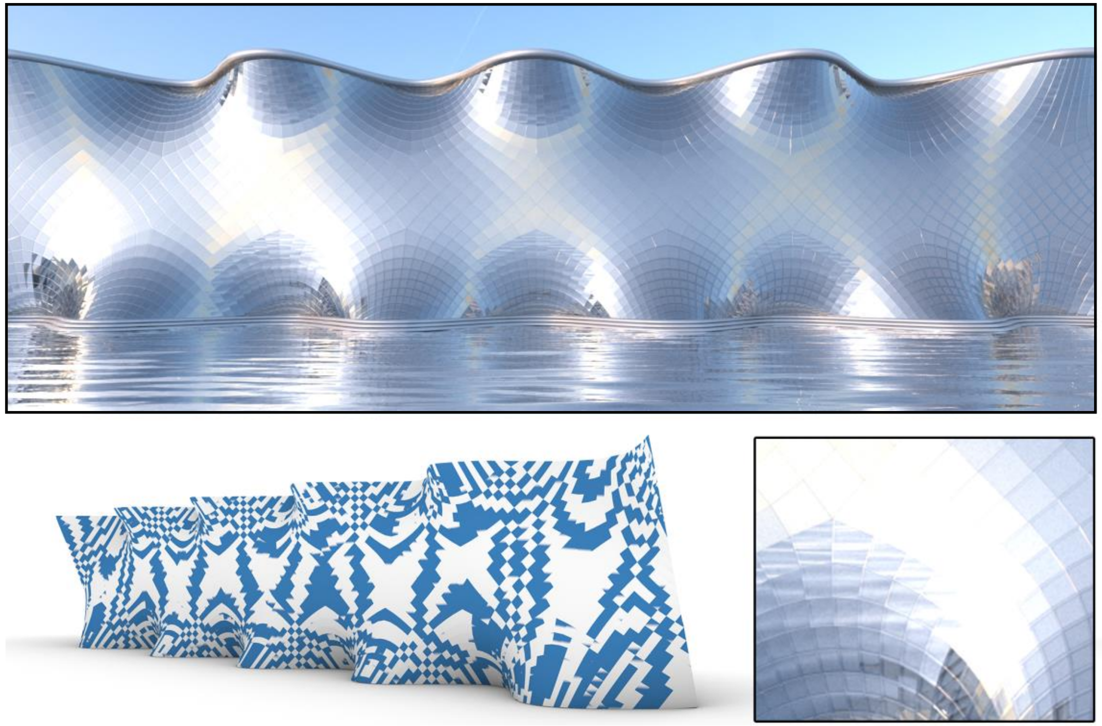

PQ mesh following principal curvature network.
Smoothest possible panelization with flat panels.
[Pellis et al., 2019]

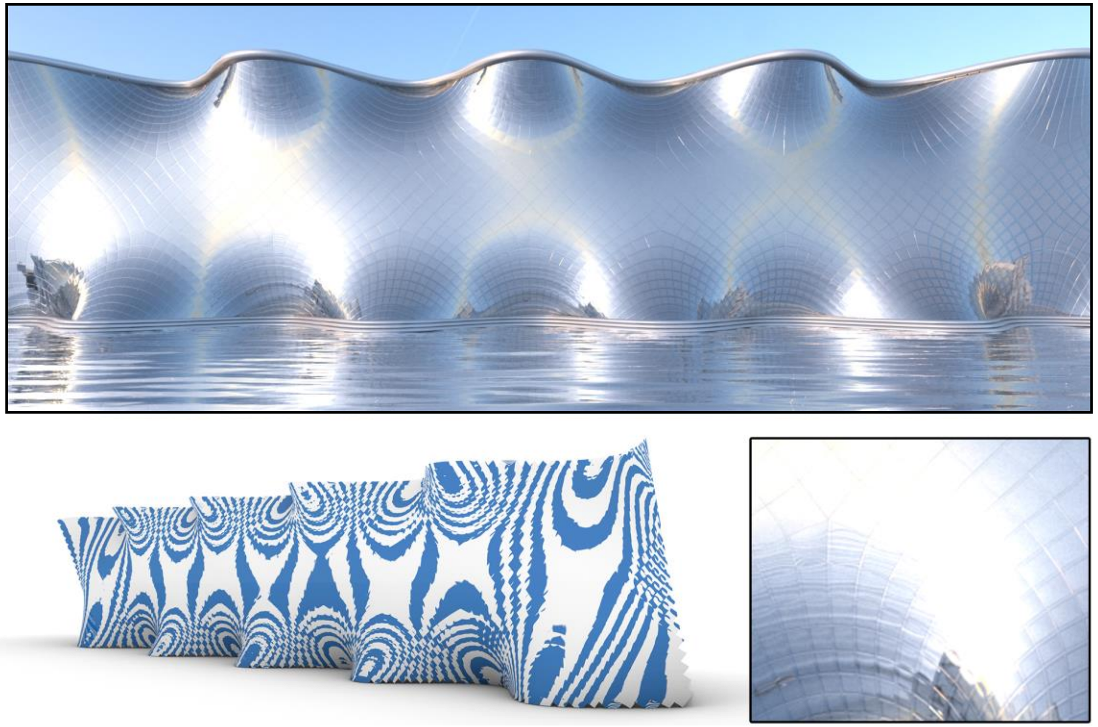

Cold bent glass panelization.
Smoothness increase.

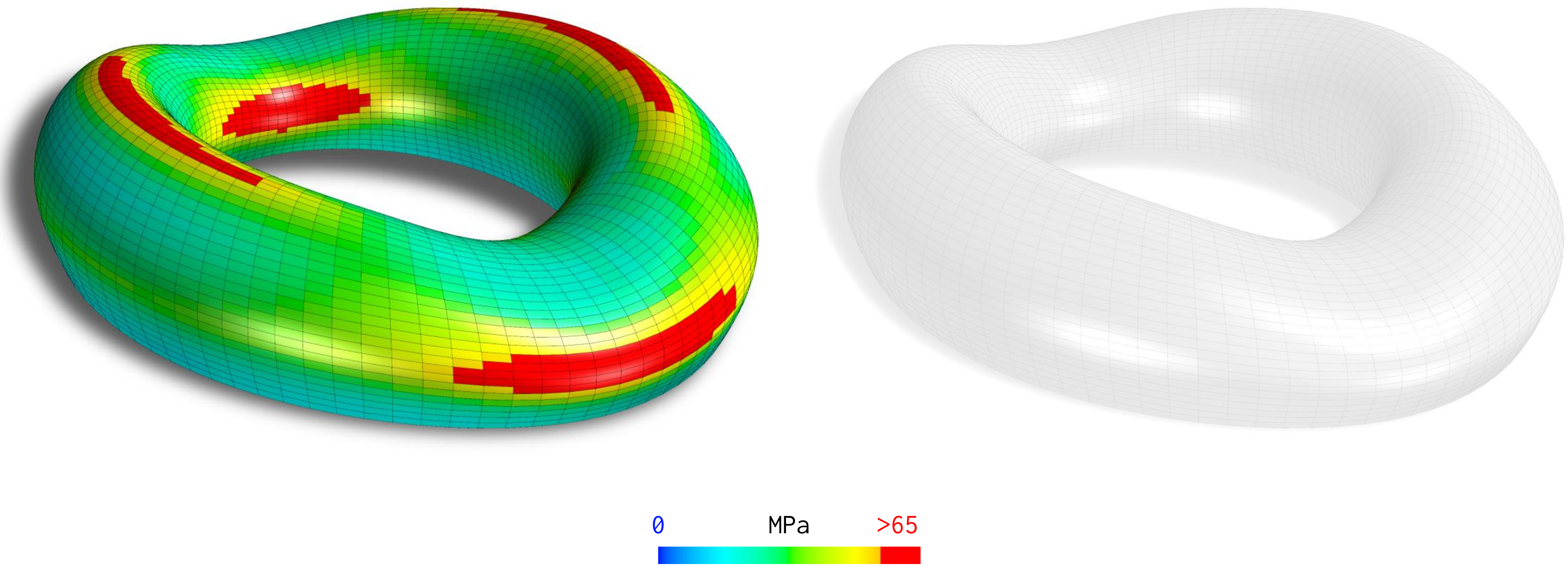

Konstantinos Gavriil

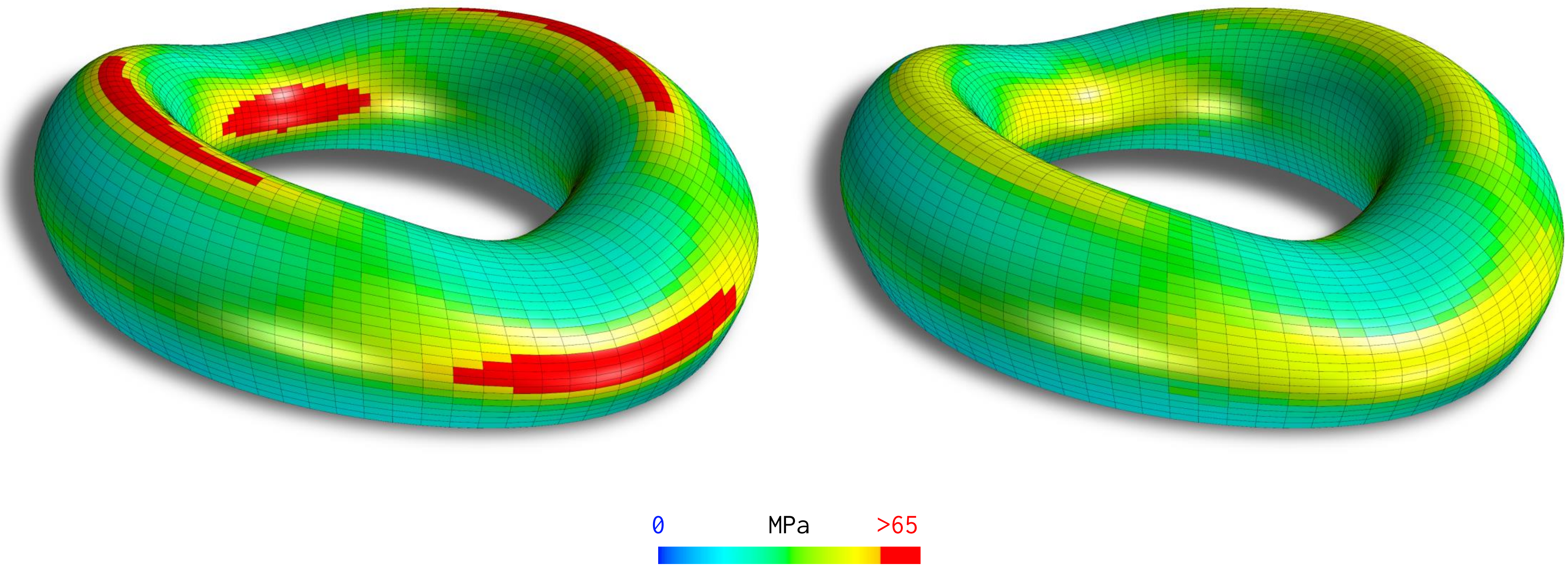
0
MPa
>65

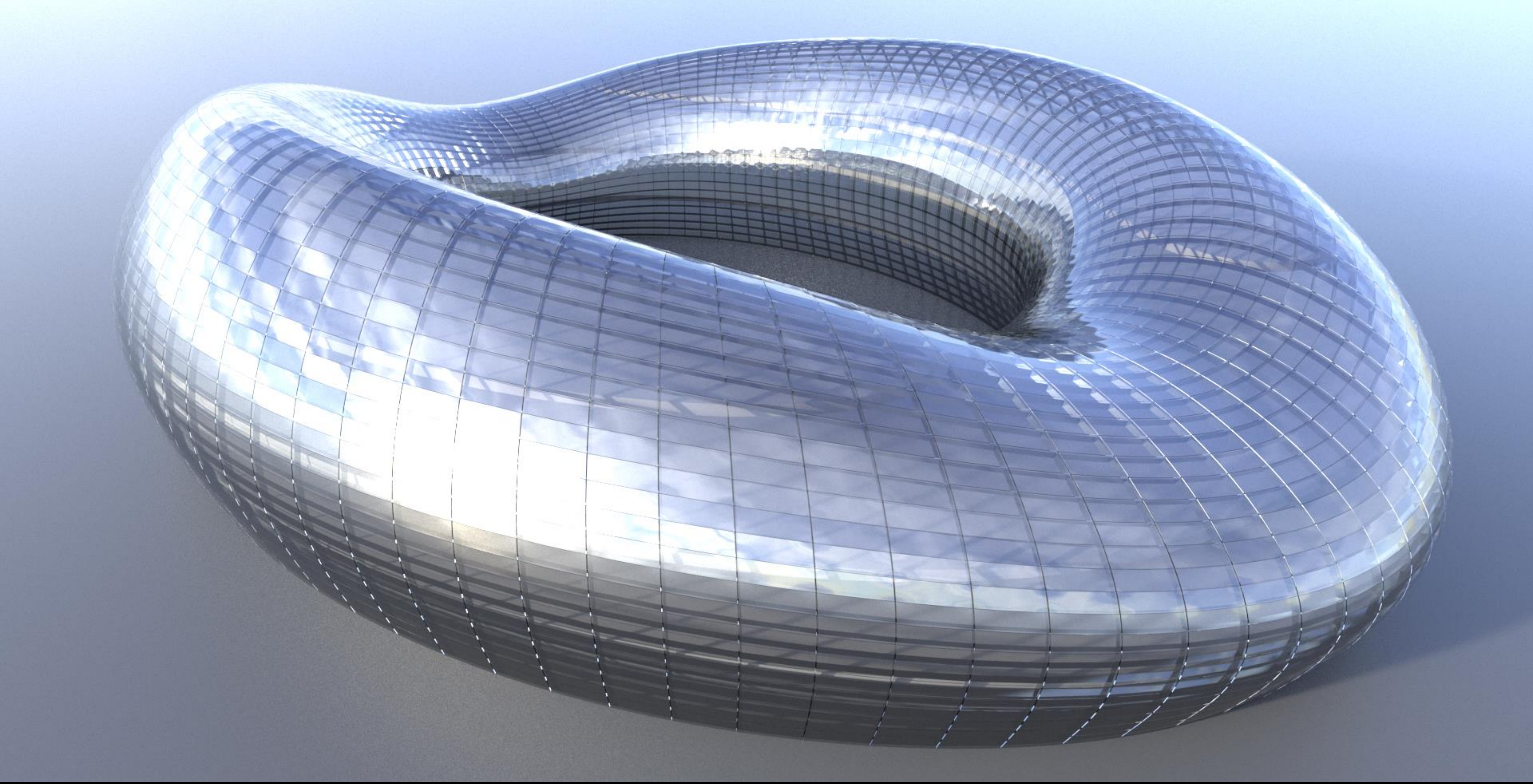

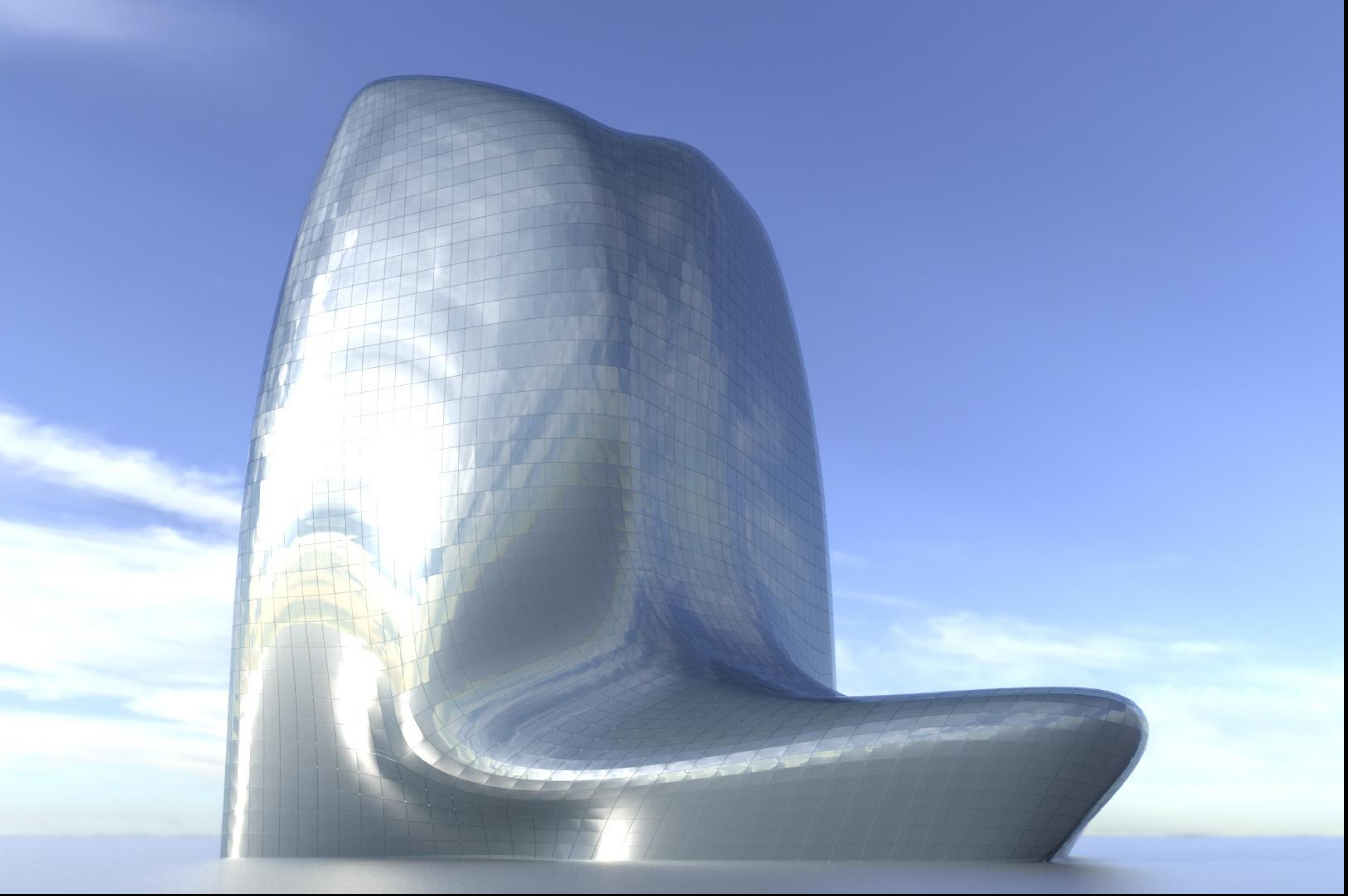

NHHQ (optimized)
Zaha Hadid Architects

Lilium Tower (optimized)
Zaha Hadid Architects

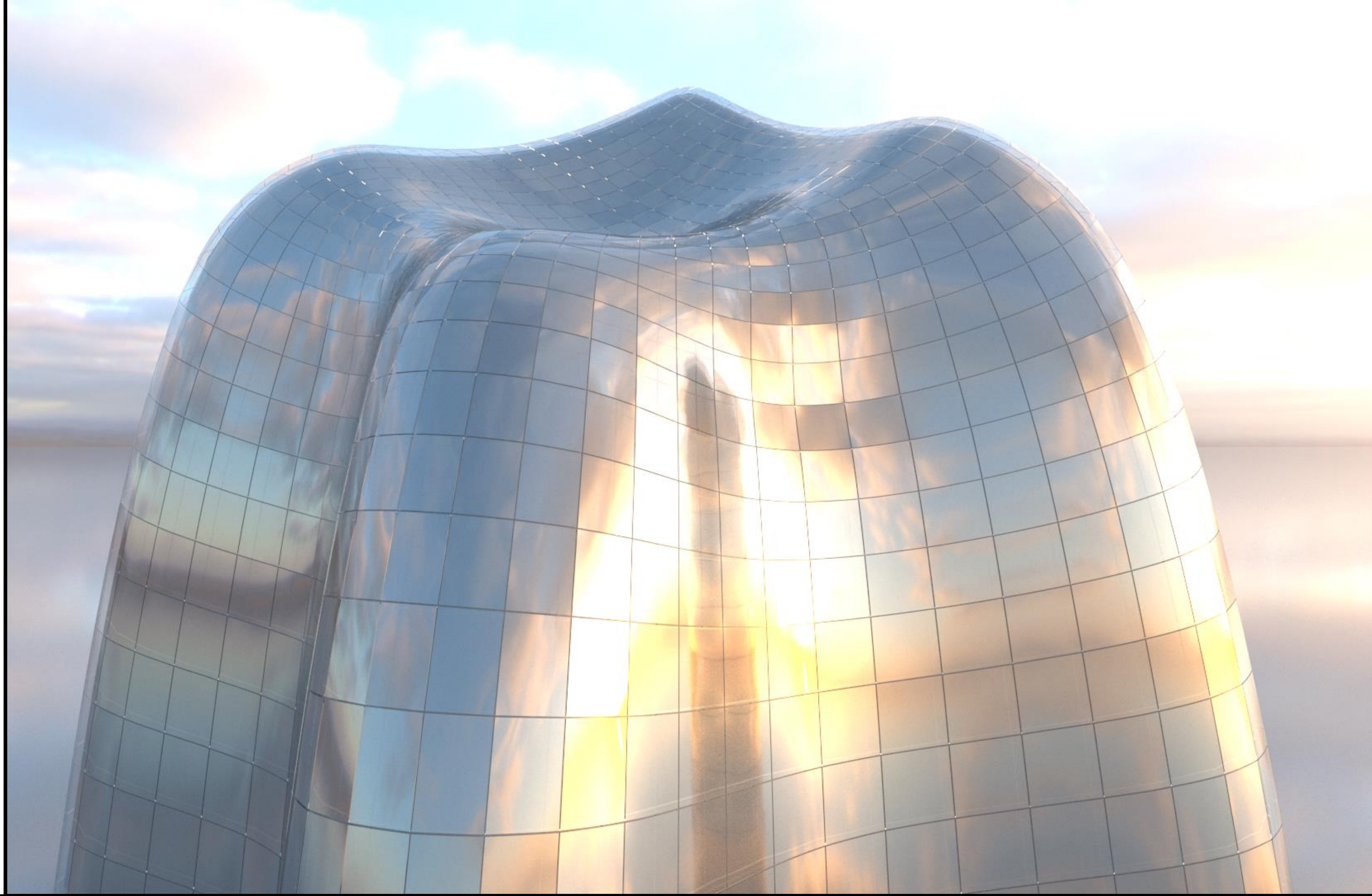

Interactive design

- Time for 1K panels:

  Prediction: 0.1 sec
  Optimization: 3.0 sec / iteration

- Total 10 - 20 iterations needed.
- Intel® Core™ i7-6700HQ CPU at 2.60 GHz and NVIDIA GeForce GTX 960M.

VS

- Average 35 sec to simulate one panel.

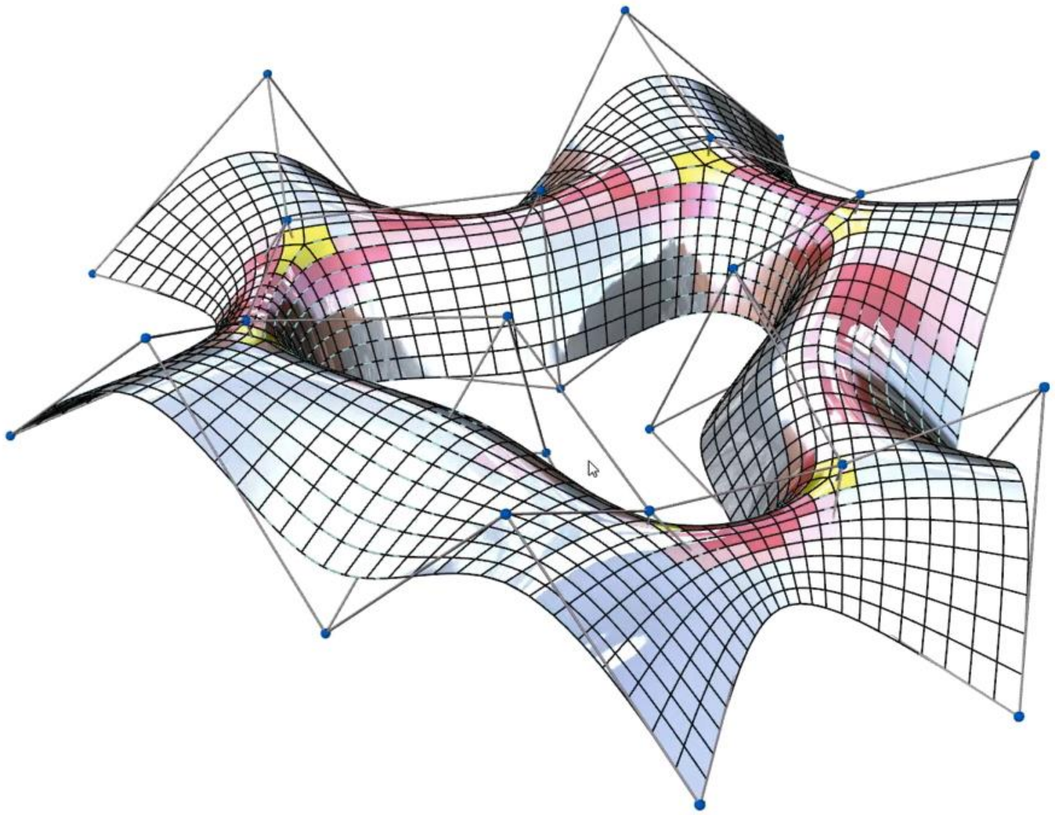

safe | critical | breaking | outside domain

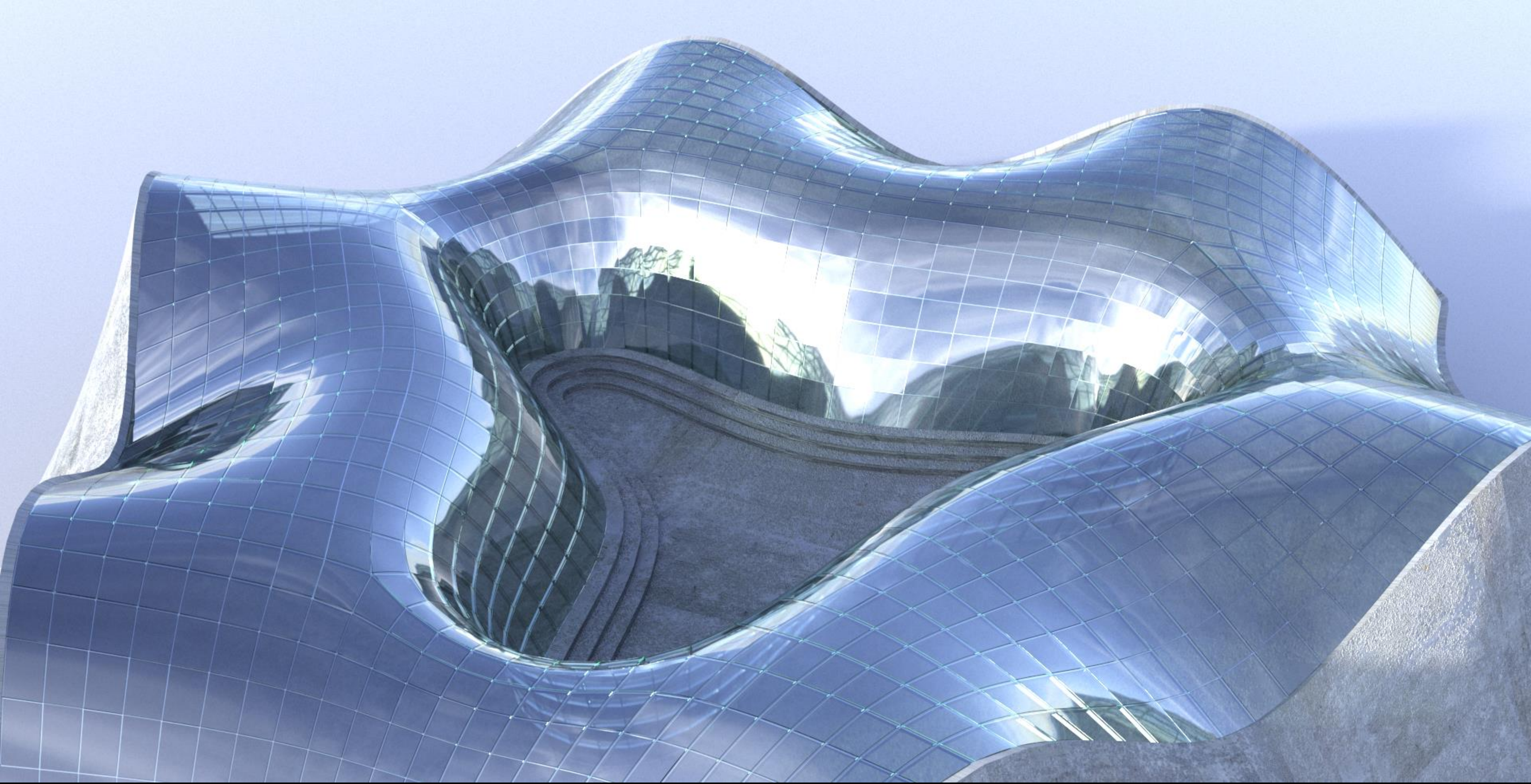

Thank you!

This project has received funding from the European Union's Horizon 2020 research and innovation programme under the Marie Skłodowska-Curie grant agreement No 675789.